4-18-2016

Dynamics of Discrete And Continuous Spatially Distributed Systems

Yury Sokolov

DYNAMICS OF DISCRETE AND CONTINUOUS SPATIALLY DISTRIBUTED SYSTEMS

by

Yury Sokolov

A Dissertation

Submitted in Partial Fulfillment of the

Requirements for the Degree of

Doctor of Philosophy

Major: Mathematical Sciences

The University of Memphis

May 2016

To my parents

ACKNOWLEDGEMENTS

This dissertation would not have been possible without the support of many people. I would like to thank my supervisor Professor Robert Kozma for his guidance and inspiration. Over the past few years he has provided me enormous support and excellent opportunities. I would also like to thank the other professors in the department. Especially, I would like to thank Professors Paul Balister and Irena Lasiecka for their support and valuable advice since they were always open to discuss mathematical and other questions.

I am thankful to my dissertation committee members: Professors George Anastassiou, Fernanda Botelho, E. Olúṣẹ́gun George, Vladimir Nikiforov, and Paul Werbos for their comments and suggestions. I am especially thankful to Professor Paul Werbos for his support, guidance, and introducing me to ADP.

I am extremely grateful to Professors Mikhail Rabinovich and Miklós Ruszinkó for their continuous support, guidance and motivation. During this process they played a crucial role for my formation both as a researcher and as a person.

I would like to express my deepest gratitude to my collaborators: Professors Valentin Afraimovich, Svante Janson, and Ludmilla D. Werbos for great discussions.

I should like to thank Quinn Culver, Joshua Davis, Kamil Popielarz, Sarah, and Carey for reading parts of the dissertation and pointing out a number of mistakes.

I would like to thank all my friends for their support especially those in Memphis for making my stay easier.

Last but not least, I would like to thank all my family for their immense love and support, for being close while afar. The constant support of my parents is invaluable and made all this undertaking real.

The research in this dissertation has been supported in part by the National Science Foundation under Grant No. DMS-13-11165.

ABSTRACT

Sokolov, Yury. Ph.D. The University of Memphis. May 2016. Dynamics of discrete and continuous spatially distributed systems. Major Professor: Robert Kozma, Ph.D.

In this dissertation we consider some dynamical systems and their properties. We study the stability of a discrete system, which corresponds to an approximate dynamic programming problem. We investigate phase transitions of a process on random graphs and find critical parameters. We analyze the bifurcation and attractor of a system given by generalized Lotka-Volterra equations. In particular:

- we study the stability of a discrete dynamical system of estimation error, which corresponds to an approximate dynamic programming (ADP) problem via Lyapunov's second method. We prove that the system is uniformly ultimately bounded;
- we show the necessary conditions for a phase transition in two randomly coupled probabilistic cellular automata in mean-field approximation and prove the existence of limit cycle behavior;
- we introduce a new random graph model $G_{\mathbb{Z}_N^2,p_d}$, a discrete torus with random edges defined with respect to graph distances between vertices on the torus. We prove that the degree probability distribution is approximately Poisson and the diameter of the graph is $D(G_{\mathbb{Z}_N^2,p_d}) = \Theta(\log N)$, whp;
- we study bootstrap percolation on $G_{\mathbb{Z}_N^2,p_d}$. Sharp conditions are derived for phase transition at different values of k with a k-threshold rule in mean-field approximation. We generalize the bootstrap percolation on $G_{\mathbb{Z}_N^2,p_d}$ to the case of two types of vertices with a modified k-threshold rule. We derive some bounds for critical probabilities in the generalized model in mean-field approximation;
- we study the bifurcation of two coupled systems each described by generalized Lotka-Volterra equations with respect to coupling. Also, we study

a dissipative system with an inhomogeneous heteroclinic cycle, that is, each equilibrium in the cycle is either with one or two unstable directions. We prove that there exists an asymptotically stable set consisting of unstable manifolds of the saddles.

Most of the results in the dissertation has been published, which represent joint work with Svante Janson, Robert Kozma, Mikhail I. Rabinovich, Miklós Ruszinkó, Ludmilla D. Werbos, and Paul J. Werbos.

TABLE OF CONTENTS

LIST OF FIGURES

INTRODUCTION

We begin this dissertation with a discussion of the stability result of a control approach which is based on approximate dynamic programming. Dynamic programming was introduced by Bellman [16] as a method for solving optimization problems by dividing them into subproblems that are easier to solve. One may be concerned that if we optimize each subproblem separately, then that would not necessarily be the optimal solution to the original problem according to some criterion. Therefore, we need to be careful at this stage. However, if one performs the division "accurately", then according to Bellman's optimality principle, [16], we will reach an optimal solution to the original problem by combining the solutions obtained for each subproblem. More precisely, a problem is reformulated as a sequence of interrelated problems, i.e., the final state of a problem is the initial state for the next one. This approach has been widely used in optimization, control theory and game theory among others.

In general, dynamic programming allows an optimal solution of an optimization problem and, moreover, it is constructive. However, in the case of a discrete optimization problem, for example, as the number of subproblems grows with a relatively small set of actions at each step, the method becomes useless due to exponential growth of the set of feasible solutions. Bellman coined this phenomenon the curse of dimensionality.

Bellman's optimality principle is associated with the Bellman (Hamilton - Jacobi - Bellman) equation with respect to value function, as defined by von Neumann's utility function [74]. The optimal policy (a collection of optimal actions from all steps) which we are looking for has to satisfy the solution of this equation. According to the method, we need to divide the problem into a sequence of subproblems and solve them iteratively. However, the solution of the original problem itself is a function. Instead of solving the problem iteratively, Werbos

considered an approximation of the solution [82], an idea which gave birth to approximate dynamic programming.

Compared with other approximation methods, for approximate dynamic programming (ADP), approximators in the form of superpositions of sigmoidal functions are of high importance. Let us call them universal function approximators, which are also known as artificial neural networks. The construction of this type of approximators relies on the ideas of Arnold and Kolmogorov. Kolmogorov first showed that a multi-variable function can be expressed as a superposition of functions of three variables. Later Arnold showed that this can be done by superposition of functions of two variables answering the 13th Hilbert problem. Finally, Kolmogorov managed to prove that a multi-variable function can be expressed as a superposition of functions of just one variable.

Mathematical justification for universal approximators was given in 1974 by Werbos who introduced the method for adjusting the parameters of the approximator [79]. Later in 1993, Barron proved fairly sharp threshold on the integrated squared error of approximation [12]. He obtained this result under the assumption for approximated functions on boundness on the first moment of the magnitude distribution of the Fourier transform.

Approximate dynamic programming has received high recognition as a very powerful method for different applications, however, without rigorous mathematical results. During the last decade some important cases were considered and the existence of a stable solution for ADP control has been shown [2, 49, 72]. Liu et al. proved the stability result for the case of the restricted function approximator [51]. This dissertation provides a proof that stability is achieved for a universal function approximator. We show that the estimation error of an ADP design is uniformly ultimately bounded under some conditions on the approximator parameters.

Next, in this dissertation we study the dynamics of discrete systems with many

interacting agents. We use probabilistic cellular automata, and bootstrap percolation with a k-threshold rule on a random graph coupled with a lattice. Let us first introduce the random graph model.

One of the most important random graph models $G_{n,m}$ was introduced by Erdős and Rényi in 1959 [32, 31]. They considered a random graph which consists of n vertices and precisely m randomly and independently chosen edges. It was shown that this model is equivalent to the random graph model introduced by Gilbert [36, 35], where each edge is presented with probability p independently of others.

Later, a different kind of random graph was considered where the distance between vertices is taken into account. In particular, in [63] a long-range percolation graph (LRPG) was introduced where an edge between a pair of points from a finite or countable metric space exists with probability inversely proportional to the distance between the points. This model is an extension of the usual percolation model where connections other than only local are also possible.

Aizenman, Kesten, and Newman [7] considered LRPG on a d-dimensional lattice. In their model a pair of sites of d-dimensional lattice $\mathbb{Z}^d$ is connected (or a bond is occupied) with a probability that depends on the graph distance. It was shown that this type of graph has small diameter in the graph size [17, 29].

Let us mention a few models of random graphs, which also have small diameter. Watts and Strogatz [75] introduced the "small world" model on the vertex set of the n-cycle, where the edges are rewired at random with probability p, starting from a circle lattice with n vertices and k edges per vertex. A different version of the "small world" model has been described by Newman and Watts [54]. Again, an n-cycle was considered and the edges of the cycle were fixed. In contrast to [75], random edges were added with some probability instead of rewiring the edges of the cycle as in [54].

We introduce a random graph model $G_{\mathbb{Z}_N^2,p_d}$ which is a combination of a lattice

and a random graph where the probability of an edge between a pair of vertices depends on graph distance between the pair. First, we consider properties of the graph. We proved that the graph diameter is of logarithmic order on the graph size and the Poisson approximation of degree distribution is shown.

Cellular automata (CA) were introduced by von Neuman [73]. A cellular automaton is a dynamical system defined on a graph with a local deterministic update rule. Every vertex is in one of two possible states described by a binary potential function. At each time step the system is updated with respect to the rule, which depends only on the states of vertices in the neighborhood of every vertex in the system.

Probabilistic cellular automata (PCA) is the generalization of CA for the case of the probabilistic update rule. For example, let us consider a usual CA with an arbitrary update rule, then we can define PCA assuming that every vertex will not follow the rule with probability p and will be updated according to the rule with probability $1 - p$. Due to the complexity of the process a few results are known. In particular, a mean-field approximation of PCA on a torus was considered in [10]. The estimate for the critical probability was derived and later the model was studied on a torus [9]. It was shown that for small p the system stays mostly in one of two configurations, moreover, the transition time from one configuration to the other is $\Theta(1/p^{n+1})$.

We consider two randomly coupled probabilistic cellular automata. The dynamics of the coupled system is analyzed in mean-field approximation. In particular, the existence of limit cycle dynamics is proven. This result provides conditions for phase transitions in the coupled system of two PCA which generalizes the study of [10].

Bootstrap percolation is a cellular automaton which describes the spread of activity (infection). Every vertex is active (infected) initially with some probability

independent on other vertices. The state of a vertex (active/inactive) is defined at each step based on the states of her neighbors. The original model was defined on a Bethe lattice by Chalupa, Leath, and Reich [27]. Since then bootstrap percolation has been extensively studied on different graphs. In 2-neighbor bootstrap percolation on a 2-dimensional lattice the first result is due to van Enter who proved $p_c(\mathbb{Z}^2) = 0$, [70]. Later, this result was generalized to all dimensions by Schonmann [62]. It was shown that for the r-neighbor rule in d dimensions the critical probability is 0 if $r \leq d$ and 1 otherwise.

Different behaviors were observed for grids [6]. In 1988, Aizenman and Lebowitz showed the existence of metastability phenomenon for a d-dimensional cube $[n]^d$. They found the order of critical probability in all dimensions. Beautiful and exciting results came later in 2003 for a 2-dimensional grid [40]. Holroyd managed to prove a sharp threshold defining precisely the constant term in asymptotic value of critical probability. Interestingly, this result contradicted numerical predictions and the reason was due to slow convergence, i.e., $o(1/\log n)$. It took another ten years to generalize this result. Balogh, Bollobás, Duminil-Copin, and Morris derived sharp thresholds for critical probabilities in bootstrap percolation on a d-dimensional cube in all dimension [11].

Recently, Janson, Łuczak, Turova, and Vallier considered bootstrap percolation model on the Erdős-Rényi random graph $G_{n,p}$ [42]. In particular, these authors obtained sharp thresholds for (almost) percolation with respect to size a of the set of initially active sites and graph parameter p. Also, time t required the termination of the bootstrap percolation process was derived.

In Lengler et al. [30] bootstrap percolation theory was generalized to the case of two types of vertices on $G_{n,p}$. However, percolation was defined according to one type. Threshold for percolation was derived with respect to size a of the set of initially active sites and graph parameter p as well as time until termination. This

model resembles bootstrap percolation on a square grid with 3-threshold rule. In the later case, the whole grid cannot be infected since there exists positive fractions of sites, which stay healthy forever, with high probability.

We consider a bootstrap percolation process with a k-threshold rule on the random graph $G_{\mathbb{Z}_N^2,p_d}$. Since there are vertices with degree four with positive probability, it is assumed that k is small. For cases where $0 \leq k \leq 3$, sharp thresholds for phase transitions are derived through a mean-field approximation of the process.

We conclude this dissertation by studying questions related to homoclinic loops and heteroclinic cycles in a dissipative system without symmetry, for the class of generalized Lotka-Volterra differential equations. A heteroclinic sequence is a collection of hyperbolic equilibria and separatrices which join them. A sequence can be either open or closed, and in the last case it is called a cycle. If the sequence consists of only one equilibrium then it is called a homoclinic loop.

For a long time it was assumed that all orbits of dissipative systems eventually go to fixed points or to periodic orbits. The first change to this idea happened when Cartwright and Littlewood proved the existence of periodic orbits with different periods for the van der Pol oscillator. Later, it was shown that dissipative systems exhibit even a more complicated type of dynamics, including chaotic dynamics.

Afraimovich et al. proved the existence of heteroclinic cycles/homoclinic loops [4], and they considered a system defined by generalized Lotka-Volterra equations. The conditions for this type of behavior were derived for the case of equilibria with a one-dimensional unstable manifold.

Mohapatra and Ott showed that nonuniformly hyperbolic dynamics emerge when flows in $\mathbb{R}^n$ with homoclinic loops or heteroclinic cycles are subjected to certain time-periodic forces [53]. In particular, the emergence of strange attractors and SRB measures with strong statistical properties were derived.

Afraimovich et al. considered a homogeneous case of mixed types of hyperbolic equilibria [3]. It was assumed that there is a subset among equilibria (that consists of $1 \leq p \leq n$ equilibria) which are on the axes of $\mathbb{R}^n$, such that each equilibrium (saddle) has two unstable directions. For this case, the topological type of the attractor depends on the size of the sequence of saddles. In particular, when p is even, it was shown that the attractor is homeomorphic to a cylinder.

We consider bifurcation of two coupled systems each described by a set of generalized Lotka-Volterra equations with respect to coupling. The systems are cyclically coupled with a fixed direction and we assume that every uncoupled system exhibits heteroclinic cycle dynamics. As coupling parameter grows complex dynamics appear. However, for a large coupling parameter we have that one system starts to dominate the other, which forces the second system eventually to die out.

Additionally, we study the case of inhomogeneous connections for the phase space in the class of generalized Lotka-Volterra equations with different dimensions of unstable manifolds of hyperbolic equilibria. That is, the sequence contains equilibria with one and two dimensional manifolds. We consider two cases, the "attractor" in each case is homeomorphic to a cylinder, however, they are of different dimensions.

The results in this dissertation may have interest by their own but also they can particularly be applied to the field of neurobiology, for example. In particular, randomly coupled probabilistic cellular automata and bootstrap percolation on the random graph $G_{\mathbb{Z}_N^2,p_d}$ are suitable for the description of dynamics on the lower hierarchical level of the brain, i.e., activity propagation among neurons and neural populations.

Rabinovich et al. introduced representation of cognition as transient dynamics with dynamical image - a heteroclinic sequence [59]. Our results for two coupled systems defined by generalized Lotka-Volterra equations may partially describe the

case of pathological dynamics in higher-level cognitive activity. The possible interpretation of different dimensions of attractors can justify dynamical origin in decision making.

CHAPTER 1

STABILITY OF APPROXIMATE DYNAMIC PROGRAMMING CONTROL DESIGN

Approximate Dynamic Programming (ADP) addresses the general challenge of optimal decision and control for sequential decision making problems with complex and often uncertain, stochastic conditions without the presumption of linearity. ADP is a relatively young branch of mathematics; in his pioneering work Werbos [79] provided powerful motivation for extensive investigations of ADP in recent decades [15, 18, 64, 82].

ADP has not only shown solid theoretical results to optimal control but also successful applications [71]. Various ADP designs demonstrated powerful results in solving complicated real-life problems, involving multi-agent systems and games [8, 83].

The stability of ADP in the general case is an open and yet unsolved problem. Significant efforts are required to develop conditions for stability in various ADP designs. We solved the stability problem for the specific ADP control case using Lyapunov's second method. Here we are addressing a discrete time dynamical system, where the dynamics is described by a second-order difference equation. We introduce a discrete time Lyapunov function and prove the uniformly ultimately bounded (UUB) property under certain conditions. We generalize the results obtained by Liu et al. [51] in deriving stability conditions for ADP with traditional three layer Multi-Layer Perceptron (MLP). A stability condition for the system with weights adapted between the hidden and output layers only is derived in [51], under the assumption that networks have a large enough number of nodes in the hidden layers.

The approach presented in [51], in effect, is equivalent to a linear basis function approach: it is easy but it leads to scalability problems. The complexity of the

system is growing exponentially for the required degree of approximation of a function of given smoothness [13]. Additional problems arise regarding the accuracy of parameter estimation, which tends to grow with the number of parameters while all other factors remain constant. If we have too many parameters for a limited set of data then it may lead to overtraining, i.e., the approximation of the data is high while there will be a large error of approximation of a different data set. We need more parsimonious models, capable of generalization, hence our intention is to use fewer parameters in truly nonlinear networks, which is made possible by implementing a more advanced learning algorithm. In this chapter we focus on studying the stability properties of the ADP system with MLP-based critic, when the weights are adapted between all layers. By using the Lyapunov approach, we study the uniformly ultimately bounded property of the ADP design.

This chapter is a joint work with Robert Kozma, Ludmila Werbos, and Paul Werbos, and results from this chapter appear in previously published papers [46, 66].

1.1 Formalization of Approximate Dynamic Programming

First, we describe the general idea of ADP in order for the reader to get an initial flavor for the subject before moving to ADP control. For this purpose let us define the discrete dynamic programming operator L

$$(LJ)(x) = \min_{u \in U(x)} \sum_{y \in S} (r(x,u) + \alpha J(y)). \tag{1.1}$$

According to the standard approach, we can find an optimal policy by backward induction starting at terminal period, T. However, we need to have additional conditions on the utility function and discount factor to guarantee a solution for the infinite horizon case. For this reason, it is enough to assume that utility function r is uniformly bounded and the discount factor $\alpha \in [0, 1)$.

Using this operator we can write the Bellman equation in the form

$$J = L(J).$$

Consider value function J from a Banach space of measurable (continuous) functions under supremum norm. One can notice that L is a contraction mapping on the Banach space. According to the Banach fixed point theorem, there exists a unique fixed point J of the operator L.

1.2 Foundations of ADP control

Let us consider a dynamical system with discrete dynamics, which is described by the following nonlinear difference equation:

$$x(t+1) = f\left(x(t), u(t)\right), \tag{1.2}$$

where x is the m-dimensional plant state vector and u is the n-dimensional control (or action) vector.

We focus on the deterministic case, as described in equation (1.2) and introduce approximate dynamic programming (ADP) to control this system. ADP is a learning algorithm for adapting a system made up of two components, the critic and the action, as shown in Figure 1. These two major components can be implemented using any kind of differentiable function approximator. Probably the most widely used value function approximators in practical applications are neural networks, linear basis function approximators, and piecewise linear value functions such as those used by [49, 56]. In this dissertation we use MLP as the universal function approximator.

The optimal value function, J^* is the solution of the Bellman equation [82], which is a function of the state variables but not of the action variables. Here we use function J, which is closely related to J^*, where J is a function of both the state and the action variables. Function J is often denoted by J' in the literature,

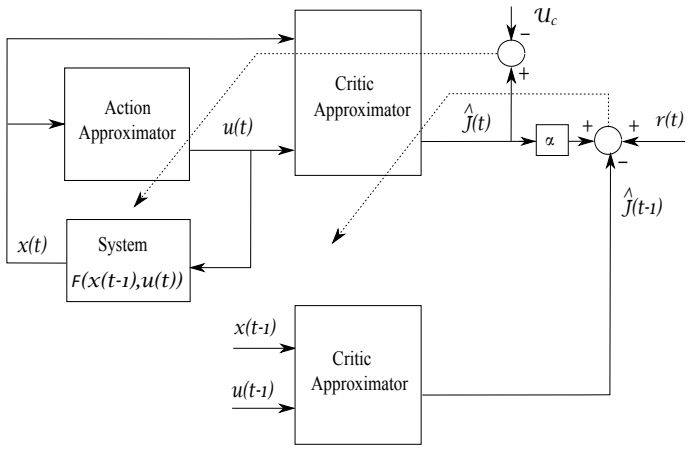

Figure 1: Representation of the ADP control design, including system, action and critic networks.

following the definition in [82]. The critic provides the estimate of function J, which is denoted as $\hat{J}$. Function Q, used in traditional Q-learning [64] is the discrete-variable equivalent of J.

The action network represents a control policy. Each combination of weights defines a different controller, hence by exploring the space of possible weights we approximate the dynamic programming solution for the optimal controller.

In ADP, the cost function is expressed as follows; see, for example, [49]:

$$J(x(t), u(t)) = \sum_{i=t}^{\infty} \alpha^{i-t} r(x(i+1), u(i+1)), \tag{1.3}$$

where $0 < \alpha \leq 1$ is a discount factor for the infinite horizon problem, and $r(x(t), u(t))$ is the reward, reinforcement or utility function. We require $r(t) = r(x(t), u(t))$ to be a bounded semidefinite function of the state $x(t)$ and control $u(t)$, so the cost function is well-defined. Using standard algebra one can derive from (1.3) that $0 = \alpha J(t) + r(t) - J(t-1)$, where $J(t) = J(x(t), u(t))$.

1.2.1 Action network

Next we introduce each component, starting with the action component. The action component is represented by a neural network (NN), and its main goal is to generate control policy. For our purpose, MLP with one hidden layer is used. At

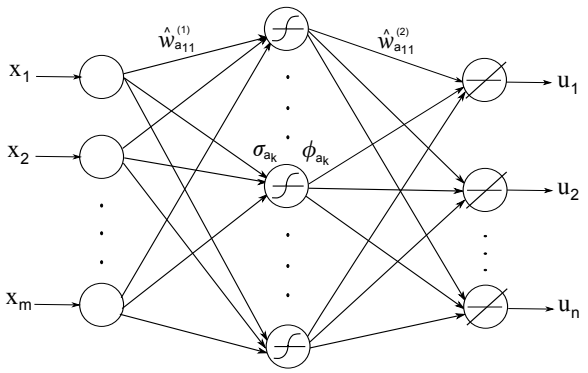

Figure 2: Illustration of the action network as a MLP with one hidden layer.

each time step this component needs to provide an action based on the state vector $x(t) = (x_1(t), \ldots, x_m(t))^T$, so $x(t)$ is used as an input for the action network. If the hidden layer of the action MLP consists of N_{h_a} nodes; the weight between the input node j and the hidden node i is denoted by $\hat{w}^{(1)}_{a_{ij}}(t)$, for $i = 1, \ldots, N_{h_a}$ and $j = 1, \ldots, m$. $\hat{w}^{(2)}_{a_{ij}}(t)$, where $i = 1, \ldots, n$, $j = 1, \ldots, N_{h_a}$ is the weight from j's hidden node to i's output. The weighted sum of all inputs, i.e., the input to a hidden node k is given as $\sigma_{a_k}(t) = \sum_{j=1}^{m} \hat{w}^{(1)}_{a_{kj}}(t) x_j(t)$. The output of hidden node k of the action network is denoted by $\phi_{a_k}(t)$.

A variety of transfer functions are in use, see, for example, [85]. Hyperbolic tangent is one of the most studied transfer function, which is used here: $\phi_{a_k}(t) = \frac{1-e^{-\sigma_{a_k}(t)}}{1+e^{-\sigma_{a_k}(t)}}$. A major advantage of the standard MLP neural network described here is the ability to approximate smooth nonlinear functions more accurately than linear basis function approximators, as the number of inputs grows [12, 13]. Finally, the output of the action MLP is a n-dimensional vector of control variables $u_i(t) = \hat{w}^{(2)}_{a_i}(t)\phi_a(t) = \sum_{j=1}^{N_{h_a}} \hat{w}^{(2)}_{a_{ij}}(t)\phi_{a_j}(t)$. The diagram of the action network is shown in Figure 2.

1.2.2 Critic network

The critic neural network, with output $\hat{J}$, learns to approximate J function and it uses the output of the action network as one of its inputs. This is shown in Figure 3. The input to the critic network is

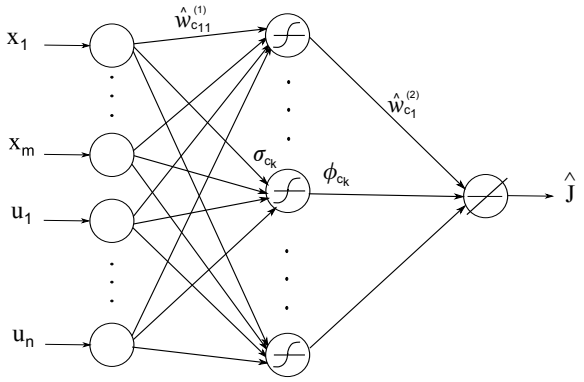

Figure 3: Illustration of the critic network as a MLP with one hidden layer.

$y(t) = (x_1(t), \ldots, x_m(t), u_1(t), \ldots, u_n(t))^T$, where $u(t) = (u_1(t), \ldots, u_n(t))^T$ is output of the action network. Just as for the action NN, here we use an MLP with one hidden layer, which contains N_{h_c} nodes. $\hat{w}_{c_{ij}}^{(1)}(t)$, for $i = 1, \ldots, N_{h_c}$ and $j = 1, \ldots, m + n$ is the weight from j's input to i's hidden node of the critic network. Here hyperbolic tangent transfer function is used. For convenience, the input to a hidden node k is split in two parts with respect to inputs $\sigma_{c_k}(t) = \sum_{j=1}^{m} \hat{w}_{c_{kj}}^{(1)}(t) x_j(t) + \sum_{j=1}^{n} \hat{w}_{c_{i(m+j)}}^{(1)}(t) u_j(t)$. The output of hidden node k of the critic network is given as $\phi_{c_k}(t) = \frac{1-e^{-\sigma_{c_k}(t)}}{1+e^{-\sigma_{c_k}(t)}}$. Since the critic network has only one output, we have N_{h_c} weights between hidden and output layers of the form $\hat{w}_{c_i}^{(2)}(t)$. Finally, the output of the critic neural network can be described in the form $\hat{J}(t) = \hat{w}_c^{(2)}(t) * \phi_c(t) = \sum_{i=1}^{N_{h_c}} \hat{w}_{c_i}^{(2)}(t) \phi_{c_i}(t)$, where $*$ denotes the inner product.

1.3 Gradient-descent Learning Algorithm

1.3.1 Adaptation of the critic network

Let $e_c(t) = \alpha \hat{J}(t) + r(t) - \hat{J}(t-1)$ be the prediction error of the critic network and $E_c(t) = \frac{1}{2} e_c^2(t)$ be the objective function, which must be minimized. Let us consider the gradient descent algorithm as the weight update rule, that is, $\hat{w}_c(t+1) = \hat{w}_c(t) + \Delta \hat{w}_c(t)$. Here the last term is $\Delta \hat{w}_c(t) = l_c \left[-\frac{\partial E_c(t)}{\partial \hat{w}_c(t)} \right]$ and $l_c > 0$ is the learning rate.

The adaptation of the critic network's weights between input layer and hidden

layer is given as follows: $\Delta\hat{w}_{c_{ij}}^{(1)}(t) = l_c\left[-\frac{\partial E_c(t)}{\partial\hat{w}_{c_{ij}}^{(1)}(t)}\right]$, which yields

$$\frac{\partial E_c(t)}{\partial\hat{w}_{c_{ij}}^{(1)}(t)} = \frac{\partial E_c(t)}{\partial\hat{J}(t)}\frac{\partial\hat{J}(t)}{\partial\phi_{c_i}(t)}\frac{\partial\phi_{c_i}(t)}{\partial\sigma_{c_i}(t)}\frac{\partial\sigma_{c_i}(t)}{\partial\hat{w}_{c_{ij}}^{(1)}(t)} = \alpha e_c(t)\hat{w}_{c_i}^{(2)}(t)\left[\frac{1}{2}(1-\phi_{c_i}^2(t))\right]y_j(t). \tag{1.4}$$

Note that the last calculation is obtained considering $\hat{J}(\cdot)$ at different time steps as different functions; see, for example, [49]. The adaptation of the critic network's weights between hidden layer and output layer is given by $\Delta\hat{w}_{c_i}^{(2)}(t) = l_c\left[-\frac{\partial E_c(t)}{\partial\hat{w}_{c_i}^{(2)}(t)}\right]$, which leads to

$$\frac{\partial E_c(t)}{\partial\hat{w}_{c_i}^{(2)}(t)} = \frac{\partial E_c(t)}{\partial\hat{J}(t)}\frac{\partial\hat{J}(t)}{\partial\hat{w}_{c_i}^{(2)}(t)} = \alpha e_c(t)\phi_{c_i}(t). \tag{1.5}$$

1.3.2 Adaptation of the action network

The training of the action network can be done by using the backpropagation adaptive critic method [82], which entails adapting the weights so as to minimize $\hat{J}(t)$. Here we used an importance-weighted training approach. We denote by U_c the desired ultimate objective function. Then the minimized error measure is given in the form $E_a(t) = \frac{1}{2}e_a^2(t)$, where $e_a(t) = \hat{J}(t) - U_c$ is the prediction error of the action NN.

In the framework of the reinforcement learning paradigm, the success corresponds to an objective function, which is zero at each time step [15]. Based on this consideration and for the sake of simplicity of the further derivations, we assume $U_c = 0$, that is, the objective function is zero at each time step, which means there is success.

Let us consider the gradient descent algorithm as the weight update rule similarly as we did for the critic network above. That is, $\hat{w}_a(t+1) = \hat{w}_a(t) + \Delta\hat{w}_a(t)$, where $\Delta\hat{w}_a(t) = l_a\left[-\frac{\partial E_a(t)}{\partial\hat{w}_a(t)}\right]$ and $l_a > 0$ is the learning rate.

The adaptation of the action network's weights between input layer and hidden layer is given as $\Delta\hat{w}_{a_{ij}}^{(1)}(t) = l_a\left[-\frac{\partial E_a(t)}{\partial \hat{w}_{a_{ij}}^{(1)}(t)}\right]$,

$$\begin{aligned}
&\frac{\partial E_a(t)}{\partial \hat{w}_{a_{ij}}^{(1)}(t)} = \frac{\partial E_a(t)}{\hat{J}(t)}\left[\frac{\partial \hat{J}(t)}{\partial u(t)}\right]^T \frac{\partial u(t)}{\partial \phi_{a_i}(t)}\frac{\partial \phi_{a_i}(t)}{\partial \sigma_{a_i}(t)}\frac{\partial \sigma_{a_i}(t)}{\partial \hat{w}_{a_{ij}}^{(1)}(t)} \\
&= \frac{\partial E_a(t)}{\hat{J}(t)}\sum_{k=1}^{n}\frac{\partial \hat{J}(t)}{\partial u_k(t)}\frac{\partial u_k(t)}{\partial \phi_{a_i}(t)}\frac{\partial \phi_{a_i}(t)}{\partial \sigma_{a_i}(t)}\frac{\partial \sigma_{a_i}(t)}{\partial \hat{w}_{a_{ij}}^{(1)}(t)} = \\
&\hat{J}(t)\sum_{k=1}^{n}\sum_{r=1}^{N_{h_c}}\left[\hat{w}_{c_r}^{(2)}(t)\frac{1}{2}(1-\phi_{c_r}^2(t))\hat{w}_{c_{r,m+k}}^{(1)}(t)\right]\times \\
&\hat{w}_{a_{ki}}^{(2)}(t)\frac{1}{2}(1-\phi_{a_i}^2(t))x_j(t),
\end{aligned} \tag{1.6}$$

where

$$\frac{\partial \hat{J}(t)}{\partial u_k(t)} = \sum_{i=1}^{N_{h_c}}\frac{\partial \hat{J}(t)}{\partial \phi_{c_i}(t)}\frac{\partial \phi_{c_i}(t)}{\partial \sigma_{c_i}(t)}\frac{\partial \sigma_{c_i}(t)}{\partial u_k(t)}. \tag{1.7}$$

Using a similar approach for the action network's weights between hidden layer and output layer, finally we get the following $\Delta\hat{w}_{a_{ij}}^{(2)}(t) = l_a\left[-\frac{\partial E_a(t)}{\partial \hat{w}_{a_{ij}}^{(2)}(t)}\right]$,

$$\begin{aligned}
\frac{\partial E_a(t)}{\partial \hat{w}_{a_{kj}}^{(2)}(t)} &= \frac{\partial E_a(t)}{\hat{J}(t)}\frac{\partial \hat{J}(t)}{\partial u_k(t)}\frac{\partial u_k(t)}{\partial \hat{w}_{a_{kj}}^{(2)}(t)} = \\
&e_a(t)\sum_{r=1}^{N_{h_c}}\left[\hat{w}_{c_r}^{(2)}(t)\frac{1}{2}(1-\phi_{c_r}^2(t))\hat{w}_{c_{r,m+k}}^{(1)}(t)\right]\phi_{a_j}(t).
\end{aligned} \tag{1.8}$$

1.4 Lyapunov stability analysis of ADP

In this section we employ the Lyapunov function approach to evaluate the stability of dynamical systems. The applied Lyapunov analysis allows us to establish the UUB property without deriving the explicit solution of the state equations.

1.4.1 Basics of the Lyapunov approach

Let w_c^*, w_a^* denote the optimal weights, that is, the following holds: $w_c^* = \arg\min_{\hat{w}_c}\left\|\alpha\hat{J}(t) + r(t) - \hat{J}(t-1)\right\|$; we assume that the desired ultimate objective $U_c = 0$ corresponds to success then $w_a^* = \arg\min_{\hat{w}_a}\left\|\hat{J}(t)\right\|$.

Consider the weight estimation error over the full ADP control, that is, over both the critic and action networks of the following form: $\tilde{w}(t) := \hat{w}(t) - w^*$. Then equations (1.4), (1.5), (1.6) and (1.8) define a dynamical system of estimation errors for some nonlinear function F in the following form

$$\tilde{w}(t+1) = \tilde{w}(t) - F\left(\hat{w}(t-1), \hat{w}(t), \phi(t-1), \phi(t)\right). \tag{1.9}$$

Definition 1. A dynamical system is said to be uniformly ultimately bounded with ultimate bound $b > 0$, if for any $a > 0$ and $t_0 > 0$, there exists a positive number $N = N(a, b)$ independent of t_0, such that $\|\tilde{w}(t)\| \leq b$ for all $t \geq N + t_0$ whenever $\|\tilde{w}(t_0)\| \leq a$.

In the present study, we make use of a theorem concerning the UUB property of a discrete dynamical system [61]. Detailed proof of this theorem appears in [52]. We adapt the notation for our situation and address the special case of discrete dynamical systems as given in (1.9).

Theorem 2. If, for system (1.9), there exists a function $L(\tilde{w}(t), t)$ such that for all $\tilde{w}(t_0)$ in a compact set K, $L(\tilde{w}(t), t)$ is positive definite and the first difference, $\Delta L(\tilde{w}(t), t) < 0$ for $\|\tilde{w}(t_0)\| > b$, for some $b > 0$, such that b-neighborhood of $\tilde{w}(t)$ is contained in K, then the system is UUB and the norm of the state is bounded to within a neighborhood of b.

Based on this theorem, which gives a sufficient condition, we can determine the UUB property of the dynamical system selecting an appropriate function L. For this reason, we first consider all components of our function candidate separately and investigate their properties, and thereafter we study the behavior of L function to match the condition from Theorem 2.

1.4.2 Preliminaries

In this subsection we introduce four lemmas which will be used in the proof of the main theorem.

Assumption 3. Let w_a^* and w_c^* be the optimal weights for action and critic networks. Assume they are bounded, i.e., $\|w_a^*\| \leq w_a^{max}$ and $\|w_c^*\| \leq w_c^{max}$.

Lemma 4. Under Assumption 3, the first difference of $L_1(t) = \frac{1}{l_c} \operatorname{tr}\left[\left(\tilde{w}_c^{(2)}(t)\right)^T \tilde{w}_c^{(2)}(t)\right]$ is expressed by

$$\begin{aligned}
&\Delta L_1(t) = -\alpha^2 \left\|\zeta_c(t)\right\|^2 - \left(1 - \alpha^2 l_c \left\|\phi_c(t)\right\|^2\right) \times \\
&\left\|\alpha \hat{w}_c^{(2)}(t)\phi_c(t) + r(t) - \hat{w}_c^{(2)}(t-1)\phi_c(t-1)\right\|^2 + \\
&\left\|\alpha w_c^{*(2)}\phi_c(t) + r(t) - \hat{w}_c^{(2)}(t-1)\phi_c(t-1)\right\|^2, \qquad (1.10)
\end{aligned}$$

where $\zeta_c(t) = \tilde{w}_c^{(2)}(t)\phi_c(t)$ is the approximation error of the output of the critic network.

Proof. Using (1.5) and taking into account that $w_c^{*(2)}$ does not depend on t, and, for example, when it is optimal for each time moment t, we get the following

$$\begin{aligned}
&\tilde{w}_c^{(2)}(t+1) = \hat{w}_c^{(2)}(t+1) - w_c^{(2)^*} = \\
&\tilde{w}_c^{(2)}(t) - \alpha l_c \phi_c \left[\alpha \hat{w}_c^{(2)}(t)\phi_c(t) + r(t) - \hat{w}_c^{(2)}(t-1)\phi_c(t-1)\right]^T. \qquad (1.11)
\end{aligned}$$

Based on the last expression, we can find the trace of multiplication of $\tilde{w}_c^{(2)}(t+1)$ by itself in the following way:

$$\begin{aligned}
&\operatorname{tr}\left[\left(\tilde{w}_c^{(2)}(t+1)\right)^T \tilde{w}_c^{(2)}(t+1)\right] = \left(\tilde{w}_c^{(2)}(t)\right)^T \tilde{w}_c^{(2)}(t) - \\
&2\alpha l_c \tilde{w}_c^{(2)}(t)\phi_c(t)\left[\alpha \hat{w}_c^{(2)}(t)\phi_c(t) + r(t) - \hat{w}_c^{(2)}(t-1)\phi_c(t-1)\right]^T + \\
&\alpha^2 l_c^2 \left\|\phi_c(t)\right\|^2 \left\|\alpha \hat{w}_c^{(2)}\phi_c(t) + r(t) - \hat{w}_c^{(2)}(t-1)\phi_c(t-1)\right\|^2. \qquad (1.12)
\end{aligned}$$

Since $\tilde{w}_c^{(2)}(t)\phi_c(t)$ is a scalar, we can rewrite the middle term in the above formula

as follows:

$$
\begin{aligned}
&-2\alpha l_c \tilde{w}_c^{(2)}(t)\phi_c(t)\left[\alpha\hat{w}_c^{(2)}(t)\phi_c(t) + r(t) - \hat{w}_c^{(2)}(t-1)\phi_c(t-1)\right] = \\
&l_c\left(\left\|\alpha\hat{w}_c^{(2)}(t)\phi_c(t) + r(t) - \hat{w}_c^{(2)}(t-1)\phi_c(t-1) - \alpha\tilde{w}_c^{(2)}(t)\phi_c(t)\right\|^2 - \right. \\
&\left.\left\|\alpha\tilde{w}_c^{(2)}(t)\phi_c(t)\right\|^2 - \left\|\alpha\hat{w}_c^{(2)}(t)\phi_c(t) + r(t) - \hat{w}_c^{(2)}(t-1)\phi_c(t-1)\right\|^2\right) = \\
&l_c\left(\left\|\alpha w_c^{*(2)}\phi_c(t) + r(t) - \hat{w}_c^{(2)}(t-1)\phi_c(t-1)\right\|^2 - \alpha^2\left\|\zeta_c(t)\right\|^2 - \right. \\
&\left.\left\|\alpha\hat{w}_c^{(2)}(t)\phi_c(t) + r(t) - \hat{w}_c^{(2)}(t-1)\phi_c(t-1)\right\|^2\right). \qquad (1.13)
\end{aligned}
$$

Here the definition of $\tilde{w}_c^{(2)}(t) = \hat{w}_c^{(2)}(t) - w_c^{*(2)}$ is applied to obtain the above expression.

Now let us consider the first difference of $L_1(t)$ in the form

$$
\Delta L_1(t) = \frac{1}{l_c}\left[\left(\tilde{w}_c^{(2)}(t+1)\right)^T\tilde{w}_c^{(2)}(t+1) - \left(\tilde{w}_c^{(2)}(t)\right)^T\tilde{w}_c^{(2)}(t)\right]. \qquad (1.14)
$$

Substituting the results for $\left(\tilde{w}_c^{(2)}(t+1)\right)^T\tilde{w}_c^{(2)}(t+1)$, finally we get the statement of the lemma, as required. □

Lemma 5. Under Assumption 3, the first difference of $L_2(t) = \frac{1}{l_a\gamma_1}\operatorname{tr}\left[\left(\tilde{w}_a^{(2)}(t)\right)^T\tilde{w}_a^{(2)}(t)\right]$ is bounded by

$$
\begin{aligned}
&\Delta L_2(t) \le \frac{1}{\gamma_1}\left(-\left(1 - l_a\left\|\phi_a(t)\right\|^2\left\|\hat{w}_c^{(2)}(t)C(t)\right\|^2\right)\left\|\hat{w}_c^{(2)}(t)\phi_c(t)\right\|^2 + \right. \\
&\left. 4\left\|\zeta_c(t)\right\|^2 + 4\left\|w_c^{*(2)}\phi_c(t)\right\|^2 + \left\|\hat{w}_c^{(2)}(t)C(t)\zeta_a(t)\right\|^2\right), \qquad (1.15)
\end{aligned}
$$

where $\zeta_a(t) = \tilde{w}_a^{(2)}(t)\phi_a(t)$ is the approximation error of the action network output and $\gamma_1 > 0$ is a weighting factor; $C(t)$ is the $N_{h_c} \times n$ matrix with coefficients $C_{ij}(t) = \frac{1}{2}\left(1 - \phi_{c_i}^2(t)\right)\hat{w}_{c_{i,m+j}}^{(1)}(t)$, where $i = 1 \ldots N_{h_c}$, and $j = 1 \ldots n$.

Proof. Let us consider the weights from the hidden layer to output layer of the

action network which are updated according to (1.8)

$$\begin{aligned}\tilde{w}_a^{(2)}(t+1) &= \hat{w}_a^{(2)}(t+1) - w_a^{*(2)} = \hat{w}_a^{(2)}(t) - \\ & l_a\phi_a(t)\hat{w}_c^{(2)}(t)C(t)\left[\hat{w}_c^{(2)}(t)\phi_c(t)\right]^T - w_a^{*(2)} = \\ & \tilde{w}_a^{(2)}(t) - l_a\phi_a(t)\hat{w}_c^{(2)}(t)C(t)\left[\hat{w}_c^{(2)}(t)\phi_c(t)\right]^T. \end{aligned} \tag{1.16}$$

Based on this expression, it is easy to see that

$$\begin{aligned}&\mathrm{tr}\left[(\tilde{w}_a^{(2)}(t+1))^T\tilde{w}_a^{(2)}(t+1)\right] = (\tilde{w}_a^{(2)}(t))^T\tilde{w}_a^{(2)}(t) + \\ &l_a^2\left\|\phi_a(t)\right\|^2\left\|\hat{w}_c^{(2)}(t)C(t)\right\|^2\left\|\hat{w}_c^{(2)}(t)\phi_c(t)\right\|^2 - 2l_a\hat{w}_c^{(2)}(t)C(t)\left[\hat{w}_c^{(2)}(t)\phi_c(t)\right]^T\zeta_a(t).\end{aligned} \tag{1.17}$$

Here the last formula is based on the assumption that all vector multiplications are under trace function.

Now let us consider the first difference of function $L_2(t)$, that is, the following expression

$$\Delta L_2(t) = \frac{1}{l_a\gamma_1}\,\mathrm{tr}\left[(\tilde{w}_a^{(2)}(t+1))^T\tilde{w}_a^{(2)}(t+1) - (\tilde{w}_a^{(2)}(t))^T\tilde{w}_a^{(2)}(t)\right]. \tag{1.18}$$

After substituting the appropriate terms in the last formula, we get

$$\begin{aligned}\Delta L_2(t) &= \frac{1}{\gamma_1}\Big(l_a\left\|\phi_a(t)\right\|^2\left\|\hat{w}_c^{(2)}(t)C(t)\right\|^2\left\|\hat{w}_c^{(2)}(t)\phi_c(t)\right\|^2 \\ &- 2\hat{w}_c^{(2)}(t)C(t)\left[\hat{w}_c^{(2)}(t)\phi_c(t)\right]^T\zeta_a(t)\Big).\end{aligned} \tag{1.19}$$

Consider the last term of (1.19)

$$\begin{aligned}-2\hat{w}_c^{(2)}(t)C(t)\left[\hat{w}_c^{(2)}(t)\phi_c(t)\right]^T\zeta_a(t) = \left\|\hat{w}_c^{(2)}(t)\phi_c(t) - \hat{w}_c^{(2)}(t)C(t)\zeta_a(t)\right\|^2 - \\ \left\|\hat{w}_c^{(2)}(t)C(t)\zeta_a(t)\right\|^2 - \left\|\hat{w}_c^{(2)}(t)\phi_c(t)\right\|^2.\end{aligned}$$

After substituting this formula into ΔL_2, we get

$$\Delta L_2(t) = \frac{1}{\gamma_1}\Big(l_a \left\|\phi_a(t)\right\|^2 \left\|\hat{w}_c^{(2)}(t)C(t)\right\|^2 \left\|\hat{w}_c^{(2)}(t)\phi_c(t)\right\|^2 + \left\|\hat{w}_c^{(2)}(t)\phi_c(t) - \hat{w}_c^{(2)}(t)C(t)\zeta_a(t)\right\|^2 - \left\|\hat{w}_c^{(2)}(t)C(t)\zeta_a(t)\right\|^2 - \left\|\hat{w}_c^{(2)}(t)\phi_c(t)\right\|^2\Big). \quad (1.20)$$

Notice that

$$\begin{aligned}
&\left\|\hat{w}_c^{(2)}(t)\phi_c(t) - \hat{w}_c^{(2)}(t)C(t)\zeta_a(t)\right\|^2 - \left\|\hat{w}_c^{(2)}(t)C(t)\zeta_a(t)\right\|^2 \leq \\
&2\left\|\hat{w}_c^{(2)}(t)\phi_c(t)\right\|^2 + \left\|\hat{w}_c^{(2)}(t)C(t)\zeta_a(t)\right\|^2 \leq \\
&2\left\|\left(\tilde{w}_c^{(2)}(t) + w_c^{*(2)}\right)\phi_c(t)\right\|^2 + \left\|\hat{w}_c^{(2)}(t)C(t)\zeta_a(t)\right\|^2 \leq \\
&2\left(\left\|\tilde{w}_c^{(2)}(t)\phi_c(t)\right\| + \left\|w_c^{*(2)}\phi_c(t)\right\|\right)^2 + \left\|\hat{w}_c^{(2)}(t)C(t)\zeta_a(t)\right\|^2 \leq \\
&4\left\|\zeta_c(t)\right\|^2 + 4\left\|w_c^{*(2)}\phi_c(t)\right\|^2 + \left\|\hat{w}_c^{(2)}(t)C(t)\zeta_a(t)\right\|^2. \qquad (1.21)
\end{aligned}$$

Finally we get the following bound for $\Delta L_2(t)$,

$$\begin{aligned}
\Delta L_2(t) \leq \frac{1}{\gamma_1}\Big(&-\left(1 - l_a\left\|\phi_a(t)\right\|^2\left\|\hat{w}_c^{(2)}(t)C(t)\right\|^2\right)\times \\
&\left\|\hat{w}_c^{(2)}(t)\phi_c(t)\right\|^2 + 4\left\|\zeta_c(t)\right\|^2 + 4\left\|w_c^{*(2)}\phi_c(t)\right\|^2 + \left\|\hat{w}_c^{(2)}(t)C(t)\zeta_a(t)\right\|^2\Big), \quad (1.22)
\end{aligned}$$

which completes the proof. □

Remark 6. If we introduce the following normalization for the network's weights $\left\|(\hat{w}_c^{(2)}(t))^T C(t)\right\|^2 = 1$ and fix the weights of the input layer, then applying Lemmas 4 and 5, we can readily obtain the results in [51].

Lemma 7. Under Assumption 3, the first difference of $L_3(t) = \frac{1}{l_c\gamma_2}\operatorname{tr}\left[\left(\tilde{w}_c^{(1)}(t)\right)^T \tilde{w}_c^{(1)}(t)\right]$ is bounded by

$$\begin{aligned}
\Delta L_3(t) \leq \frac{1}{\gamma_2}\Big(&\alpha^2 l_c\left\|\alpha\hat{w}_c^{(2)}(t)\phi_c(t) + r(t) - \hat{w}_c^{(2)}(t-1)\phi_c(t-1)\right\|^2\left\|a(t)\right\|^2\left\|y(t)\right\|^2 + \\
&\alpha\left\|\tilde{w}_c^{(1)}(t)y(t)a^T(t)\right\|^2 + \alpha\left\|\alpha\hat{w}_c^{(2)}(t)\phi_c(t) + r(t) - \hat{w}_c^{(2)}(t-1)\phi_c(t-1)\right\|^2\Big), \quad (1.23)
\end{aligned}$$

where $\gamma_2 > 0$ is a weighting factor and $a(t)$ is a vector, with

$a_i(t) = \frac{1}{2}\left(1 - \phi_{c_i}^2(t)\right)\hat{w}_{c_i}^{(2)}(t)$ for $i = 1 \ldots N_{h_c}$.

Proof. Let us consider the weight update rule of the critic network between input layer and hidden layer in the form

$$\hat{w}_c^{(1)}(t+1) = \hat{w}_c^{(1)}(t) - \alpha l_c \left(\alpha \hat{w}_c^{(2)}(t)\phi_c(t) + r(t) - \hat{w}_c^{(2)}(t-1)\phi_c(t-1)\right)^T B(t), \tag{1.24}$$

where $B_{ij}(t) = \frac{1}{2}(1 - \phi_{c_i}^2(t))\hat{w}_{c_i}^{(2)}(t)y_j(t)$, for $i = 1, \ldots, N_{h_c}, j = 1, \ldots, m+n$.

Following the same approach as earlier, we can express $\tilde{w}_c^{(1)}(t+1)$ by

$$\tilde{w}_c^{(1)}(t+1) = \hat{w}_c^{(1)}(t+1) - w_c^{*(1)} = \tilde{w}_c^{(1)}(t) - \alpha l_c \left(\alpha \hat{w}_c^{(2)}(t)\phi_c(t) + r(t) - \hat{w}_c^{(2)}(t-1)\phi_c(t-1)\right)^T B(t). \tag{1.25}$$

For convenience, we introduce the following notation
$B^T(t)B(t) = y^T(t)a^T(t)a(t)y(t) = \|a(t)\|^2 \|y(t)\|^2$. Then the trace of multiplication can be written as

$$\begin{aligned}\operatorname{tr}\left[\left(\tilde{w}_c^{(1)}(t+1)\right)^T \tilde{w}_c^{(1)}(t+1)\right] &= \left(\tilde{w}_c^{(1)}(t)\right)^T \tilde{w}_c^{(1)}(t) + \alpha^2 l_c^2 \left\|\alpha \hat{w}_c^{(2)}(t)\phi_c(t) + r(t) - \hat{w}_c^{(2)}(t-1)\phi_c(t-1)\right\|^2 B^T(t)B(t) - \\ &2\alpha l_c \left(\alpha \hat{w}_c^{(2)}(t)\phi_c(t) + r(t) - \hat{w}_c^{(2)}(t-1)\phi_c(t-1)\right) B^T(t)\tilde{w}_c^{(1)}(t).\end{aligned} \tag{1.26}$$

Using the property of trace function, that is, the following
$\operatorname{tr}\left(y(t)a^T(t)\tilde{w}_c^{(1)}(t)\right) = \operatorname{tr}\left(\tilde{w}_c^{(1)}(t)y(t)a^T(t)\right)$, we can express the last term of (1.26) as follows:

$$\begin{aligned}&-2\alpha l_c \left(\alpha \hat{w}_c^{(2)}(t)\phi_c(t) + r(t) - \hat{w}_c^{(2)}(t-1)\phi_c(t-1)\right) y(t)a^T(t)\tilde{w}_c^{(1)}(t) = \\ &\alpha l_c \left(\left\|\alpha \hat{w}_c^{(2)}(t)\phi_c(t) + r(t) - \hat{w}_c^{(2)}(t-1)\phi_c(t-1) - \right.\right. \\ &\left.\tilde{w}_c^{(1)}(t)y(t)a^T(t)\right\|^2 - \left\|\tilde{w}_c^{(1)}(t)y(t)a^T(t)\right\|^2 - \\ &\left.\left\|\alpha \hat{w}_c^{(2)}(t)\phi_c(t) + r(t) - \hat{w}_c^{(2)}(t-1)\phi_c(t-1)\right\|^2\right).\end{aligned} \tag{1.27}$$

Therefore, using (1.26), (1.27), the first difference of $L_3(t)$ can be bounded by

$$\Delta L_3(t) \leq \frac{1}{\gamma_2}\Big(\alpha^2 l_c \left\|\alpha\hat{w}_c^{(2)}(t)\phi_c(t) + r(t) - \hat{w}_c^{(2)}(t-1)\phi_c(t-1)\right\|^2 \|a(t)\|^2 \|y(t)\|^2 + \alpha\left\|\tilde{w}_c^{(1)}(t)y(t)a^T(t)\right\|^2 + \alpha\left\|\alpha\hat{w}_c^{(2)}(t)\phi_c(t) + r(t) - \hat{w}_c^{(2)}(t-1)\phi_c(t-1)\right\|^2\Big). \quad (1.28)$$

□

Lemma 8. Under Assumption 3, the first difference of $L_4(t) = \frac{1}{l_a\gamma_3}\operatorname{tr}\left[\left(\tilde{w}_a^{(1)}(t)\right)^T \tilde{w}_a^{(1)}(t)\right]$ is bounded by

$$\Delta L_4(t) \leq \frac{1}{\gamma_3}\Big(l_a\left\|\hat{w}_c^{(2)}(t)\phi_c(t)\right\|^2\left\|\hat{w}_c^{(2)}(t)C(t)D^T(t)\right\|^2 \times \|x(t)\|^2 + \left\|\hat{w}_c^{(2)}(t)\phi_c(t)\right\|^2 + \left\|\hat{w}_c^{(2)}(t)C(t)D^T(t)\right\|^2\left\|\tilde{w}_a^{(1)}(t)x(t)\right\|^2\Big), \quad (1.29)$$

where $\gamma_3 > 0$ is a weighting factor; and $D_{ij}(t) = \frac{1}{2}\left(1 - \phi_{a_i}^2(t)\right)\hat{w}_{a_{ji}}^{(2)}(t)$ for $i = 1\ldots N_{h_a}$ and $j = 1\ldots n$.

Proof. Let us consider the weights from the input layer to the hidden layer of the action network

$$\tilde{w}_a^{(1)}(t+1) = \hat{w}_a^{(1)}(t+1) - w_a^{*(1)} = \tilde{w}_a^{(1)}(t) - l_a\hat{w}_c^{(2)}(t)\phi_c(t)D(t)C^T(t)\left(\hat{w}_c^{(2)}(t)\right)^T x^T(t). \quad (1.30)$$

Let us consider also that

$$\operatorname{tr}\left[(\tilde{w}_a^{(1)}(t+1))^T\tilde{w}_a^{(1)}(t+1)\right] = (\tilde{w}_a^{(1)}(t))^T\tilde{w}_a^{(1)}(t) + l_a^2\left\|\hat{w}_c^{(2)}(t)\phi_c(t)\right\|^2\left\|\hat{w}_c^{(2)}(t)C(t)D^T(t)\right\|^2\|x(t)\|^2 - 2l_a\hat{w}_c^{(2)}(t)C(t)D^T(t)\phi_c^T(t)\left(\hat{w}_c^{(2)}(t)\right)^T\tilde{w}_a^{(1)}(t)x(t). \quad (1.31)$$

We obtained the last term since

$\operatorname{tr}(A^TB + B^TA) = \operatorname{tr}(A^TB) + \operatorname{tr}([A^TB]^T) = 2\operatorname{tr}(A^TB)$ and $\operatorname{tr}(AB) = \operatorname{tr}(BA)$

The last term in (1.30) can be transformed into the form:

$$-2l_a\hat{w}_c^{(2)}(t)C(t)D^T(t)\phi_c^T(t)\left(\hat{w}_c^{(2)}(t)\right)^T\tilde{w}_a^{(1)}(t)x(t)\leq$$
$$l_a\left(\left\|\hat{w}_c^{(2)}(t)\phi_c(t)\right\|^2+\left\|\hat{w}_c^{(2)}(t)C(t)D^T(t)\right\|^2\left\|\tilde{w}_a^{(1)}(t)x(t)\right\|^2\right). \quad (1.32)$$

Based on the last result, we can obtain the upper bound for $\Delta L_4(t)$, which is given in the statement of the lemma:

$$\Delta L_4(t)\leq\frac{1}{\gamma_3}\left(l_a\left\|\hat{w}_c^{(2)}(t)\phi_c(t)\right\|^2\left\|\hat{w}_c^{(2)}(t)C(t)D^T(t)\right\|^2\times\right.$$
$$\left.\|x(t)\|^2+\left\|\hat{w}_c^{(2)}(t)\phi_c(t)\right\|^2+\left\|\hat{w}_c^{(2)}(t)C(t)D^T(t)\right\|^2\left\|\tilde{w}_a^{(1)}(t)x(t)\right\|^2\right). \quad (1.33)$$

□

1.4.3 Stability analysis of the dynamical system

In this section we introduce a candidate of the Lyapunov function for analyzing the dynamical system of estimation error. To this aim, we utilize the following auxiliary function $L=L_1+L_2+L_3+L_4$.

Theorem 9. Let the weights of the critic network and the action network be updated according to the gradient descent algorithm, and assume that the utility function is a bounded semidefinite function. Then under Assumption 3, the errors between the optimal weights w_a^*, w_c^* and their estimates $\hat{w}_a(t)$, $\hat{w}_c(t)$ are uniformly ultimately bounded (UUB), if the following conditions are fulfilled:

$$l_c<\min_t\frac{\gamma_2-\alpha}{\alpha^2\gamma_2\left(\left\|\phi_c(t)\right\|^2+\frac{1}{\gamma_2}\left\|a(t)\right\|^2\left\|y(t)\right\|^2\right)}, \quad (1.34)$$

$$l_a<\min_t\frac{\gamma_3-\gamma_1}{\gamma_3\left\|(\hat{w}_c^2(t))^TC(t)\right\|^2\left\|\phi_a(t)\right\|^2+\gamma_1\left\|\hat{w}_c^{(2)}(t)C(t)D^T(t)\right\|^2\left\|x(t)\right\|^2}. \quad (1.35)$$

Proof. At first, let us collect all terms of $\Delta L(t)$ based on the results of lemmas 4 - 8.

Hence $\Delta L(t)$ is bounded by

$$\Delta L(t) \leq \left\{-\alpha^2 \left\|\zeta_c(t)\right\|^2 - \left(1-\alpha^2 l_c \left\|\phi_c(t)\right\|^2\right) \left\|\alpha \hat{w}_c^{(2)}(t)\phi_c(t) + r(t) - \right. \tag{1.36}$$
$$\left. \hat{w}_c^{(2)}(t-1)\phi_c(t-1)\right\|^2 + \left\|\alpha w_c^{*(2)}\phi_c(t) + r(t) - \hat{w}_c^{(2)}(t-1)\phi_c(t-1)\right\|^2\Big\} +$$
$$\frac{1}{\gamma_1}\left\{-\left(1 - l_a \left\|\phi_a(t)\right\|^2 \left\|\hat{w}_c^{(2)}(t)C(t)\right\|^2\right)\left\|\hat{w}_c^{(2)}(t)\phi_c(t)\right\|^2 + 4\left\|\zeta_c(t)\right\|^2 + \right.$$
$$\left. 4\left\|w_c^{*(2)}\phi_c(t)\right\|^2 + \left\|\hat{w}_c^{(2)}(t)C(t)\zeta_a(t)\right\|^2\right\} + \frac{1}{\gamma_2}\left\{\alpha^2 l_c \left\|\alpha \hat{w}_c^{(2)}(t)\phi_c(t) + \right.\right.$$
$$\left.\left. r(t) - \hat{w}_c^{(2)}(t-1)\phi_c(t-1)\right\|^2 \left\|a(t)\right\|^2 \left\|y(t)\right\|^2 + \alpha\left\|\tilde{w}_c^{(1)}(t)y(t)a^T(t)\right\|^2 + \right.$$
$$\left.\alpha\left\|\alpha \hat{w}_c^{(2)}(t)\phi_c(t) + r(t) - \hat{w}_c^{(2)}(t-1)\phi_c(t-1)\right\|^2\right\} + \frac{1}{\gamma_3}\left\{l_a \left\|\hat{w}_c^{(2)}(t)\phi_c(t)\right\|^2 \times \right.$$
$$\left\|\hat{w}_c^{(2)}(t)C(t)D^T(t)\right\|^2 \left\|x(t)\right\|^2 + \left\|\hat{w}_c^{(2)}(t)\phi_c(t)\right\|^2 +$$
$$\left.\left\|\hat{w}_c^{(2)}(t)C(t)D^T(t)\right\|^2 \left\|\tilde{w}_a^{(1)}(t)x(t)\right\|^2\right\}. \tag{1.37}$$

The first difference of $L(t)$ can be rewritten as

$$\Delta L(t) \leq -(\alpha^2 - \frac{4}{\gamma_1})\left\|\zeta_c(t)\right\|^2 - \left(1-\alpha^2 l_c \left\|\phi_c(t)\right\|^2 - \right.$$
$$\left.\frac{\alpha^2 l_c}{\gamma_2}\left\|a(t)\right\|^2 \left\|y(t)\right\|^2 - \frac{\alpha}{\gamma_2}\right)\left\|\alpha \hat{w}_c^{(2)}(t)\phi_c(t) + r(t) - \right.$$
$$\left.\hat{w}_c^{(2)}(t-1)\phi_c(t-1)\right\|^2 - \left\|\hat{w}_c^{(2)}(t)\phi_c(t)\right\|^2\left(\frac{1}{\gamma_1} - \frac{l_a}{\gamma_1}\left\|\hat{w}_c^{(2)}(t)C(t)\right\|^2 \left\|\phi_a(t)\right\|^2 - \right.$$
$$\left.\frac{l_a}{\gamma_3}\left\|\hat{w}_c^{(2)}(t)C(t)D^T(t)\right\|^2 \left\|x(t)\right\|^2 - \frac{1}{\gamma_3}\right) + \frac{4}{\gamma_1}\left\|w_c^{*(2)}\phi_c(t)\right\|^2 +$$
$$\frac{1}{\gamma_1}\left\|\hat{w}_c^{(2)}(t)C(t)\right\|^2 \left\|\zeta_a(t)\right\|^2 + \left\|\alpha w_c^{*(2)}\phi_c(t) + r(t) - \hat{w}_c^{(2)}(t-1)\phi_c(t-1)\right\|^2 +$$
$$\frac{\alpha}{\gamma_2}\left\|\tilde{w}_c^{(1)}(t)y(t)\right\|^2 \left\|a(t)\right\|^2 + \frac{1}{\gamma_3}\left\|\hat{w}_c^{(2)}(t)C(t)D^T(t)\right\|^2 \left\|\tilde{w}_a^{(1)}(t)x(t)\right\|^2. \tag{1.38}$$

To guarantee that the second and third terms in the last expression are negative, we need to choose learning rates in the following manner

$$1 - \alpha^2 l_c \left\|\phi_c(t)\right\|^2 - \frac{\alpha^2 l_c}{\gamma_2}\left\|a(t)\right\|^2 \left\|y(t)\right\|^2 - \frac{\alpha}{\gamma_2} > 0. \tag{1.39}$$

Therefore,

$$l_c < \min_t \frac{\gamma_2 - \alpha}{\alpha^2 \gamma_2 \left(\left\|\phi_c(t)\right\|^2 + \frac{1}{\gamma_2}\left\|a(t)\right\|^2 \left\|y(t)\right\|^2\right)}. \tag{1.40}$$

In particular, when $\gamma_2 > \alpha$, similarly, for the action network we obtain:

$$\frac{1}{\gamma_1} - \frac{1}{\gamma_1} l_a \left\| (\hat{w}_c^{(2)}(t))^T C(t) \right\|^2 \left\| \phi_a(t) \right\|^2 - \frac{l_a}{\gamma_3} \left\| D(t) C^T(t) \hat{w}_c^{(2)}(t) \right\|^2 \left\| x(t) \right\|^2 - \frac{1}{\gamma_3} > 0,$$

$$l_a < \min_t \frac{\gamma_3 - \gamma_1}{\gamma_3 \left\| (\hat{w}_c^{(2)}(t))^T C(t) \right\|^2 \left\| \phi_a(t) \right\|^2 + \gamma_1 \left\| \hat{w}_c^{(2)}(t) C(t) D^T(t) \right\|^2 \left\| x(t) \right\|^2}. \quad (1.41)$$

In particular, when $\gamma_3 > \gamma_1$, notice that the norm of the sum can be bounded by the sum of the norms, thus we have the following

$$\begin{aligned} &\left\| \alpha w_c^{*(2)} \phi_c(t) + r(t) - \hat{w}_c^{(2)}(t-1) \phi_c(t-1) \right\|^2 \leq \\ &4\alpha^2 \left\| w_c^{*(2)} \phi_c(t) \right\|^2 + 4r^2(t) + 2 \left\| \hat{w}_c^{(2)}(t-1) \phi_c(t-1) \right\|^2. \end{aligned} \quad (1.42)$$

Let $\overline{C}$, $\overline{w}_{a1}$, $\overline{w}_{a2}$, $\overline{w}_{c1}$, $\overline{\phi}_a$, $\overline{y}$, $\overline{x}$, $\overline{a}$, $\overline{D}$ be upper bounds of $C(t)$, $\tilde{w}_a^{(1)}(t)$, $\tilde{w}_a^{(2)}(t)$, $\tilde{w}_c^{(1)}(t)$, $\phi_a(t)$, $y(t)$, $x(t)$, $a(t)$, $D(t)$, respectively; while $\overline{w}_{c2}$=max $\{w_c^{*(2)}, w_{c2}^{(M)}\}$, where $w_{c2}^{(M)}$ is the upper bound of $\hat{w}_c^{(2)}(t)$. Finally, we obtain the following bound:

$$\begin{aligned} &\frac{4}{\gamma_1} \left\| w_c^{*(2)} \phi_c(t) \right\|^2 + \frac{1}{\gamma_1} \left\| \hat{w}_c^{(2)}(t) C(t) \right\|^2 \left\| \zeta_a(t) \right\|^2 + \\ &\left\| \alpha w_c^{*(2)} \phi_c(t) + r(t) - \hat{w}_c^{(2)}(t-1) \phi_c(t-1) \right\|^2 + \\ &\frac{\alpha}{\gamma_2} \left\| \tilde{w}_c^{(1)}(t) y(t) \right\|^2 \left\| a(t) \right\|^2 + \frac{1}{\gamma_3} \left\| \hat{w}_c^{(2)}(t) C(t) D^T(t) \right\|^2 \left\| \tilde{w}_a^{(1)}(t) x(t) \right\|^2 \leq \\ &\left(\frac{4}{\gamma_1} + 4\alpha^2 + 2 \right) (\overline{w}_{c2} \overline{\phi}_c)^2 + 4\overline{r}^2 + \frac{1}{\gamma_1} (\overline{w}_{c2} \overline{C}\, \overline{w}_{a2} \overline{\phi}_a)^2 + \frac{\alpha}{\gamma_2} (\overline{w}_{c1} \overline{y}\, \overline{a})^2 + \\ &\frac{1}{\gamma_3} (\overline{w}_{c2} \overline{C}\, \overline{D} \overline{w}_{a1} \overline{x})^2 = M. \end{aligned} \quad (1.43)$$

Therefore, if $\alpha^2 - \frac{4}{\gamma_1} > 0$, that is, $\gamma_1 > \frac{4}{\alpha^2}$ and $\alpha \in (0, 1)$, then for l_a and l_c with constraints from (1.40), (1.41) and $\left\| \zeta_c(t) \right\|^2 > \frac{M}{\alpha^2 - \frac{4}{\gamma_1}}$, we get $\Delta L(t) < 0$. Based on Theorem 1, we deerive that the system of estimation errors is ultimately uniformly bounded. □

Remark 10. It is to be emphasized that the present results do not pose any

restrictions on the discount factor α, as opposed to the results found in [51]. The choice of the discount factor depends on the given problem. A constraint on the discount factor can reduce the performance of the ADP control. Also it should be mentioned that parameters γ_1, γ_2, and γ_3 allow fine-tuning of the learning in different layers of the networks, thus leading to further improved performance.

As the above remark says it is possible to expect a difference between the control design considered in this chapter and one studied in [51]. A comparison of these two methods was performed in [66]. Our study showed that two control algorithms have nearly the same performance in controlling a linear system. However, our algorithm, which uses universal function approximators, significantly outperforms the one considered by Liu et al. in the case of a nonlinear system.

CHAPTER 2

RANDOM GRAPH MODEL $G_{\mathbb{Z}_N^2,P_D}$ AND ITS MAIN PROPERTIES

In this chapter we introduce a model of random graph coupled with a lattice. The probabilities of random edges are defined to get a sparser graph with respect to additional random edges. We study several properties, including diameter and degree distribution.

This chapter is a joint work with Svante Janson, Robert Kozma, and Miklós Ruszinkó; and is partly based on our submitted paper, [43].

2.1 Background on random graphs with distant-dependent probabilities

In general, there are not many models with the property that the probability of an edge depends on the distance between a pair of vertices. Schulman [63] introduced a long-range percolation graph (LRPG) where vertices are defined on at most a countable metric space. In his model, the probability of an edge between a pair of vertices is inversely proportional to the distance between the pair.

Benjamini and Berger considered LRPG on a finite discrete n-circle [17]. In their settings vertices of distance one are connected with probability one and with probability $1 - exp(-\beta/|v_i - v_j|^s)$ otherwise, where $v_i, v_j \in 1, \ldots, n$. From the definition of the random graph it follows that the graph is connected and the appropriate question to ask is; what is the diameter of the graph? This question was studied by Benjamini and Berger, and Coppersmith, Gamarnik and Sviridenko in [17, 29] and sharp results were derived for different regimes with respect to s.

2.2 Random graph model

We consider a random graph G that is built as follows. We start with the $\mathbb{Z}^2$ lattice over a $(N+1) \times (N+1)$ grid; for the sake of simplicity we assume periodic boundary conditions. Thus, we have a torus $\mathbb{T}^2 = (\mathbb{Z}/N\mathbb{Z})^2$, with the short notation $\mathbb{Z}_N^2$. The set of vertices of G consists of all vertices of $\mathbb{Z}_N^2$, in total N^2 vertices. All

the edges from the torus $\mathbb{Z}_N^2$ are included in the graph G. In addition, we introduce random edges as follows; for every pair of vertices we assign an edge with probability that depends on the graph distance d between the two vertices, i.e., d is the length of the shortest path between the given pair of vertices in the torus grid. Accordingly, the probability of a long edge is described as follows:

$$p_d = \mathbb{P}\left((u,v) \in E(G) \;\middle|\; dist(u,v) = d\right) = \frac{c}{N} \times d^{-\alpha}, \tag{2.1}$$

where c and α are positive constants, $d > 1$ (no multiple edges are allowed between any pair of vertices) and N is large enough so that each $p_d < 1$. We assume $\alpha = 1$ throughout this study. We will denote this model the $G_{\mathbb{Z}_N^2, p_d}$ graph. The edges of the torus are called *short edges*, while the randomly added ones are called *long edges*.

We will use the following standard notation; for non-negative sequences a_m and b_m, $a_m = O(b_m)$ if $a_m \le cb_m$ holds for some constant $c > 0$ and every m; $a_m = \Theta(b_m)$ if both $a_m = O(b_m)$ and $b_m = O(a_m)$ hold; $a_m \sim b_m$ if $\lim_{m\to\infty} a_m/b_m = 1$; $a_m = o(b_m)$ if $\lim_{m\to\infty} a_m/b_m = 0$. A sequence of events A_n occurs with high probability, *whp*, if the probability $\mathbb{P}(A_n) = 1 - o(1)$.

2.3 Properties of $G_{\mathbb{Z}_N^2, p_d}$

First notice that the expected number of long edges $E_\ell \subseteq E(G_{\mathbb{Z}_N^2, p_d})$ is proportional to N^2.

Claim 11. $\mathbb{E}(|E_\ell|) \sim (2c \ln 2)N^2$, i.e., $\lim_{N\to\infty} \dfrac{\mathbb{E}(|E_\ell|)}{2cN^2 \ln 2} = 1$.

Proof. Indeed, the number of vertices $|\Lambda_d|$ in $\mathbb{Z}_N^2$ which are exactly at distance d from a fixed vertex is

$$|\Lambda_d| = \begin{cases} 4d, & 1 \le d \le \lfloor N/2 \rfloor \\ 4(N-d), & \lfloor N/2 \rfloor < d \le N \end{cases}$$

for N odd, and

$$|\Lambda_d| = \begin{cases} 4d, & 1 \leq d < N/2 \\ 4d-2, & d = N/2 \\ 4(N-d), & N/2 < d < N \\ 1, & d = N \end{cases}$$

for N even. The number of pairs of vertices in $\mathbb{Z}_N^2$ having distance d is $\frac{N^2|\Lambda_d|}{2}$. Therefore, for N odd

$$\begin{aligned} \mathbb{E}(|E_\ell|) &= \sum_{d=2}^{N} \frac{N^2|\Lambda_d|}{2} \frac{c}{Nd} = \sum_{d=2}^{N/2} \frac{4N^2 d}{2} \frac{c}{Nd} + \sum_{d=N/2+1}^{N} \frac{4N^2(N-d)}{2} \frac{c}{Nd} \\ &= (2c\ln 2)N^2 + O(N) \sim (2c\ln 2)N^2. \end{aligned} \tag{2.2}$$

For N even a similar computation gives the same result.

□

2.3.1 Degree distribution

The degree distribution of a vertex $v \in G_{\mathbb{Z}_N^2, p_d}$ with respect to long edges can be approximated by a Poisson distribution. Let W be the random variable describing the degree of a particular vertex v considering long edges only. Then clearly, the degree of a vertex $v \in G_{\mathbb{Z}_N^2, p_d}$ considering the short edges too, is $W + 4$.

Lemma 12. The probability that a vertex has degree k considering only the long edges is given by

$$\mathbb{P}(W = k) = \sum_{k_2 + \ldots + k_N = k} \prod_{i=2}^{N} \binom{|\Lambda_i|}{k_i} \left(\frac{c}{Ni}\right)^{k_i} \left(1 - \frac{c}{Ni}\right)^{|\Lambda_i| - k_i}. \tag{2.3}$$

The total variation distance

$$d_{TV}\left(\mathcal{L}(W), \mathrm{Po}(\lambda)\right) = \frac{1}{2} \sum_{j \geq 0} |\mathbb{P}(W = j) - \mathbb{P}(Y = j)| = O(1/N), \tag{2.4}$$

where the random variable Y has a Poisson distribution $\mathrm{Po}(\lambda)$, with $\lambda = 4c\ln 2$.

Proof. The probability of the event A_i that a vertex has k_i edges of length i is clearly

$$\mathbb{P}(A_i) = \binom{|\Lambda_i|}{k_i} \left(\frac{c}{Ni}\right)^{k_i} \left(1 - \frac{c}{Ni}\right)^{|\Lambda_i|-k_i} \tag{2.5}$$

Therefore, the probability that a vertex has degree exactly to the value of k is

$$\begin{aligned}\mathbb{P}(W = k) = \mathbb{P}\left(\bigcup_{k_2+\ldots+k_N=k} \bigcap_{i=2}^{N} A_i\right) &= \sum_{k_2+\ldots+k_N=k} \prod_{i=2}^{N} \mathbb{P}(A_i) \\ &= \sum_{k_2+\ldots+k_N=k} \prod_{i=2}^{N} \binom{|\Lambda_i|}{k_i} \left(\frac{c}{Ni}\right)^{k_i} \left(1 - \frac{c}{Ni}\right)^{|\Lambda_i|-k_i}. \end{aligned} \tag{2.6}$$

The last expression is not very convenient to use, however, a standard Poisson approximation can be given using Le Cam's argument [47], see also for example [14]. Let us choose an arbitrary vertex v and enumerate the other $N^2 - 5$ vertices by u_i, $i = 1, \ldots, N^2 - 5$, excluding the nearest neighbors, i.e., vertices at distance one. Note that the long edges that connect the vertex v to other vertices of the graph are independent 0–1 random variables with a Bernoulli distribution, $\mathrm{Be}(p_i)$. In other words, let $I_i = 1$ be the event that there is an edge between vertices v and u_i, so that $\mathbb{P}(I_i = 1) = p_i$ and $\mathbb{P}(I_i = 0) = 1 - p_i$, where p_i may in general vary for a different i. Consider now the degree $W = \sum_{i=1}^{N^2-5} I_i$ of the vertex v. Let

$$\lambda_1 = \sum_{i=1}^{N^2-5} p_i = 4c \ln 2 + O(1/N),$$

where the last equality follows from (2.2). By triangle inequality,

$$d_{TV}\left(\mathcal{L}(W), \mathrm{Po}(\lambda)\right) \le d_{TV}\left(\mathcal{L}(W), \mathrm{Po}(\lambda_1)\right) + d_{TV}\left(\mathrm{Po}(\lambda_1), \mathrm{Po}(\lambda)\right) \tag{2.7}$$

The first term, by Le Cam [47], see also [14, Theorem 2.M], is at most

$$\begin{aligned}\sum_{i=1}^{N^2-5} p_i^2 &= \sum_{d=2}^{N} |\Lambda_d| p_d^2 \le \sum_{d=1}^{N} |\Lambda_d| p_d^2 = \sum_{d=1}^{N/2} 4d \left(\frac{c}{Nd}\right)^2 \\ &+ \sum_{d=N/2+1}^{N} 4(N-d) \left(\frac{c}{Nd}\right)^2 \le \sum_{d=1}^{N} 4d \left(\frac{c}{Nd}\right)^2 = O\left(\frac{\ln N}{N^2}\right). \end{aligned} \tag{2.8}$$

and by Theorem 1.C (i) in [14]

$$d_{TV}\left(\mathrm{Po}(\lambda_1), \mathrm{Po}(\lambda)\right) = O\left(|\lambda_1 - \lambda|\right) = O\left(\frac{1}{N}\right). \tag{2.9}$$

□

Clearly, Lemma 12 also implies that in (2.4) each term satisfies

$$|\mathbb{P}(W = j) - \mathbb{P}(Y = j)| = O(1/N).$$

2.3.2 The diameter of $G_{\mathbb{Z}_N^2, p_d}$

Next we show that the addition of long edges to the torus grid significantly reduces its diameter in the number of vertices from linear to logarithmic.

Theorem 13. There exist constants C_1, C_2, which depend on c only, such that for the diameter $D(G_{\mathbb{Z}_N^2, p_d})$ the following hold:

$$\lim_{N\to\infty} \mathbb{P}\left(C_1 \log N \leq D(G_{\mathbb{Z}_N^2, p_d}) \leq C_2 \log N\right) = 1,$$

that is, $D(G_{\mathbb{Z}_N^2, p_d}) = \Theta(\log N),\ whp.$

Proof. The lower bound is trivial. The expected degree $\mathbb{E}(d(v))$ of a vertex v is a constant $k = k(c)$ by Claim 11. Thus, the expected number of vertices A_m we can reach in at most $m \geq 0$ steps from a given vertex v is less than or equal to $1 + \sum_{i=1}^{m} k(k-1)^{i-1}$. For $m \geq 3$, this is less than k^m, and thus, by Markov's inequality,

$$\mathbb{P}(A_m \geq N^2) \leq \frac{\mathbb{E}(A_m)}{N^2} \leq \frac{k^m}{N^2}. \tag{2.10}$$

If we choose $m \leq C_1 \log N$ with C_1 sufficiently small, the probability in (2.10) tends to zero, i.e., even from a given vertex v we cannot reach all vertices within distance $C_1 \log N$. Hence, $C_1 \log N$ bounds the diameter from below.

To prove the upper bound, let us partition the vertices of $G_{\mathbb{Z}_N^2,p_d}$ into consecutive $k \times k$ blocks $B_{ij}, i, j = 1, \ldots, \frac{N}{k}$, where k is a constant $k(c)$ to be chosen later. (For simplicity, we will assume that everywhere divisibility holds during the proof; otherwise we let some blocks be $(k+1) \times (k+1)$.) Define the graph G' as follows; the vertices are the blocks, and two blocks $B_{i,j}$ and $B_{k,\ell}$, $(1, \leq i, j, k, \ell \leq N/k)$ are connected iff there is a long edge from a vertex of $B_{i,j}$ to a vertex of $B_{k,\ell}$ in $G_{\mathbb{Z}_N^2,p_d}$. We obtain a random graph on N^2/k^2 vertices where the edge probabilities can be obtained from the ones of $G_{\mathbb{Z}_N^2,p_d}$. For an arbitrary pair of vertices $B_{i,j}$ and $B_{k,\ell}$, the probability of the event $A_{i,j;k,l}$ that they are connected is bounded from below by the probability, that two blocks which are most distant from each other in $\mathbb{Z}_N^2$ are connected. Therefore, for large N,

$$\begin{aligned}
\mathbb{P}(A_{i,j;k,l}) &\geq \mathbb{P}(A_{1,1;N/(2k),N/(2k)}) = 1 - \mathbb{P}(\overline{A_{1,1,\frac{N}{2k},\frac{N}{2k}}}) \\
&\geq 1 - (1-p_N)^{k^4} = 1 - \left(1 - \frac{c}{N^2}\right)^{k^4} \\
&\geq 1 - e^{-ck^4/N^2} \geq ck^4/2N^2.
\end{aligned}$$

For the second inequality we chose the two most distant vertices from each block, and the last one follows from $e^x \leq 1 + x/2$ for $x < 0$ sufficiently close to 0.

By, for example, Theorem 9.b, in the seminal paper of Erdős and Rényi [32] there is a constant c_1 such that in the Erdős-Rényi random graph $G_{n,p}$ with $p = c_1/n$ there is a giant component on at least, say, $n/2$ vertices, *whp.* Choosing

$$k \geq (2c_1/c)^{1/2}$$

we get that the probability that G' has an edge for an arbitrary pair of vertices is at least

$$ck^4/2N^2 \geq c_1 k^2/N^2.$$

Since the edges of G' are chosen independently, it will contain a giant component on

at least $N^2/2k^2$ vertices, *whp*. The diameter of the giant component of $G_{n,p}$ with $p = c_1/n$ is known to be of the order of $O(\log n)$, *whp*. (See, e.g. Table 1 in [28].)

First, assume that vertices $u, v \in G_{\mathbb{Z}_N^2, p_d}$ are contained in blocks $B(u)$ and $B(v)$ which are vertices of the giant component in G'. Find the shortest path, say, $B(u) = B(x_0), B(x_1), B(x_2), \ldots, B(x_m) = B(v)$, between $B(u)$ and $B(v)$ in G'. Let (x_0, x_1), (x'_1, x_2), (x'_2, x_3), $\ldots$, (x'_{m-1}, x_m), $x_i, x'_i \in B(x_i)$ be the edges in $G_{\mathbb{Z}_N^2, p_d}$ inducing this path in G'.

Now go from u to x_0 in $B(u)$ along short ($\mathbb{Z}^2$) edges. Jump from x_0 to x_1, then go from x_1 to x'_1 in $B(x_1)$ along short edges. After that, jump from x_1 to x'_2, and so on. The total length of the path from u to v, will be at most

$$m + 2k(m+1) \leq (2k+1)(m+1).$$

Indeed, we make m jumps, and within each block we make at most $2k$ steps along short edges. Since $m = O(\log N)$, *whp*, the proof of this case is completed.

Next we show that, *whp,* every vertex $v \in G_{\mathbb{Z}_N^2, p_d}$ is close to some block B of the giant component in G'. Indeed, by symmetry, the set A of vertices in the giant component can be any set of vertices of the same size, with the same probability. Therefore, one can regard A as a uniformly random subset on at least half of the vertices in G'.

For some large constant D, the number of vertices with distance at most $D\sqrt{\log_2 N}$ from a fixed vertex v in $\mathbb{Z}^2$ is

$$\sum_{d=1}^{D\sqrt{\log_2 N}} 4d \geq 4D^2 \log_2 N,$$

i.e., this neighborhood contains a vertex from at least

$$\frac{4D^2 \log_2 N}{k^2}$$

blocks. Since A contains at least half of the vertices in G', the probability that none

of those blocks is in A is

$$\leq 2^{-\frac{4D^2 \log_2 N}{k^2}} = N^{-4D^2/k^2}.$$

Therefore, the probability that there is a vertex $v \in G_{\mathbb{Z}^2_N, p_d}$ for which there is no vertex u within distance $D\sqrt{\log_2 N}$ such that $B(u) \in A$ is

$$\leq N^2 \cdot N^{-4D^2/k^2} < N^{-2},$$

assuming that D is large enough.

Now, consider two arbitrary vertices $u, v \in G_{\mathbb{Z}^2_N, p_d}$. If one, or neither of them is in block from A, then, *whp,* each of them can reach a block from A within $D\sqrt{\log_2 N}$ steps in $\mathbb{Z}^2$, and then proceed as in case $B(u), B(v) \in A$. Since the number of additional steps *whp* is $O(\sqrt{\log N})$, the proof is finished. □

CHAPTER 3

BOOTSTRAP PERCOLATION ON $G_{\mathbb{Z}_N^2,P_D}$ WITH ONE TYPE OF VERTICES

In this chapter we consider bootstrap percolation with one type of vertices on random graph $G_{\mathbb{Z}_N^2,p_d}$ defined in Chapter 2. We prove sharp thresholds on critical probabilities for different values of k with a k-threshold rule.

This chapter is partly based on joint work with Svante Janson, Robert Kozma, and Miklós Ruszinkó, [43].

3.1 Recent developments in the theory of bootstrap percolation

During the last decade, several important results on bootstrap percolation defined on random graphs were derived. In particular, bootstrap percolation has been studied on Erdős-Rényi random graph $G_{n,p}$ in [42], where percolation is defined with respect to the size a of the set of initially active vertices. Results include sharp threshold for phase transition for parameters p and a, and results for the time t required to the termination of the bootstrap percolation process.

Turova and Vallier[69] considered bootstrap percolation over the combination of the lattice $\mathbb{Z}^d$ and the random graph $G_{n,p}$, where the edges of $\mathbb{Z}^d$ and $G_{n,p}$ are selected with probability q and p, respectively. Sharp threshold for phase transition was derived. These authors got asymptotic results for the time when the bootstrap percolation process stops.

3.2 Non-monotonous bootstrap percolation

Let us begin with the definition of a stochastic process on the random graph we built in Chapter 2. Each vertex is described by its *state*. The state of a vertex can be either active or inactive. At the beginning the state of a vertex is chosen independently at random, so that a vertex is active with probability p.

Let $A(t)$ denote the set of all active vertices at time t. We also define a potential function $\chi_v(t)$ for each vertex v such that $\chi_v(t) = 1$ if vertex v is active at time t, and $\chi_v(t) = 0$ if v is inactive. Therefore, $A(t) = \{v \in V(G_{\mathbb{Z}_N^2,p_d}) \mid \chi_v(t) = 1\}$. Let $A(0)$ be a random subset of active vertices, each is activated at the beginning with probability p, independently of others. Each vertex may change its activity based on the states of its neighbors based on the following non-monotone k-threshold rule

$$\chi_v(t+1) = \mathbb{1}\left(\sum_{u \in N(v)} \chi_u(t) \geq k\right), \tag{3.1}$$

where $N(v)$ denotes the closed neighborhood of the vertex v; and $\mathbb{1}$ is the indicator function. Here k is a nonnegative integer that specifies a threshold required for the vertex to be active at the next time step.

It is important to note that the set of active vertices does not necessarily grow monotonically during the process, whereas monotonicity is usually assumed in bootstrap percolation. The above rule says that a vertex will be active at the next time step if it has at least k active neighbors including itself. We assume for simplicity that k is not greater than 3. Notice that if there are only local edges, the case $k = 3$ yields bootstrap percolation with majority rule. The choice of small k is motivated by the fact that there are vertices with degree 4 with positive probability. Therefore, if k could be 5 or more, then there would be vertices that cannot become active unless they were activated at the beginning.

3.3 Mean-field approximation of the process

For simplicity we consider here the mean-field (MF) approximation of the model. The mean-field approximation assumes that the activation and degrees of the various nodes are well-mixed; hence we ignore any dependencies between activation and vertex degrees, as well as any dependencies between the state of a vertex and the state of its neighbors [10]. Effectively, we sample a new set of neighbors at each step. This, in particular, implies that the MF approximation does

not depend on the structure of the graph but only on the degree distribution and on the cardinality of $A(t)$. Thus, the transition probabilities from one state to another depend only on the number of active nodes. Furthermore, we assume that the vertices are activated independently of each other, ignoring the small dependencies between degrees and activities for different vertices.

3.3.1 Phase transition in mean-field model

Let $\rho_t = A(t)/N^2$, where N^2 is the size of the graph. Clearly, $\rho_t \in [0, 1]$ and it defines the density of active nodes at time t.

The mean-field analysis is an analytical approach of finding phase transitions in a stochastic process by averaging the system over space. Thus, the mean-field model reduces the analysis of a system with distributed components to a system with a single component. Let $f(\rho_t)$ denote the conditional mean of ρ_{t+1} given ρ_t, for the mean-field approximation. The main task of the mean-field approximation is to find solutions to the $x = f(x)$, where the solutions of this equation are called fixed points. This approach is based on the observation that the critical behavior of the original system often occurs near the unstable fixed points of mean-field model [19, 68]. A fixed point is called stable if it attracts all the trajectories that start from some neighborhood of the fixed point. Otherwise, a fixed point is unstable. For a discrete time one-dimensional dynamical system, if $f(x)$ is continuously differentiable in an open neighborhood of a fixed point x_0, a sufficient condition for x_0 to be stable or unstable is $|f'(x_0)| < 1$ or $|f'(x_0)| > 1$, respectively; see, e.g., [39].

Let $\mathrm{Bin}(n, p)$ be a binomial random variable. Then the density ρ_t in the mean-field model satisfies the stochastic recursion defined in Lemma 14. Recall from Chapter 2 that $\deg(v)$ denotes the degree with respect to the long edges only in $G_{\mathbb{Z}_N^2, p_d}$, so the total degree of a vertex v is $\deg(v) + 4$.

Lemma 14. For the mean-field approximation of the process on $G_{\mathbb{Z}_N^2, p_d}$ with N^2

vertices, ρ_t is a Markov process given by

$$N^2\rho_{t+1} = \mathrm{Bin}(N^2\rho_t, f^+(\rho_t)) + \mathrm{Bin}(N^2(1-\rho_t), f^-(\rho_t)), \tag{3.2}$$

where

$$f^+(x) = \sum_{n=4}^{N^2-1} \mathbb{P}\left(\deg(v) = n-4\right) \sum_{i=k}^{n+1} \binom{n}{i-1} x^{i-1}(1-x)^{n-i+1}, \tag{3.3}$$

$$f^-(x) = \sum_{n=4}^{N^2-1} \mathbb{P}\left(\deg(v) = n-4\right) \sum_{i=k}^{n} \binom{n}{i} x^{i}(1-x)^{n-i}. \tag{3.4}$$

Moreover, given ρ_t, ρ_{t+1} has mean $f(\rho_t)$ and variance $g(\rho_t)/N^2$ where

$$f(x) = xf^+(x) + (1-x)f^-(x), \tag{3.5}$$

$$g(x) = xf^+(x)(1-f^+(x)) + (1-x)f^-(x)(1-f^-(x)). \tag{3.6}$$

Proof. Clear, since in the MF approximation, each vertex is assumed to have $\deg(v)+4$ neighbors, each is active with probability ρ_t, independently of each other and of $\deg(v)$; furthermore, different vertices are regarded as independent. □

Remark 15. In our model, the state of a vertex at the next time step is deterministic given the number of active vertices in the closed neighborhood. More generally, one can consider a model where an active (inactive) vertex with i active neighbors is activated with some probability p_i^+ (p_i^-), where $p_i^\pm$ are some given probabilities. In this more general case, (3.3)–(3.4) become

$$f^+(x) = \sum_{n=4}^{N^2-1} \mathbb{P}\left(\deg(v) = n-4\right) \sum_{i=1}^{n+1} p_i^+ \binom{n}{i-1} x^{i-1}(1-x)^{n-i+1}, \tag{3.7}$$

$$f^-(x) = \sum_{n=4}^{N^2-1} \mathbb{P}\left(\deg(v) = n-4\right) \sum_{i=0}^{n} p_i^- \binom{n}{i} x^{i}(1-x)^{n-i}. \tag{3.8}$$

Lemma 14 shows that the conditional variance of ρ_{t+1} is $g(\rho_t)/N^2 = O(N^{-2})$; thus ρ_{t+1} is well concentrated for large N, and we can approximate ρ_{t+1} by the mean $f(\rho_t)$.

The function $f(\cdot)$ given by (3.5) can be simplified to

$$\begin{aligned} f(x) &= xf^+(x) + (1-x)f^-(x) \\ &= \sum_{n=4}^{N^2-1} \mathbb{P}\left(\deg(v) = n-4\right) \sum_{i=k}^{n+1} \binom{n}{i-1} x^i (1-x)^{n-i+1} \\ &\quad + \sum_{n=4}^{N^2-1} \mathbb{P}\left(\deg(v) = n-4\right) \sum_{i=k}^{n} \binom{n}{i} x^i (1-x)^{n-i+1} \\ &= \sum_{n=4}^{N^2-1} \mathbb{P}\left(\deg(v) = n-4\right) \left(\sum_{i=k}^{n+1} \binom{n+1}{i} x^i (1-x)^{n-i+1} \right). \end{aligned} \tag{3.9}$$

This can also be seen directly, since if $\deg(v) = n-4$ with respect to the long edges, then the closed neigborhood of v contains $n+1$ vertices, of which k have to be active for activation of v, and in the MF approximation, these $n+1$ vertices are active independently of each other.

In Section 2.3.1 we showed that the degree distribution can be approximated by Poisson $\mathrm{Po}(\lambda)$ distribution. We use the last fact to approximate $f(x)$. Consider the function

$$\bar{f}(x) = \bar{f}_k(x) = \sum_{n=4}^{\infty} \frac{e^{-\lambda}\lambda^{n-4}}{(n-4)!} \sum_{i=k}^{n+1} \binom{n+1}{i} x^i (1-x)^{n-i+1}. \tag{3.10}$$

The difference between $f(x)$ and $\bar{f}(x)$ can be bounded by

$$\begin{aligned} |f(x) - \bar{f}(x)| &\le \sum_{n=4}^{\infty} \left| \mathbb{P}\left(\deg(v) = n-4\right) - \frac{e^{-\lambda}\lambda^{n-4}}{(n-4)!} \right| \sum_{i=k}^{n+1} \binom{n+1}{i} x^i (1-x)^{n-i+1} \\ &\le \sum_{n=4}^{\infty} \left| \mathbb{P}\left(\deg(v) = n-4\right) - \frac{e^{-\lambda}\lambda^{n-4}}{(n-4)!} \right| = O\left(\frac{1}{N}\right) \end{aligned} \tag{3.11}$$

where the last equality follows from Lemma 12.

3.3.2 Critical initialization probability for various k values

We rewrite $\bar{f} = \bar{f}_k$ defined in (3.10) as

$$\bar{f}_k(x) = \sum_{n=0}^{\infty} \frac{e^{-\lambda}\lambda^{n}}{n!} \left(\sum_{i=k}^{n+5} \binom{n+5}{i} x^i (1-x)^{n+5-i} \right). \tag{3.12}$$

For $k = 0, 1, 2$ and 3, respectively, the internal sums in (3.12) are

$$\sum_{i=0}^{n+5} \binom{n+5}{i} x^i (1-x)^{n+5-i} = 1, \tag{3.13}$$

$$\sum_{i=1}^{n+5} \binom{n+5}{i} x^i (1-x)^{n+5-i} = 1 - (1-x)^{n+5}, \tag{3.14}$$

$$\sum_{i=2}^{n+5} \binom{n+5}{i} x^i (1-x)^{n+5-i} = 1 - (1-x)^{n+5} - (n+5)(1-x)^{n+4}x, \tag{3.15}$$

$$\sum_{i=3}^{n+5} \binom{n+5}{i} x^i (1-x)^{n+5-i} = 1 - (1-x)^{n+5} - (n+5)(1-x)^{n+4}x - \frac{(n+5)(n+4)}{2}(1-x)^{n+3}x^2. \tag{3.16}$$

Hence, (3.12) yields, by simple calculations,

$$\bar{f}_0(x) = \sum_{n=0}^{\infty} \frac{e^{-\lambda}\lambda^n}{n!} = 1, \tag{3.17}$$

$$\bar{f}_1(x) = \sum_{n=0}^{\infty} \frac{e^{-\lambda}\lambda^n}{n!} \left(1 - (1-x)^{n+5}\right) = 1 - e^{-\lambda x}(1-x)^5, \tag{3.18}$$

$$\bar{f}_2(x) = \sum_{n=0}^{\infty} \frac{e^{-\lambda}\lambda^n}{n!} \left(1 - (1-x)^{n+5} - (n+5)(1-x)^{n+4}x\right) \tag{3.19}$$

$$= 1 - e^{-\lambda x}\left((1-x)^5 + 5x(1-x)^4 + \lambda x(1-x)^5\right),$$

$$\bar{f}_3(x) = \sum_{n=0}^{\infty} \frac{e^{-\lambda}\lambda^n}{n!} \left(1 - (1-x)^{n+5} - (n+5)(1-x)^{n+4}x - \frac{(n+5)(n+4)}{2}(1-x)^{n+3}x^2\right) \tag{3.20}$$

$$= 1 - e^{-\lambda x}\left((1-x)^5 + 5x(1-x)^4 + \lambda x(1-x)^5 + \frac{\lambda^2}{2}x^2(1-x)^5 + 5\lambda x^2(1-x)^4 + 10x^2(1-x)^3\right).$$

Proposition 16. Let $\bar{f}_k(x) : [0,1] \to [0,1]$ be a family of maps for $k = 0, 1, 2, 3$ defined by (3.17) - (3.20). These maps have the following fixed points:

(i) for $k = 0$ the only fixed point is 1 and it is stable.

(ii) for $k = 1$ there are two fixed points: 1 is stable and 0 is unstable.

(iii) for $k = 2$ there are three fixed points: 0 and 1 are stable and $x_2(\lambda) \in (0, 1)$ is unstable;

(iv) for $k = 3$ there are three fixed points: 0 and 1 are stable and $x_3(\lambda) \in (0, 1)$ is unstable.

Proof. For $k = 0$, the equation $\bar{f}_0(x) = x$ reduces just to

$$x = 1. \tag{3.21}$$

In this case the fixed point $x = 1$ is stable since $\bar{f}_0'(x) = 0$.

For $k = 1$, $\bar{f}_1(x) = x$ can be written

$$(1 - x)e^{\lambda x} = (1 - x)^5. \tag{3.22}$$

This equation has only two solutions 0 and 1 in $[0, 1]$, where 0 is an unstable fixed point since $\bar{f}_1'(0) = 5 + \lambda > 1$, while 1 is a stable fixed point because $\bar{f}_1'(1) = 0$.
For $k = 2$, $\bar{f}_2(x) = x$ we obtain

$$(1 - x)e^{\lambda x} = (1 - x)^4(1 + 4x + \lambda x - \lambda x^2). \tag{3.23}$$

Clearly, 0 and 1 are solutions of (3.23). Divide both sides of (3.23) by $1 - x$ and let denote the LHS of the resulting equation by $g(x) = e^{\lambda x}$ and the RHS by $h(x)$.

Since $g(0) = h(0) = 1$, $g(1) = e^{\lambda} > 0 = h(1)$ and $h'(0) = 1 + \lambda > \lambda = g'(0)$, $h(x) = g(x)$ has a solution in $(0, 1)$.

This solutions is unique. To see this, first observe that $h''(x) = 0$ has a unique solution $x_{\text{infl}} \in (0, 0.5)$. Indeed, $h''(x)$ is a polynomial of degree three, i.e., it has at most three real roots. Clearly, $h''(1) = 0$, and since $h''(0) = -8\lambda - 18 < 0$ and $h''(0.5) = 0.5\lambda + 3 > 0$, by the intermediate value theorem $h''(x) = 0$ has a solution in $(0, 0.5)$. Moreover, $h'''(1) = -30 < 0$ and the leading coefficient of $h''(x)$ is positive; therefore, the third solution has to be greater than one.

Also, observe, that $h'(x) = 0$ has a unique solution $x_{\max} \in (0, 1)$. Indeed, $h'(x)$ is a polynomial of degree four, i.e., it has at most four real roots. Since $h'(1) = h''(1) = 0$ and $h'''(1) < 0$, 1 is a root of multiplicity two of $h'(x) = 0$ and $h'(1 \pm \varepsilon(\lambda)) < 0$ for $\varepsilon(\lambda)$ sufficiently small. Since the leading coefficient of $h'(x)$ is positive, $h'(x)$ must have two additional real roots, such that one is bigger and the other is smaller than 1. Moreover, $h'(0) > 0$, therefore, there is a unique root $x_{\max}$ in $(0, 1)$ and $h(x)$ has a unique maximum in $x_{\max}$ on $(0, 1)$.

Since $h(x)$ is concave on $[0, x_{\text{infl}})$ but $g(x)$ is convex, by Rolle's theorem they may have at most two intersections over that interval and one of those is at $x = 0$; furthermore, if there is an intersection in $(0, x_{\text{infl}})$, then $h(x_{\text{infl}}) < g(x_{\text{infl}})$.

On $(x_{\text{infl}}, 1)$, $h''(x) > 0$ and since also $h'(1) = 0$, it follows that $h'(x) < 0$ and $h(x)$ is decreasing on $(x_{\text{infl}}, 1)$. Furthermore, $g(x)$ is increasing, and thus the functions $h(x)$ and $g(x)$ may intersect at most once in $(x_{\text{infl}}, 1)$; moreover, if there is such an intersection, then $h(x_{\text{infl}}) > g(x_{\text{infl}})$.

Consequently, $h(x) = g(x)$ has a unique root $x_2(\lambda)$ in $(0, 1)$, and thus $x_2(\lambda)$ is the unique fixed point of $\bar{f}_2(x)$ in $(0, 1)$. In this case 0 and 1 are stable fixed points since $\bar{f}_2'(x)$ is zero at those points. The function $\bar{f}_2(x)$ is increasing on $[0, 1]$ and since the fixed points 0 and 1 are stable, one can see that $x_2(\lambda)$ is an unstable fixed point.

Finally, in the case $k = 3$, $\bar{f}_3(x) = x$ reduces to

$$(1-x)e^{\lambda x} = \frac{1}{2}(1-x)^3(2+6x+2\lambda x+x^2(12+6\lambda+\lambda^2)-x^3(8\lambda+2\lambda^2)+\lambda^2x^4). \quad (3.24)$$

Equation (3.24) has solutions 0 and 1 for any λ.

There is also a solution $x_3(\lambda) \in (0, 1)$ for any $\lambda > 0$. Indeed, divide each side of (3.24) by $(1 - x)$ and denote the RHS and the LHS of the resulting expression by $h(x)$ and $g(x)$, correspondingly. The fact that $g(0) = h(0) = 1$, $g(1) = e^{\lambda} > 0 = h(1)$, and $h'(0) = 1 + \lambda > \lambda = g'(0)$ verifies the statement.

Thus, $g(x) = h(x)$ has at least two solutions on $[0, 1)$, including $x = 0$, so by

Rolle's theorem $g'(x) = h'(x)$ has at least one solution on $(0, 1)$. It is enough to show that $g'(x) = h'(x)$ has a unique solution on $[0, 1]$ to guarantee that that $x_3(\lambda)$ is a unique solution of $g(x) = h(x)$ on $(0, 1)$.

The first two derivatives of $h(x)$ are

$$\begin{aligned} h'(x) = 3\lambda^2 x^5 - (10\lambda^2 + 20\lambda)x^4 + (12\lambda^2 + 44\lambda + 24)x^3 \\ - (6\lambda^2 + 27\lambda + 27)x^2 + (\lambda^2 + 2\lambda + 2)x + \lambda + 1 \end{aligned} \tag{3.25}$$

and

$$\begin{aligned} h''(x) = 15\lambda^2 x^4 - (40\lambda^2 + 80\lambda)x^3 + (36\lambda^2 + 132\lambda + 72)x^2 \\ - (12\lambda^2 + 54\lambda + 54)x + \lambda^2 + 2\lambda + 2. \end{aligned} \tag{3.26}$$

First, we show that $h''(x) = 0$ has two solutions on $[0, 1]$. Note that 0 and 1 are not solutions since $h''(0) = \lambda^2 + 2\lambda + 2 > 0$ and $h''(1) = 20$. If $p(x)$ is a univariate polynomial of degree n then the variation of signs $V_c(p)$ of $p(x)$ at $x = c$ is the number of sign changes of consecutive elements in the sequence $\{p^{(j)}(x)\}_{j=0}^{n} \big|_{x=c} = \{p(c), p'(c), \ldots, p^{(n)}(c)\}$ (ignoring any terms that are 0). By Budan-Fourier theorem, the number of roots on $[0, 1]$ of $h''(x) = 0$ is $V_0(h'') - V_1(h'') - 2k$ where $k \in \mathbb{N} \cup 0$. We have at $x = 0$

$$\begin{aligned} h''(0) &= \lambda^2 + 2\lambda + 2 \\ h'''(0) &= -12\lambda^2 - 54\lambda - 54 \\ h^{(4)}(0) &= 72\lambda^2 + 264\lambda + 144 \\ h^{(5)}(0) &= -240\lambda^2 - 480\lambda \\ h^{(6)}(0) &= 360\lambda^2 \end{aligned} \tag{3.27}$$

and at $x = 1$

$$\begin{aligned} h''(1) &= 20 \\ h'''(1) &= -30\lambda + 90 \\ h^{(4)}(1) &= 12\lambda^2 - 216\lambda + 144 \\ h^{(5)}(1) &= 120\lambda^2 - 480\lambda \\ h^{(6)}(1) &= 360\lambda^2 \end{aligned} \tag{3.28}$$

Clearly, $V_0(h'') = 4$ for any $\lambda > 0$. However, there are different sequences $\{h^{(2+j)}(x)\}_{j=0}^{4} \big|_{x=1}$ for $\lambda > 0$. Nevertheless, $V_1(h'') = 2$ for any $\lambda > 0$. To see this, one has to consider sequences, which correspond to different λ. It is easily verified by inspection, considering the intervals $(0, 9 - \sqrt{69}]$, $(9 - \sqrt{69}, 3]$, $(3, 4]$, $(4, 9 + \sqrt{69}]$ and $(9 + \sqrt{69}, \infty)$ separately, that $V_1(h'') = 2$ for every $\lambda > 0$.

Therefore, the number of solutions on $[0, 1]$ to $h''(x) = 0$ is at most $V_0(h'') - V_1(h'') = 2$, counted with multiplicity. Furthermore, by (3.27) and (3.28) $h''(0) > 0$ and $h''(1) > 0$ for any $\lambda > 0$. However, $h''(0.5) = -0.0625\lambda^2 - 2\lambda - 7 < 0$ for any $\lambda > 0$. Thus, $h''(x) = 0$ has exactly two roots on $[0, 1]$ and let us denote them by x_1 and x_2, so that we have $0 < x_1 < 0.2 < x_2 < 1$.

Moreover, $h''(x) > 0$ for $x \leq 0$ and any $\lambda > 0$. Indeed, $h''(0) > 0$ by (3.27), $\lim_{x \to -\infty} h''(x) = \infty$ and by Descartes rule of signs $h''(x) = 0$ does not have a negative solution.

Consider the third derivative of function $h(x)$,

$$h'''(x) = 60\lambda^2 x^3 - 120\lambda(\lambda + 2)x^2 + (72\lambda^2 + 264\lambda + 144)x - 12\lambda^2 - 54\lambda - 54. \tag{3.29}$$

By Descartes' rule of signs the equation $h'''(x) = 0$ does not have a negative root and $h'''(0) = -12\lambda^2 - 54\lambda - 54 < 0$ for any $\lambda > 0$, that is, $h'''(x) < 0$ for $x \leq 0$.

Thus, function $h'(x)$ has two critical points on $(-\infty, 1]$, i.e., at x_1 and x_2. Since $h''(x) > 0$ and $h'''(x) < 0$ for $x \leq 0$ then x_1 corresponds to a maximum point while

x_2 to a minimum point of $h'(x)$. Also, note that $h'(1) = 0$ since $x = 1$ is a root of multiplicity 2 of $h(x) = 0$. Hence, $\min_{[0,1]} h'(x) < 0$. From this, it also follows that $h'(x) = 0$ has a unique root on $(0, 1)$, denote the root by $\hat{x}$.

Equation $g'(x) = h'(x)$ has a unique negative solution. To see this note that $h'(0) = 1 + \lambda > \lambda = g'(0)$ and the limits of $g'(x)$ and $h'(x)$ as $x \to -\infty$ are 0 and $-\infty$, respectively. The solution is unique since otherwise by Rolle's theorem $g''(x) = h''(x)$ would have a negative solution which contradicts to the above consideration. Denote the solution by $\bar{x}$.

Let x^* be the smallest inflection point of $h'(x)$ on $(-\infty, x_2)$, i.e., the smallest solution of $h'''(x) = 0$ on $(-\infty, x_2)$ where existence follows by Rolle's theorem from the above consideration of $h''(x)$, that is, $h''(x) = 0$ has exactly two roots on $(-\infty, 1]$. Moreover, $x^* \in (x_1, x_2)$. To see this it is enough to show that $h'''(x)$ does not have a solution on $[0, x_1 + \epsilon]$ for some small $\epsilon > 0$. Consider interval $[0, 0.2]$ and show that $h''(x) = 0$ has a unique root on the interval while $h'''(x) = 0$ does not have a solution on the interval. Again, by Budan-Fourier theorem the number of roots on $[0, 0.2]$ of $h''(x) = 0$ is $V_0(h'') - V_{0.2}(h'') - 2k$ where $k \in \mathbb{N} \cup 0$ and $h'''(x) = 0$ has $V_0(h''') - V_{0.2}(h''') - 2j$ roots on $[0, 0.2]$, where $j \in \mathbb{N} \cup 0$. We have already found the values of $h''(x)$ with her derivatives at $x = 0$ in Eqns. (3.27). Now we consider functions at $x = 0.2$

$$\begin{aligned} h''(0.2) &= -0.256\lambda^2 - 4.16\lambda - 5.92 \\ h'''(0.2) &= -1.92\lambda^2 - 10.8\lambda - 25.2 \\ h^{(4)}(0.2) &= 31.2\lambda^2 + 168\lambda + 144 \\ h^{(5)}(0.2) &= -168\lambda^2 - 480\lambda \\ h^{(6)}(0.2) &= 360\lambda^2 \end{aligned} \tag{3.30}$$

From (3.27) and (3.30), it is easy to see that $V_0(h'') - V_{0.2}(h'') = 1$ and $V_0(h''') - V_{0.2}(h''') = 0$ for any $\lambda > 0$. That is, $h''(x) = 0$ has a unique solution on

$[0, 0.2]$ and $h'''(x) = 0$ does not have solutions on that interval. Since $h'''(x) < 0$ for $x \leq 0$ there is no solution of $h'''(x) = 0$ on $(-\infty, x^*)$, i.e., x^* is the overall smallest solution of $h'''(x) = 0$. Thus, $h'''(x) < 0$ for $x \in (0, x^*)$, in particular, for $x \in (0, x_1) \subset (0, x^*)$. Indeed, $h'''(x) = 0$ does not have solutions on $(-\infty, x^*)$ and $h'''(0) < 0$.

At the beginning, we showed that there is a solution on $(0, 1)$ of $g'(x) = h'(x)$. Now, we show that it is unique.

Clearly, there is no solution to $g'(x) = h'(x)$ on $(\hat{x}, 1)$ since $h'(x) < 0 < g'(x)$. Consider two cases with respect to x^*. First, if $\hat{x} < x^*$ then there exists a unique solution to $g'(x) = h'(x)$ on $(0, \hat{x}) \subset (0, 1)$. Indeed, $g'(x)$ is convex and $h'(x)$ is concave on $(-\infty, \hat{x})$ so there are at most two solutions. One solution is $\bar{x}$ and the other one is in $(0, \hat{x})$ since $h'(0) > g'(0)$ while $h'(\hat{x}) = 0 < g'(\hat{x})$ for any $\lambda > 0$.

Now, consider $\hat{x} > x^*$ then $g'(x)$ and $h'(x)$ have qualitatively similar behavior on $[\bar{x}, \hat{x}]$ as $g(x)$ and $h(x)$ on $[0, 1]$ in the case $k = 2$. Since $h'(0) > g'(0)$ and $h'(\hat{x}) < g'(\hat{x})$ there is a solution to $g'(x) = h'(x)$ on $(0, \hat{x}) \subset (0, 1)$. Assume first that there is a solution on $(0, x^*) \subset [\bar{x}, x^*)$ then it is unique since $g'(x)$ is convex and $h'(x)$ is concave on the last interval and $\bar{x} < 0$ is a solution, moreover, in this case $h'(x^*) < g'(x^*)$.

If there is a solution on $(x^*, \hat{x})$ then it is unique since $g'(x)$ is strictly increasing and $h'(x)$ is strictly decreasing on this interval. In particular, one must have in this case that $h'(x^*) > g'(x^*)$.

Moreover, the last two sub-cases for $\hat{x} > x^*$ are mutually exclusive due to the values of functions at $x = x^*$. Hence, combining the above results we get that $g'(x) = h'(x)$ has a unique solution on $[0, 1]$ for any $\lambda > 0$. As said above, this implies that for any $\lambda > 0$ there is a unique root $x_3(\lambda)$ in $(0, 1)$ of $g(x) = h(x)$, and thus a unique fixed point $x_3(\lambda)$ in $(0, 1)$ of $\bar{f}_3$.

One can check that $\bar{f}_3'(x) = 0$ at 0 and 1, and thus these two fixed points are

stable. Furthermore, $\bar{f}_3(x)$ is increasing on $[0,1]$ and using the stability of the fixed points 0 and 1, and the uniqueness of the fixed point $x_3(\lambda)$, it follows that $x_3(\lambda)$ is an unstable fixed point. □

For all cases considered above 0 is a fixed point of $\bar{f}$. As we noted before, the error $f(x) - \bar{f}(x)$ is 0 at 0, so this fixed point is also a fixed point of $f(x)$ for any N. If x is an unstable fixed point of $\bar{f}$ with $\bar{f}'(x) > 1$, then (3.11) implies that $f(x)$ has a fixed point shifted from x at most by $O(1/N)$. These arguments are valid in case λ is a fixed constant independent of N.

Let p denote the probability that a node is initially activated and p_c be the nontrivial solution(s) derived above. Since ρ_t is a Markov process, for the mean-field approximation we obtain the following theorem.

Theorem 17. In the mean-field approximation of the bootstrap percolation on random graph $G_{\mathbb{Z}_N^2,p_d}$ there exists a critical probability p_c such that for a fixed p, with high probability for large N, all vertices will eventually be active if $p > p_c$, while all vertices will eventually be inactive for $p < p_c$. The value of p_c is given as the function of k and λ as follows:

(i) For $k = 0$ and any λ, $p_c = 0$ and all vertices will become active in one step for any p.

(ii) For $k = 1$ and any λ, $p_c = 0$, i.e., for any fixed $p > 0$, all vertices will eventually become active with high probability.

(iii) For $k = 2$ and any λ, $p_c = x_2(\lambda)$, where $x_2(\lambda) \in (0,1)$ is a nontrivial solution to $x = \bar{f}_2(x)$.

(iv) For $k = 3$ and any λ, $p_c = x_3(\lambda)$, where $x_3(\lambda) \in (0,1)$ is a nontrivial solution to $x = \bar{f}_3(x)$.

Proof. Consider the case $0 \le p < p_c$ (and thus (iii) or (iv)); the case $p_c < p \le 1$ is similar and (i) and (ii) are trivial. In the limit as $N \to \infty$, $\rho_0 = p$ and ρ_t is

deterministic with $\rho_{t+1} = \bar{f}(\rho_t)$. Since $p < p_c$, the sequence $\rho_t = \bar{f}^t(p)$ converges, as $t \to \infty$, to the fixpoint 0. Furthermore, because $\bar{f}'(0) = 0$, the convergence is (at least) quadratic, and in particular geometric.

Now consider a fixed positive integer N. The deterministic sequence $\bar{f}^t(p)$ just considered reaches below $1/N$ for $t \geq t_N$, where $t_N = O(\log N)$. The sequence ρ_t is a random perturbation of $\bar{f}^t(p)$. In each step, we have two sources of error: the difference in mean $f(\rho_t) - \bar{f}(\rho_t) = O(1/N)$, by (3.11), and the random error coming from the binomial distributions in (3.2), which by a standard Chernoff bound is $O(N^{-0.9})$ with probability $1 - O(N^{-1})$, say. Since further $|f'(x)| \leq 1$ for small x, the combined error from the first t_N steps is $t_N(O(N^{-1}) + O(N^{-0.9})) = O(N^{-0.8})$ with probability $1 - O(t_N N^{-1}) = 1 - o(1)$. Hence, with high probability, we reach a state with $\rho_t = O(N^{-0.8})$. Then $f(\rho_t) = O(\rho_t^2) = O(N^{-1.6})$, and by another Chernoff bound (or Chebyshev's inequality), $\rho_{t+1} = O(N^{-1.6})$ with high probability. But then $f(\rho_{t+1}) = O(\rho_{t+1}^2) = O(N^{-3.2})$, and thus (conditionally given ρ_{t+1}), the expected number of active vertices at time $t + 2$ is $N^2 f(\rho_{t+1}) = O(N^{-1.2}) = o(1)$, and thus with high probability there are no active vertices at all at time $t + 2$. □

Lemma 18. For $k = 2, 3$, $p_c = x_k(\lambda)$, is a non-increasing function of λ.

We provide two proofs of Lemma 18. The first proof is based on the definition of random graph $G_{\mathbb{Z}_N^2, p_d}$. The second one utilizes the properties of functions $g(x)$ and $h(x)$ defined in the proof of Proposition 16.

Proof. 1. If we increase λ, then the average number of edges is increased. Moreover, if $G_N(\lambda)$ denotes the random graph $G_{\mathbb{Z}_N^2, p_d}$ with parameter λ, and $\lambda_1 < \lambda_2$, then we can couple the random graphs $G_N(\lambda_1)$ and $G_N(\lambda_2)$ such that $G_N(\lambda_1) \subseteq G_N(\lambda_2)$; it is then evident that if all vertices eventually are activated in $G_N(\lambda_1)$ (for a given initially active set), then so are all vertices in $G_N(\lambda_2)$. The same holds for the mean-field approximation, where again we can couple two models with parameters

λ_1 and λ_2, with $\lambda_1 < \lambda_2$, such that the set of activated vertices for λ_1 is a subset of the set of activated vertices for λ_2. It follows that in Theorem 17, $p_c(\lambda_1) \geq p_c(\lambda_2)$, i.e., p_c is a non-increasing function of λ. □

Proof. 2. For $k = 2$ or 3, denote the functions $g(x)$ and $h(x)$ from corresponding cases of the proof of Proposition 16 by $g_k(x)$ and $h_k(x)$, and let $F_k(\lambda, x) = g_k(x) - h_k(x)$. Then $x_k(\lambda)$ is a root of $F_k(\lambda, x) = 0$. We have shown that $g_k(x) = h_k(x)$ has a unique root in $(0, 1)$ and the proofs also show that the root is simple, so $\partial F_k/\partial x = g_k'(x) - h_k'(x) \neq 0$ at $x = x_k(\lambda)$. It follows from the implicit function theorem that $x_k(\lambda)$ is an infinitely differentiable function of $\lambda \in (0, \infty)$, and that

$$\frac{dx_k(\lambda)}{d\lambda} = -\frac{\partial F_k/\partial \lambda}{\partial F_k/\partial x}(\lambda, x_k(\lambda)). \tag{3.31}$$

Now, $F_k(\lambda, 1) = g_k(1) - h_k(1) > 0$, and thus $F_k(\lambda, x) > 0$ for $x > x_k(\lambda)$. Consequently, $\partial F_k/\partial x > 0$ at $x = x_k(\lambda)$.

The denominator of (3.31), $\partial F_k/\partial x$, is always positive for $k = 2, 3$. To see this, first, recall that $x_k(\lambda)$ is the unique root of $F_k(\lambda, x) = 0$ on $(0, 1)$ and $x = 0$ is also a root. It was shown that $g_3'(x) = h_3'(x)$ has a unique root $\hat{x}$ on $(0, 1)$ for $k = 3$, that is, $\hat{x}$ is the unique solution on $(0, 1)$ of $\partial F_3/\partial x = 0$.

In the case $k = 2$ there is also a unique solution on $(0, 1)$ of $g_2'(x) = h_2'(x)$. Indeed, as it was shown in the uniqueness part, both equations $h_2'(x) = 0$ and $h_2''(x) = 0$ have unique solution on $(0, 1)$ which are unique on $(-\infty, 1)$, denote the solutions by $\hat{x}$ and x_1, correspondingly. Moreover, $x = 1$ is the solution of multiplicity two of $h_2'(x) = 0$. This implies that $x_1 \in (\hat{x}, 1)$. Since $h_2'(0) > g_2'(0)$ and $h_2'(1) < g_2'(1)$ for any $\lambda > 0$ the equation $g_2'(x) = h_2'(x)$ has a solution on $(0, 1)$. Furthermore, $h_2''(0) = -8\lambda - 18 < 0$ for any $\lambda > 0$. Therefore, $h_2'(x)$ is decreasing on $(-\infty, \hat{x})$ and the function is negative on $(\hat{x}, 1)$, see proof of Proposition 16. However, $g_2'(x)$ is a strictly increasing, positive function for any x and $\lambda > 0$. Hence,

there is no negative solutions and the solution on $(0, \hat{x})$ is unique.

Thus, in both cases $k = 2, 3$ by Rolle's theorem $0 < \hat{x} < x_k(\lambda)$. At $x = 0$, $\partial F_k(\lambda, x)/\partial x \mid_{x=0} = g_k'(0) - h_k'(0) = -1 < 0$ for any $\lambda > 0$. Therefore, at the solution $x_k(\lambda)$, $0 < \hat{x} < x_k(\lambda)$, we have $\partial F_k(\lambda, x)/\partial x \mid_{x=x_k(\lambda)} > 0$, that is, the the denominator of (3.31) is positive for any $\lambda > 0$.

In the case $k = 2$ the numerator of (3.31) is

$$\begin{aligned} \partial F_2/\partial\lambda \mid_{x=x_2(\lambda)} &= x\left(e^{\lambda x} - (1-x)^4\right) \mid_{x=x_2(\lambda)} \\ &= x_2(\lambda)\left(e^{\lambda x_2(\lambda)} - (1-x_2(\lambda))^4\right) > 0, \end{aligned}$$

because $(1 - x_2(\lambda))^4 < 1 \leq e^{\lambda x_2(\lambda)}$. Hence, $dx_2(\lambda)/d\lambda < 0$ for any $\lambda > 0$.

For $k = 3$ the numerator of (3.31) is given by

$$\begin{aligned} &\partial F_3/\partial\lambda \mid_{x=x_3(\lambda)} = x\left(e^{\lambda x} - (1-x)^3(1 + 4x + \lambda x - \lambda x^2)\right) \mid_{x=x_3(\lambda)} \\ = \;& x_3(\lambda)\left(e^{\lambda x_3(\lambda)} - (1-x_3(\lambda))^3(1 + 4x_3(\lambda) + \lambda x_3(\lambda) - \lambda x_3^2(\lambda))\right). \end{aligned}$$

Note that in this case the numerator of (3.31) is $\partial F_3/\partial\lambda(\lambda, x) = xF_2(x)$. Therefore, $\partial F_3/\partial\lambda > 0$ if $F_2(x_3(\lambda)) > 0$ (the first factor of $\partial F_3/\partial\lambda$ is positive because $x_3(\lambda) \in (0, 1)$). Since $x_2(\lambda)$ is the unique solution of $F_2(x) = 0$ on $(0, 1)$ and $F_2(1) > 0$ it is enough to show that $x_2(\lambda) < x_3(\lambda)$ for any $\lambda > 0$.

In both cases, $k = 2, 3$, the left hand sides of $g_k(x) = h_k(x)$ are the same, i.e., $g_k = e^{\lambda x}$ and this is a strictly increasing function. We also know that $x = 0$ is the solution of $g_k(x) = h_k(x)$ for $k = 2, 3$. Thus, if $h_3(x) > h_2(x)$ then $F_2(x_3(\lambda)) > 0$. First, we need to solve $h_3(x) = h_2(x)$ which reduces to $\frac{1}{2}x^2(1-x)^2(\lambda^2x^2 - (2\lambda^2 + 10\lambda)x + \lambda^2 + 10\lambda + 20) = 0$. Clearly, 0 and 1 are solutions of multiplicity 2 and the other two solutions are $1 + (5 \pm \sqrt{5})/\lambda$. Since $1 + (5 \pm \sqrt{5})/\lambda > 1$ for any $\lambda > 0$ the sign of $h_3(x) - h_2(x)$ is not changed on $(0, 1)$ for any $\lambda > 0$. We have that $h_3(x) - h_2(x) > 0$ on $(0, 1)$ because the difference of two functions is positive at $-\infty$, $x = 0$ is a root of multiplicity 2 and there is no

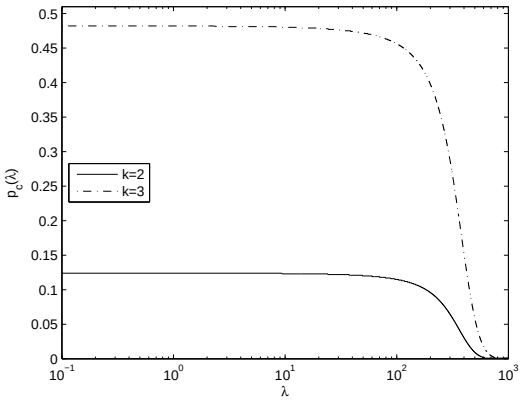

Figure 4: Critical probability p_c as a function of λ for $k = 2, 3$. The curves are calculated as the unique solutions in $(0, 1)$ of equations (3.23) and (3.24), respectively.

negative solutions of $h_3(x) = h_2(x)$.

Thus, $h_3(x) > h_2(x)$ on $(0, 1)$ for any $\lambda > 0$ which implies that $F_2(x_3(\lambda)) > 0$. Consequently, in case $k = 3$ the numerator of (3.31) is positive at $x_3(\lambda)$ for any $\lambda > 0$. □

Corollary 19. Cases (*iii*) and (*iv*) of Theorem 17 can be sharpened as follows.

(iii) For $k = 2$ and any λ, $p_c = x_2(\lambda)$, where $x_2(\lambda) \in (0, x_2(0)]$ is a unique solution to $x = \bar{f}_2(x)$ and $x_2(0) \approx 0.132$.

(iv) For $k = 3$ and any λ, $p_c = x_3(\lambda)$, where $x_3(\lambda) \in (0, x_3(0)]$ is a unique solution to $x = \bar{f}_3(x)$ and $x_3(0) = 0.5$.

Proof. The values
$x_2(0) = \frac{11}{12} - \frac{1}{12}(235 + 6\sqrt{1473})^{1/3} - \frac{13}{12}(235 + 6\sqrt{1473})^{-1/3} \approx 0.131123$, and
$x_3(0) = \frac{1}{2}$ can be easily obtained from (3.23) and (3.24), respectively. Assuming Lemma 18, for $k = 2, 3$ we have that $x_k(\lambda) \leq x_k(0)$, i.e., Corollary 19 holds. □

It is also easy to see that for any fixed $p > 0$, if λ is large enough, then the proportion of vertices active after the first step is more than, say, $0.6 > p_c$, and thus eventually all vertices will be active. Consequently, $p_c = x_k(\lambda) \to 0$ as $\lambda \to \infty$. The dependence of p_c on λ (for $k = 2, 3$) is shown in Figure 4.

Remark 20. Note that for $k \geq 5$, an inactive vertex will remain inactive for ever. Hence, unless all vertices are activated at the beginning, there is at each step a set of inactive vertices. Furthermore, every neighbor of an inactive vertex becomes inactive; hence, for the graph $G_{\mathbb{Z}_N^2, p_d}$, every vertex will become inactive after at most N steps. For the mean-field approximation, every vertex has at least a fixed positive probability of becoming inactive at every step; hence (almost surely) every vertex will eventually become inactive in the mean-field approximation, too.

CHAPTER 4

BOOTSTRAP PERCOLATION ON $G_{\mathbb{Z}_N^2,P_D}$ WITH TWO TYPES OF VERTICES

In this chapter we generalize a non-monotone bootstrap percolation with one type of vertex on random graph $G_{\mathbb{Z}_N^2,p_d}$ considered in Chapter 3 for the case of two types of vertices. In order to study the process, we will utilize the properties of the graph, which we studied in Chapter 2.

This chapter is a joint work with Robert Kozma, and Miklós Ruszinkó; and is partly based on our forthcoming paper.

4.1 The present state of bootstrap percolation with two types of vertices

In the last decades, interest in bootstrap percolation has increased significantly. The direct connection between bootstrap percolation models on $\mathbb{Z}^2$ and cellular automata has plaeds an important role in the development of both fields [23, 22].

In all the models mentioned a unique type of vertices was considered. In [30] bootstrap percolation theory was generalized to the case of two types of vertices. Authors considered the bootstrap percolation process on $G_{n,p}$ where vertices are of two types. Percolation was defined according to one type. Thresholds for percolation with respect to the size of the set of initially active sites, a, and graph parameter p as well as the time until termination were derived.

4.2 Definition of the process

We define the bootstrap percolation with two types of vertices on $G_{\mathbb{Z}_N^2,p_d}$ as follows. Each vertex of the graph is defined by two variables: *type* and *state*. The vertex is either of the first (excitatory E) or second (inhibitory I) type. The state of the vertex is either active or inactive. We assume that the type of vertex is selected randomly at the beginning and it remains unchanged through the process, during which a vertex is of the first type with probability ω. However, the state of the

vertex changes over time according to a non-monotone bootstrap percolation with two types of vertices (for a short - activation process) which will be defined next.

Let $A(t)$ be the set of all active vertices at time t, while $A_1(t)$ and $A_2(t)$ are the sets of active vertices of the first and second types at time t, respectively; $A(t) = A_1(t) \cup A_2(t)$. The state of a vertex v is defined by the potential function $\chi_v(t)$ such that $\chi_v(t) = 1$ if vertex v is active at time t, otherwise $\chi_v(t) = 0$. Therefore,

$$A_i(t) = \{v \in V(G_{\mathbb{Z}_N^2, p_d}) \mid \chi_v(t) = 1 \ \& \ v \text{ is of type } i\},$$

where $i = 1, 2$. At the beginning, we activate each vertex with probability p, independently of its type and of all other vertices. Let $A(0)$ be the random subset of initially active vertices.

Non-monotone bootstrap percolation with two types of vertices is defined for each type separately. For a vertex v of the first type,

$$\chi_v(t+1) = \mathbb{1}\left(\sum_{u \in N^1(v)} \chi_u(t) - \sum_{u \in N^2(v)} \chi_u(t) \geq k\right), \tag{4.1}$$

where $N^1(v)$ and $N^2(v)$ denote the subsets of vertices in the closed neighborhood of the vertex v, of the first and second types, respectively; and $\mathbb{1}$ is the indicator function. Here $k \in \mathbb{Z}_+$ is a threshold required for the vertex to be in the active state. The rule for a vertex v of the second type is defined as

$$\chi_v(t+1) = \mathbb{1}\left(\sum_{u \in N^1(v)} \chi_u(t) + \sum_{u \in N^2(v)} \chi_u(t) \geq k\right) = \mathbb{1}\left(\sum_{u \in N(v)} \chi_u(t) \geq k\right), \tag{4.2}$$

where $N(v) = N^1(v) \cup N^2(v)$ is the closed neighborhood of vertex v.

It can be observed that $A(t)$ does not necessarily grow monotonically during the activation process even in the absence of vertices of the second type, as discussed in Chapter 3, whereas monotonicity is a typical assumption in most bootstrap

percolation models considered previously.

4.2.1 Mean-field approximation

In the case where there are two types of vertices we need to take into account the evolution of two density functions that correspond to active vertices of each type. Let

$$\rho_t^{(1)} = \frac{|A_1(t)|}{\omega N^2} \tag{4.3}$$

and

$$\rho_t^{(2)} = \frac{|A_2(t)|}{(1-\omega)N^2} \tag{4.4}$$

be the densities of active vertices of the first and second types relative to the total number of vertices of these types, correspondingly. Then, in particular, the density of all active vertices is given by

$$\rho_t = \omega\rho_t^{(1)} + (1-\omega)\rho_t^{(2)} = \frac{|A_1(t)| + |A_2(t)|}{N^2}.$$

Based on definitions (4.3) and (4.4), we can also find the probability of the event $B_i(t) = \{\text{an active vertex at time } t \text{ is of the type } i\}$

$$\mathbb{P}(B_1(t)) = \frac{A_1(t)}{A_1(t) + A_2(t)} = 1 - \frac{(1-\omega)\rho_t^{(2)}}{\omega\rho_t^{(1)} + (1-\omega)\rho_t^{(2)}} \tag{4.5}$$

and

$$\mathbb{P}(B_2(t)) = \frac{A_2(t)}{A_1(t) + A_2(t)} = \frac{(1-\omega)\rho_t^{(2)}}{\omega\rho_t^{(1)} + (1-\omega)\rho_t^{(2)}}. \tag{4.6}$$

The function from the last expression can be denoted by $h(x, y, \omega) = \frac{(1-\omega)y}{\omega x + (1-\omega)y}$, where it is assumed that $\omega x + (1-\omega)y > 0$.

Next, some functions and their meaning will be introduced, which we will use in the following lemmas. As in Chapter 3, we are interested in the dynamics of the

density function; here we consider $\rho_t^{(1)}$ and $\rho_t^{(2)}$. In this section we need to study the dynamics of a coupled system (4.3) and (4.4) since $A_1(t)$ and $A_2(t)$ are dependent. However, we can still consider the expectations of $\rho_t^{(1)}$ and $\rho_t^{(2)}$ to study their dynamics. In order to do this, we introduce functions $f_i^{\pm}(x,y)$, $i=1,2$, which describe the probabilities for vertices of i-th type to stay active $(+)$ or to become active $(-)$ at the next time step.

Let us first consider events which describe functions $f_i^{\pm}(x,y,\omega)$. For simplicity, we show the derivation of only function $f_1^{+}(x,y,\omega)$; the other functions can be derived in a similar way. Let $C=\{v \text{ will be active } \big|\ v \text{ is active excitatory}\}$. Let $D_{n-4}=\{v \text{ will be active } \big|\ v \text{ is active excitatory and } \deg(v)=n-4\}$. Let $F_{i-1}=\{v$ will be active$\big|\ v$ is active excitatory and $\deg(v)=n-4$ and out of n neighbors exactly $i-1$ are active$\}$. Finally, $H_{i-1}=\{$out of n neighbors exactly $i-1$ are active$\}$. Then we have

$$\begin{aligned} f_1^{+}(x,y,\omega) &= \mathbb{P}(C)=\sum_{n=4}^{N^2-1}\mathbb{P}(D_{n-4})\mathbb{P}(\deg(v)=n-4)= \\ &\quad \sum_{n=4}^{N^2-1}\mathbb{P}(\deg(v)=n-4)\sum_{i=1}^{n+1}\mathbb{P}(F_{i-1})\mathbb{P}(H_{i-1}) \end{aligned} \tag{4.7}$$

Thus,

$$\begin{aligned} f_1^{+}(x,y,\omega) &= \sum_{n=4}^{N^2-1}\mathbb{P}(\deg(v)=n-4)\sum_{i=1}^{n+1}p_i^{1+}(x,y,\omega)\cdot \\ &\quad \binom{n}{i-1}(\omega x+(1-\omega)y)^{i-1}(1-\omega x-(1-\omega)y)^{n-i+1} \end{aligned} \tag{4.8}$$

$$\begin{aligned} f_1^{-}(x,y,\omega) &= \sum_{n=4}^{N^2-1}\mathbb{P}(\deg(v)=n-4)\sum_{i=0}^{n}p_i^{1-}(x,y,\omega)\cdot \\ &\quad \binom{n}{i}(\omega x+(1-\omega)y)^{i}(1-\omega x-(1-\omega)y)^{n-i} \end{aligned} \tag{4.9}$$

$$f_2^+(x,y,\omega) = \sum_{n=4}^{N^2-1} \mathbb{P}(\deg(v)=n-4) \sum_{i=1}^{n+1} p_i^{2+} \cdot \binom{n}{i-1} (\omega x + (1-\omega)y)^{i-1} (1-\omega x - (1-\omega)y)^{n-i+1} \quad (4.10)$$

$$f_2^-(x,y,\omega) = \sum_{n=4}^{N^2-1} \mathbb{P}(\deg(v)=n-4) \sum_{i=0}^{n} p_i^{2-} \cdot \binom{n}{i} (\omega x + (1-\omega)y)^{i} (1-\omega x - (1-\omega)y)^{n-i} \quad (4.11)$$

where $p_i^{j-} = \mathbb{P}(\text{a vertex will be active} \mid \text{the vertex is non-active, of type } j \text{ and it has } i \text{ active neighbors in the closed neighborhood})$ and $p_i^{j+} = \mathbb{P}(\text{a vertex will be active} \mid \text{the vertex is active, of type } j \text{ and it has } i \text{ active neighbors in the closed neighborhood})$, for $j = 1, 2$, and are defined as follows

$$p_i^{1+}(x,y,\omega) = \sum_{t=0}^{\lfloor \frac{i-k}{2} \rfloor} \binom{i-1}{t} h^t(x,y,\omega)(1-h(x,y,\omega))^{i-t-1}, \quad (4.12)$$

$$p_i^{1-}(x,y,\omega) = \sum_{t=0}^{\lfloor \frac{i-k}{2} \rfloor} \binom{i}{t} h^t(x,y,\omega)(1-h(x,y,\omega))^{i-t}, \quad (4.13)$$

$$p_i^{2\pm} = \begin{cases} 1 & , i \geq k, \\ 0 & i \leq k-1 \end{cases} \quad (4.14)$$

where ω is the probability that a vertex is of the first type (defined at the beginning of the process).

Remark 21. For simplicity we mostly omit the argument ω from the functions $f_1(x,y,\omega)$, $f_2(x,y,\omega)$, and $f_1^{\pm}(x,y,\omega)$, $f_2^{\pm}(x,y,\omega)$. In particular, all statement are for an arbitrary $\omega \in (0,1)$ unless additionally stated.

Lemma 22. For the mean-field approximation on the graph $G_{\mathbb{Z}_N^2, p_d}$ with N^2 vertices of two types, and a vertex is of the first type with probability w, $\rho_t^{(i)}$ is a

Markov process for $i = 1, 2$ given by

$$\begin{aligned} \omega N^2 \rho_{t+1}^{(1)} &= Bin(\omega N^2 \rho_t^{(1)}, f_1^+(\rho_t^{(1)}, \rho_t^{(2)})) \\ &+ Bin(\omega N^2 (1 - \rho_t^{(1)}), f_1^-(\rho_t^{(1)}, \rho_t^{(2)})), \end{aligned} \tag{4.15}$$

$$\begin{aligned} (1-\omega) N^2 \rho_{t+1}^{(2)} &= Bin((1-\omega) N^2 \rho_t^{(2)}, f_2^+(\rho_t^{(1)}, \rho_t^{(2)})) \\ &+ Bin((1-\omega) N^2 (1 - \rho_t^{(2)}), f_2^-(\rho_t^{(1)}, \rho_t^{(2)})), \end{aligned} \tag{4.16}$$

respectively, where $f_i^{\pm}(x, y)$ are defined in (4.8)-(4.11).

Moreover, given $\rho_t^{(i)}$, $\rho_{t+1}^{(i)}$ has mean $f_i(\rho_t^{(1)}, \rho_t^{(2)})$, for $i = 1, 2$, and variance $g_1(\rho_t^{(1)}, \rho_t^{(2)})/\omega N^2$ and $g_2(\rho_t^{(1)}, \rho_t^{(2)})/((1-\omega)N^2)$, respectively, where

$$f_1(x, y) = x f_1^+(x, y) + (1 - x) f_1^-(x, y), \tag{4.17}$$

$$f_2(x, y) = y f_2^+(x, y) + (1 - y) f_2^-(x, y), \tag{4.18}$$

and

$$g_1(x, y) = x f_1^+(x, y)(1 - f_1^+(x, y)) + (1 - x) f_1^-(x, y)(1 - f_1^-(x, y)), \tag{4.19}$$

$$g_2(x, y) = y f_2^+(x, y)(1 - f_2^+(x, y)) + (1 - y) f_2^-(x, y)(1 - f_2^-(x, y)). \tag{4.20}$$

Proof. This is clear, since it is assumed in the MF approximation that a vertex has $\deg(v) + 4$ neighbors, each is active with probability $\rho_t^{(i)}$, for $i = 1, 2$, and of the first type with probability ω, independent of one another and of $\deg(v)$; and different vertices are considered as independent. □

The explicit study of the dynamics of $\rho_t^{(1)}$ and $\rho_t^{(2)}$ requires solutions for the following system of fixed-point equations

$$\begin{cases} f_1(x, y) = x, \\ f_2(x, y) = y. \end{cases} \tag{4.21}$$

However, due to the complex form of function $f_i(x, y)$, $i = 1, 2$, it is hard to find a

solution for the system. Instead, in the next section we approximate the behavior of $\rho_t^{(1)}$ and $\rho_t^{(2)}$ for some values of the initialization probability, i.e., the probability that a vertex is active at $t = 0$, using results from Chapter 3.

4.2.2 Special cases of $f_2(x, y) = y$

In Section 3 it was pointed out that for $k \geq 5$ there will be vertices which will stay inactive for ever as long as they were not activated at the beginning. This is because there are vertices with degree 4 with positive probability.

In the case of two types of vertices, the closed neighborhood of a vertex contains a vertex of each type with positive probabilities. Combining this with the fact that there are vertices of degree 4 with positive probability, one can consider $k \leq 4$ since otherwise there will be vertices which are inactive unless they were activated at the beginning. Here we consider for simplicity $k = 0, 1, 2$.

The analysis of the second equation of (4.21) is much easier than that of the first one due to the definition of $p_i^{2\pm}$. For this reason, we begin with (4.18). For $k = 0$ one gets

$$\begin{aligned} &f_2(x,y) = yf_2^+(x,y) - (1-y)f_2^-(x,y) = \\ &y\sum_{n=4}^{N^2-1}\mathbb{P}(\deg(v)=n-4)\sum_{i=1}^{n+1}\binom{n}{i-1}(\omega x+(1-\omega)y)^{i-1}(1-\omega x-(1-\omega)y)^{n-i+1}+ \\ &(1-y)\sum_{n=4}^{N^2-1}\mathbb{P}(\deg(v)=n-4)\sum_{i=0}^{n}\binom{n}{i}(\omega x+(1-\omega)y)^{i}(1-\omega x-(1-\omega)y)^{n-i}, \end{aligned} \tag{4.22}$$

and for $k > 0$

$$\begin{aligned} &f_2(x,y) = y\sum_{n=4}^{N^2-1}\mathbb{P}(\deg(v)=n-4)\sum_{i=k}^{n+1}\binom{n}{i-1}(\omega x+(1-\omega)y)^{i-1}(1-\omega x-(1-\omega)y)^{n-i+1} \\ &+(1-y)\sum_{n=4}^{N^2-1}\mathbb{P}(\deg(v)=n-4)\sum_{i=k}^{n}\binom{n}{i}(\omega x+(1-\omega)y)^{i}(1-\omega x-(1-\omega)y)^{n-i}. \end{aligned} \tag{4.23}$$

The simplified versions of the above equations for $k = 0, 1, 2$ are

$$f_2^0(x, y) = 1, \tag{4.24}$$

$$f_2^1(x, y) = 1 + (y - 1) \sum_{n=4}^{N^2-1} \mathbb{P}(\deg(v) = n - 4)(1 - \omega x - (1 - \omega)y)^n, \tag{4.25}$$

$$f_2^2(x, y) = 1 - \sum_{n=4}^{N^2-1} \mathbb{P}(\deg(v) = n - 4)(1 - \omega x - (1 - \omega)y)^n + \tag{4.26}$$

$$(y - 1) \sum_{n=4}^{N^2-1} \mathbb{P}(\deg(v) = n - 4)n(\omega x + (1 - \omega)y)(1 - \omega x - (1 - \omega)y)^{n-1},$$

where we denoted $f_2(x, y)$ for a particular k by $f_2^k(x, y)$.

The feasible solutions of (4.21) are the solutions of $f_2(x, y) = y$. For $k = 0$ one has pair(s) of the form $(x^*, 1)$ where x^* is the solution of $x = f_1^0(x, 1)$ since $y = 1$ is the unique solution of $f_2^0(x, y) = y$ for any x.

Using an approximation of the degree distribution by the Poisson distribution, Lemma 12, for $k = 1$ the equation $f_2^1(x, y) = y$ becomes

$$(1 - y)e^{\lambda(\omega x+(1-\omega)y)} = (1 - y)(1 - \omega x - (1 - \omega)y)^4. \tag{4.27}$$

Clearly, $y = 1$ is a solution. Let $z = \omega x + (1 - \omega)y$ then after dividing each side of the above equation by $(y - 1)$ it can be written as

$$e^{\lambda z} = (1 - z)^4 \tag{4.28}$$

which has a unique solution $z = 0$ on $[0, 1]$. Since $\omega \neq 0, 1$, we have that $z = 0$ is, if and only if, $x = 0, y = 0$. Thus, for $k = 1$ there are two feasible solutions $(0, 0)$ and $(x^*, 1)$ where x^* is a solution of $f_1^1(x, 1) = x$.

Finally, for $k = 2$ the equation $f_2^2(x, y) = y$ can be rewritten using the

approximation of degree distribution, Lemma (12), as

$$(1-y)e^{\lambda(\omega x+(1-\omega)y)} = (1-y)(1-\omega x-(1-\omega)y)^3\,(4+\lambda-\lambda(\omega x+(1-\omega)y))$$
$$(\omega x+(1-\omega)y)+(1-\omega x-(1-\omega)y)^4 \quad (4.29)$$

In the last equation there are no obvious solutions. Even solution $y = 1$ exists only if $x = 1$ in contrast to the cases $k = 0, 1$, i.e., $(1, 1)$ is a feasible solution.

Another special case is found when $y = 0$, and in this case we have

$$e^{\lambda\omega x} = (1-\omega x)^3\left(1+\lambda\omega x+3\omega x-\omega^2x^2\right) \quad (4.30)$$

which is closely related to the case $k = 2$ as considered in Chapter 3. However, the above equation has the (only unique) solution $\omega x = 0$, that is, $x = 0$, since the derivatives of the LHS and the RHS of (4.30) have the same derivative at $x = 0$ and the other properties of the functions are the same as in the corresponding case considered in Chapter 3.

Thus, there are at least two feasible solutions of (4.21), namely, $(0, 0)$ and $(1, 1)$.

4.2.3 Estimation of function $f_1(x, y)$

Consider now function $f_1(x, y)$ and that by using the definition of $f_1^{\pm}$ and $p_i^{1\pm}$ we get

$$f_1(x,y) = \sum_{n=4}^{N^2-1}\mathbb{P}(\deg(v)=n-4)\sum_{i=0}^{n}\binom{n}{i}(\omega x+(1-\omega)y)^i$$
$$(1-\omega x-(1-\omega)y)^{n-i}\left(xp_{i+1}^{1+}+(1-x)p_i^{1-}\right) \quad (4.31)$$

By the definition $f_1(x, y) \leq 1$. In fact, $f_1(x, y) = 1$ iff $y = 0$ and $x > 0$. To see this, note that (4.31) without the last factor adds up to 1. Let us estimate this factor

$$xp_{i+1}^{1+} + (1-x)p_i^{1-} = x \sum_{t=0}^{\lfloor \frac{i-k+1}{2} \rfloor} \binom{i}{t} h^t(x,y,\omega)(1-h(x,y,\omega))^{i-t} + (1-x) \sum_{t=0}^{\lfloor \frac{i-k}{2} \rfloor} \binom{i}{t} h^t(x,y,\omega)(1-h(x,y,\omega))^{i-t}, \tag{4.32}$$

which is at most 1 since each sum is so. Moreover, (4.32) is 1 iff $y = 0$ (as before we assume $\omega \neq 0, 1$).

Therefore, $f_1(x,y) < 1$ for any x and $y > 0$. This observation is intuitively clear since if there is some portion of active veritces of the second type then they will reduce the total activation of vertices of the first type. Hence, the density of active vertices of the first type $\rho_t^{(1)}$ is never 1.

By simple substitution, it can be seen that $x = 0, y = 0$ satisfies $f_1(x,y) = x$ for any ω and k. Combining this with consideration of $f_2(x,y) = y$ we have that $(0,0)$ is a solution of (4.21) for $k = 1, 2$.

4.3 Properties of transition probabilities

In this section we consider the properties of $f_1(x,y)$ and $f_2(x,y)$, and build some bounds of these functions, which are useful in the description of certain types of dynamics of the model. As discussed in Chapter 3, we will focus on the case of $k \leq 3$. Nevertheless, the following statement may be obtained.

Claim 23. Functions $f_1(x,y)$ and $f_2(x,y)$ are non-increasing in k for fixed x, y, ω.

Proof. The statement follows from the definitions of the functions. □

For the purpose of this work, an auxiliary result for stochastic ordering will be stated next. Let a measurable space $(\mathbb{R}, \mathcal{B}(\mathbb{R}))$ be equipped with two probability measures P_1 and P_2, thus the stochastic ordering is the partial ordering

$$P_1 \leq_{st} P_2 \quad \text{iff} \quad P_1([x,\infty)) \leq P_2([x,\infty)) \ \text{ for all } \ x \in \mathbb{R}. \tag{4.33}$$

The last condition is equivalent to the existence of a real-valued random variable X_i with distribution P_i, $i = 1, 2$, such that $X_1 \leq X_2$ almost surely. In the case of binomial distributions, the following criterion can be used

Lemma 24. Let X_i be a binomial random variable Bin(n, p_i), i=1,2. Then for any $k \in \mathbb{N}_0$, $\mathbb{P}(X_1 \geq k) \leq \mathbb{P}(X_2 \geq k)$, if and only if, $p_1 \leq p_2$.

The statement can be proved, for example, by a coupling technique; for a proof see, e.g., [44].

Lemma 25. Function $f_2(x, y)$ is nondecreasing with respect to x for any fixed y, and with respect to y for any fixed x. In particular, $f_2(0, y) \leq f_2(x, y)$, and $0 \leq f_2(0, y) < 1$ for any $k > 0$.

Proof. Let us consider the following difference

$$f_2(x+\delta, y) - f_2(x, y) = y\left(f_2^+(x+\delta, y) - f_2^+(x, y)\right) + (1-y)\left(f_2^-(x+\delta, y) - f_2^-(x, y)\right), \tag{4.34}$$

for an arbitrary $\delta > 0$. According to the definition of functions $f_2^{\pm}(x, y)$, and Lemma 24, it follows that $f_2^{\pm}(x, y)$ is a nondecreasing function in x for any fixed y, that is, $f_2^{\pm}(x+\delta, y) - f_2^{\pm}(x, y) \geq 0$, which implies that so is $f_2(x, y)$. Hence, $f_2(0, y) \leq f_2(x, y)$.

Let δ be an arbitrary positive number, and consider the statement with respect to y,

$$\begin{aligned} &f_2(x, y+\delta) - f_2(x, y) = \\ &(y+\delta) f_2^+(x, y+\delta) + (1-y-\delta) f_2^-(x, y+\delta) y f_2^+(x, y) - (1-y) f_2^-(x, y) = \\ &y\left(f_2^+(x, y+\delta) - f_2^+(x, y)\right) + (1-y)\left(f_2^-(x, y+\delta) - f_2^-(x, y)\right) + \\ &\delta\left(f_2^+(x, y+\delta) - f_2^-(x, y+\delta)\right). \end{aligned} \tag{4.35}$$

The first two terms are nonnegative since $f_2^{\pm}(x, y+\delta) - f_2^{\pm}(x, y) \geq 0$, which follow on from Lemma 24. The last term is also nonnegative because after a change of

variables $f_2^+(x, y+\delta)$ can be expressed as $f_2^-(x, y+\delta) + \tilde{\delta}$, for some $\tilde{\delta} \geq 0$.

Now we can consider the bounds of $f_2(0, y)$. The lower bound of $f_2(0, y)$ can be easily seen from the above consideration. Indeed, $0 = f_2(0, 0) \leq f_2(0, y)$. For the upper bound $f_2(0, y) \leq f_2(0, 1) \leq f_2(1, 1)$, where the last inequality is an equality only if $k = 0$. □

Lemma 26. Function $f_1(x, y)$ is nondecreasing with respect to x for any fixed y, and non-increasing with respect to y for any fixed x.

Proof. The monotonicity can be proved in a similar way as it was done in Lemma 25. However, it is hard to show it directly using (4.8)- (4.9). Here, we first introduce equivalent functions of $f_1^{\pm}$ and then apply the argument.

Let us recall that $f_1^+(x, y, \omega) = \mathbb{P}(C) = \mathbb{P}(\{v \text{ will be active} \mid v \text{ is active excitatory}\})$. However, instead of conditioning first by the number of active neighbors, and then choosing only those events, which constitute the rule (4.1), here we first condition on the types and choose events so that (4.1) holds.

If we consider first the number of neighbors of the second type then

$$f_1^+(x, y) = \sum_{n=4}^{N^2-1} \mathbb{P}(\deg(v) = n-4) \sum_{j=0}^{n} \binom{n}{j} \omega^{n-j} (1-\omega)^j \cdot \sum_{l=0}^{j} \binom{j}{l} y^l (1-y)^{j-l} \sum_{i=k+l}^{n+1-j} \binom{n-j}{i-1} x^{i-1} (1-x)^{n+1-j-i}, \tag{4.36}$$

$$f_1^-(x, y) = \sum_{n=4}^{N^2-1} \mathbb{P}(\deg(v) = n-4) \sum_{j=0}^{n} \binom{n}{j} \omega^{n-j} (1-\omega)^j \cdot \sum_{l=0}^{j} \binom{j}{l} y^l (1-y)^{j-l} \sum_{i=k+l}^{n-j} \binom{n-j}{i} x^{i} (1-x)^{n-j-i}. \tag{4.37}$$

While, if we first condition on the number of neighbors of the first type then

$$f_1^+(x,y) = \sum_{n=4}^{N^2-1} \mathbb{P}(\deg(v)=n-4) \sum_{j=k-1}^{n} \binom{n}{j} \omega^j (1-\omega)^{n-j} \cdot \sum_{l=k-1}^{j} \binom{j}{l} x^l (1-x)^{j-l} \sum_{i=0}^{l-k+1} \binom{n-j}{i} y^i (1-y)^{n-j-i}, \tag{4.38}$$

$$f_1^-(x,y) = \sum_{n=4}^{N^2-1} \mathbb{P}(\deg(v)=n-4) \sum_{j=k}^{n} \binom{n}{j} \omega^j (1-\omega)^{n-j} \cdot \sum_{l=k}^{j} \binom{j}{l} x^l (1-x)^{j-l} \sum_{i=0}^{l-k} \binom{n-j}{i} y^i (1-y)^{n-j-i}. \tag{4.39}$$

Let us consider (4.36)-(4.37). It follows from Lemma 24 that $f_1^{\pm}(x,y)$ are nondecreasing in x for any fixed y. Since $f_1^+(x,y) \geq f_1^-(x,y)$ a similar estimation as in the proof of Lemma 25 shows that $f_1(x,y)$ is a nondecreasing function in x for fixed y.

Since the last sums in (4.38)-(4.39) are the left tails of binomial distribution, $f_1^{\pm}(x,y)$ decreases in y for any fixed x as indicated by Lemma 24. Hence, so is $f_1(x,y)$ as this is a convex combination of decreasing functions. □

Lemma 27. For any $x \leq y$ the following holds $f_2(x,y) \geq f_1(x,y)$ a.s.

Proof. At the initial time moment the type and state of a vertex are chosen independently of each other. Thus, by the definition of $\rho_t^{(i)}$, $i = 1, 2$, we have $\mathbb{P}(\rho_0^{(1)} = \rho_0^{(2)}) = 1$, i.e., $x = y$. The difference of the two functions is given by

$$f_2(x,y) - f_1(x,y) = \tag{4.40}$$
$$\sum_{n=4}^{N^2-1} \mathbb{P}(\deg(v)=n-4) \sum_{i=1}^{n+1} \binom{n}{i-1} (\omega x + (1-\omega)y)^{i-1} (1-\omega x - (1-\omega)y)^{n-i+1} \times$$
$$\left[y p_i^{2+}(x,y,\omega) - x p_i^{1+}(x,y,\omega) \right] +$$

$$+\sum_{n=4}^{N^2-1}\mathbb{P}(\deg(v)=n-4)\sum_{i=0}^{n}\binom{n}{i}(\omega x+(1-\omega)y)^i(1-\omega x-(1-\omega)y)^{n-i}\times$$
$$\big[(1-y)p_i^{2-}(x,y,\omega)-(1-x)p_i^{1-}(x,y,\omega)\big],$$

where the expressions in square brackets are zero for $i \le k-1$. Let us consider the expressions at the initial time moment, i.e., when $x = y = p$. By the definitions of $p_i^{1\pm}(x,y,\omega)$ and $p_i^{2\pm}(x,y,\omega)$, for any x, y, ω we have

$$p_i^{1\pm}(x,y,\omega) \le p_i^{2\pm}(x,y,\omega). \tag{4.41}$$

Therefore, $f_2(p,p) \ge f_1(p,p)$ a.s., i.e., $x \le y$, since after the initial time moment we apply the deterministic functions. Now, we shall show that $f_2(x,y) \ge f_1(x,y)$ will remain so. Let us rewrite (4.40) as

$$f_2(x,y)-f_1(x,y)=$$
$$\sum_{n=4}^{N^2-1}\mathbb{P}(\deg(v)=n-4)\sum_{i=0}^{n}\binom{n}{i}(\omega x+(1-\omega)y)^i(1-\omega x-(1-\omega)y)^{n-i}$$
$$\big[yp_{i+1}^{2+}(x,y,\omega)-xp_{i+1}^{1+}(x,y,\omega)+(1-y)p_i^{2-}(x,y,\omega)-(1-x)p_i^{1-}(x,y,\omega)\big]. \tag{4.42}$$

Assume that $x \le y$ then using (4.41) we get

$$yp_{i+1}^{2+}(x,y,\omega)-xp_{i+1}^{1+}(x,y,\omega)+(1-y)p_i^{2-}(x,y,\omega)-(1-x)p_i^{1-}(x,y,\omega)\ge$$
$$yp_{i+1}^{2+}(x,y,\omega)-xp_{i+1}^{2+}(x,y,\omega)+(1-y)p_i^{2-}(x,y,\omega)-(1-x)p_i^{2-}(x,y,\omega)=0, \tag{4.43}$$

since $p_i^{2-}(x,y,\omega) = p_i^{2+}(x,y,\omega) = 1$ for $i \ge k$. □

Let p_{exc} be the critical initialization probability for the mean-field approximation of the bootstrap percolation model with one type, which was derived in Chapter 3. Also, we will use function $f(\cdot)$ defined in Lemma 14 for the model with one type of vertex. Then we have the following

Lemma 28. In the mean-field approximation of bootstrap percolation with two

types of vertices over $G_{\mathbb{Z}^2_N,p_d}$, all vertices of both types will eventually be inactive if the initialization probability $p < p_{exc}$.

Proof. Assume $p < p_{exc}$. According to Lemma 22 $\rho^{(i)}_{t+1} = f_i(\rho^{(1)}_t, \rho^{(2)}_t)$ for $i = 1, 2$. As it was stated in the proof of Lemma 27 $\rho^{(1)}_0 = \rho^{(2)}_0$ a.s., which is equal to p. By simple substitution one can check that $f_2(p, p) = f(p)$. In Chapter 3 it was shown that $f(p) < p$ for $p < p_{exc}$, see Theorem 17. Therefore, $f_2(p, p) < p$, and $f_1(p, p) \leq f_2(p, p) < p$ as stated in Lemma 27. That is, $\rho^{(1)}_1 \leq \rho^{(2)}_1 < p$.

For any fixed $\rho^{(2)}_1 < p$ by Lemma 25 we have

$$f_2(\rho^{(1)}_1, \rho^{(2)}_1) \leq f_2(\rho^{(2)}_1, \rho^{(2)}_1) < \rho^{(2)}_1. \tag{4.44}$$

On the other hand, $f_1(\rho^{(1)}_1, \rho^{(2)}_1) \leq f_2(\rho^{(1)}_1, \rho^{(2)}_1)$ since $\rho^{(1)}_1 \leq \rho^{(2)}_1$ as stated in Lemma 27.

Therefore, for an arbitrary t

$$\rho^{(1)}_{t+1} = f_1(\rho^{(1)}_t, \rho^{(2)}_t) < \rho^{(2)}_t \tag{4.45}$$

$$\rho^{(2)}_{t+1} = f_2(\rho^{(1)}_t, \rho^{(2)}_t) < \rho^{(2)}_t \tag{4.46}$$

Functions $f_1(x, y)$ and $f_2(x, y)$ are nonnegative, and $\rho^{(i)}_t$ are non-increasing for $p < p_{exc}$ following the above consideration of $i = 1, 2$. Since $\rho^{(2)}_t$ is, in fact, decreasing by (4.46), it can be proven by contradiction that $\lim_{t\to\infty} \rho^{(2)}_t = 0$. However, $\rho^{(2)}_t$ is a majorant of $\rho^{(1)}_t$, i.e., $0 \leq \rho^{(1)}_t \leq \rho^{(2)}_t$, therefore $\lim_{t\to\infty} \rho^{(1)}_t = 0$. □

According to the above results we can derive the relation between function $f(x)$ defined in Chapter 3, and functions $f_1(x, y)$ and $f_2(x, y)$

$$f_1(x, y) \leq f(\omega x + (1 - \omega)y) \leq f_2(x, y). \tag{4.47}$$

CHAPTER 5

RANDOMLY CONNECTED PROBABILISTIC CELLULAR AUTOMATA

In this chapter we consider two coupled probabilistic cellular automata (PCA). The process is defined on a random graph obtained by random coupling of two grids such that a node (vertex) of one grid may have at most one edge to a node from the other grid. This graph can be obtained, for example, by considering a random injection.

Let us assume that a node in one grid can have an edge to a node in the other grid. For simplicity, we eliminate one edge to a neighbor of the node in the same grid, if the specific node has an edge to the other grid as shown in Figure 5.

Each automaton has a majority update rule. In contrast to bootstrap percolation considered in the previous chapters nodes may have the opposite state due to the rule with probability ϵ.

This chapter is partly based on a joint work with Robert Kozma, [65].

5.1 Model

Let us first outline a PCA on a two-dimensional torus $\mathbb{T}^2 = (\mathbb{Z}/n\mathbb{Z})^2$, that is, a finite grid with periodic boundary conditions. A neighborhood of a node z, Λ, is a finite subset of $\mathbb{T}^2$. For simplicity, it can be assumed that Λ contains only the nearest neighbors of a node. At each time step, node z becomes either active or inactive according to an update rule. Instead of considering a deterministic rule, the following generalization is made in PCA, a node, which is inactive according to the update rule, can randomly become active with probability ϵ at the next time step. Let us call ϵ the transition probability. In this chapter, two PCA's are coupled, so that the processes are defined on two coupled tori. Modified rules for each of the coupled PCA's will be described next.

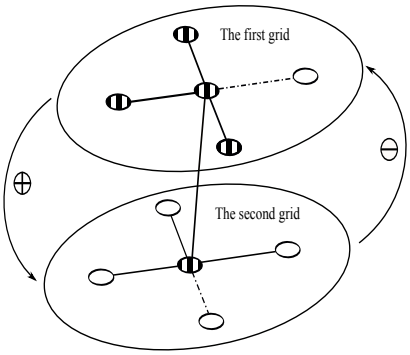

Figure 5: The underlying graph structure of the coupled PCA. The shaded nodes constitute the closed neighborhood of the node shown in the center position in the first grid.

We distinguish nodes from the grids of the coupled PCA so that they have different influences on each other. If a node in the first grid has an edge to a node from the second grid, then there are two possible scenarios:

1. If the node from the second grid is inactive at a certain time step, then it does not have any influence on the node from the first grid.
2. However, if the node from the second grid is active then the cumulative activation of the node from the first grid calculated by the summation over neighbors from the first grid of the given node is reduced by one.

The influence of a node from the first grid connected to a node from the second grid is defined as

1. If the node from the first grid is inactive then it does not affect the node in the other grid which has an edge to the given node.
2. On the other hand, if the node from the first grid is active then the cumulative activation of the node from the second grid calculated by the summation over neighbors from the second grid of the given node is increased by one.

Let us define a process on the randomly coupled square grids as follows. Every node is described by its state. The state of a node can be either active or inactive. At the beginning every node is active with probability p. Note, however, that one

can consider the case, where the initialization probabilities are different for each of the coupled grids.

As we did in the previous chapter, let us define the set of all active nodes from the first grid by $A_1(t)$ and from the second one by $A_2(t)$. For an arbitrary node v let $\chi_v(t)$ be its potential function, so that $\chi_v(t) = 1$ if the node is active, and otherwise $\chi_v(t) = 0$. The state of a node can be changed according to a probabilistic grid-majority rule. For a node v from the first grid we have

$$\begin{aligned}\chi_v(t+1) &= (1-\epsilon)\,\mathbb{1}\left(\sum_{u\in N_1(v)}\chi_u(t) - \sum_{u\in N(v)\setminus N_1(v)}\chi_u(t) \geq \left\lceil\frac{|N_1(v)|}{2}\right\rceil\right) \\ &+ \epsilon\,\mathbb{1}\left(\sum_{u\in N_1(v)}\chi_u(t) - \sum_{u\in N(v)\setminus N_1(v)}\chi_u(t) < \left\lceil\frac{|N_1(v)|}{2}\right\rceil\right), \qquad (5.1)\end{aligned}$$

where $\mathbb{1}$ is the indicator function, $N_1(v)$ is the closed neighborhood of the node v within the first grid, and $N(v)$ is the closed neighborhood of the node v including nodes from both grids. The probability that a node will follow the minority of its neighbors is ϵ. Due to the definition of the graph on which the process is defined $|N(v) \setminus N_1(v)|$ may be at most 1. The rule for a node v from the second grid is given by

$$\begin{aligned}\chi_v(t+1) &= (1-\epsilon)\,\mathbb{1}\left(\sum_{u\in N_2(v)}\chi_u(t) + \sum_{u\in N(v)\setminus N_2(v)}\chi_u(t) \geq \left\lceil\frac{|N_2(v)|}{2}\right\rceil\right) \\ &+ \epsilon\,\mathbb{1}\left(\sum_{u\in N_2(v)}\chi_u(t) + \sum_{u\in N(v)\setminus N_2(v)}\chi_u(t) < \left\lceil\frac{|N_2(v)|}{2}\right\rceil\right), \qquad (5.2)\end{aligned}$$

where $N_2(v)$ is the closed neighborhood of the node v within the second grid, and $|N(v) \setminus N_2(v)|$ may be at most 1.

The meaning of the rule is the following. Each node follows the majority of its neighbors with probability $1 - \epsilon$ and the minority with probability ϵ. The size of $N_j(v)$, where $j = 1, 2$, for different nodes from the same grid depends on the edges

between the grids, and can differ by 1.

Let β be the probability that a node has an edge to a node from the other grid independently on other nodes.

5.2 Mean-field approximation

For simplicity we consider the mean-field (MF) approximation of the process. The usual assumptions of the MF approximations were discussed in Chapter 3. In this section we consider the evolution of two density functions that correspond to active nodes of the first and second grids. Let

$$\rho_t^{(1)} = \frac{|A_1(t)|}{n^2} \tag{5.3}$$

and

$$\rho_t^{(2)} = \frac{|A_2(t)|}{n^2} \tag{5.4}$$

be the densities of active nodes from the first and second grids, relative to the total number of nodes in a grid, respectively.

Lemma 29. For the mean-field approximation of the bootstrap percolation process with grid-majority update rule on randomly coupled grids with n^2 nodes on a grid, and each node has degree N, $\rho_t^{(i)}$ is a Markov process, for $i = 1, 2$, given by

$$\begin{aligned} n^2\rho_{t+1}^{(1)} = (1-\epsilon)\left(Bin\left(n^2\rho_t^{(1)}, f_1^+(\rho_t^{(1)}, \rho_t^{(2)})\right) + Bin\left(n^2(1-\rho_t^{(1)}), f_1^-(\rho_t^{(1)}, \rho_t^{(2)})\right)\right) \\ + \epsilon\left(Bin\left(n^2\rho_t^{(1)}, 1 - f_1^+(\rho_t^{(1)}, \rho_t^{(2)})\right) + Bin\left(n^2(1-\rho_t^{(1)}), 1 - f_1^-(\rho_t^{(1)}, \rho_t^{(2)})\right)\right), \end{aligned} \tag{5.5}$$

$$\begin{aligned} n^2\rho_{t+1}^{(2)} = (1-\epsilon)\left(Bin\left(n^2\rho_t^{(2)}, f_2^+(\rho_t^{(1)}, \rho_t^{(2)})\right) + Bin\left(n^2(1-\rho_t^{(2)}), f_2^-(\rho_t^{(1)}, \rho_t^{(2)})\right)\right) \\ + \epsilon\left(Bin\left(n^2\rho_t^{(2)}, 1 - f_2^+(\rho_t^{(1)}, \rho_t^{(2)})\right) + Bin\left(n^2(1-\rho_t^{(2)}), 1 - f_2^-(\rho_t^{(1)}, \rho_t^{(2)})\right)\right), \end{aligned} \tag{5.6}$$

respectevily, where $f_i^{\pm}(x,y)$ are defined as follows

$$f_1^+(x,y) = (1-\beta)\sum_{i=\lceil \frac{N}{2} \rceil}^{N} \binom{N-1}{i-1} x^{i-1}(1-x)^{N-i} + \beta \left(y \sum_{i=\lceil \frac{N-1}{2} \rceil + 1}^{N-1} \binom{N-2}{i-1} x^{i-1}(1-x)^{N-i-1} + (1-y)\sum_{i=\lceil \frac{N-1}{2} \rceil}^{N-1} \binom{N-2}{i-1} x^{i-1}(1-x)^{N-i-1} \right) \quad (5.7)$$

$$f_1^-(x,y) = (1-\beta)\sum_{i=\lceil \frac{N}{2} \rceil}^{N-1} \binom{N-1}{i} x^{i}(1-x)^{N-i-1} + \beta \left(y \sum_{i=\lceil \frac{N-1}{2} \rceil + 1}^{N-2} \binom{N-2}{i-1} x^{i}(1-x)^{N-i-2} + (1-y)\sum_{i=\lceil \frac{N-1}{2} \rceil}^{N-2} \binom{N-2}{i} x^{i}(1-x)^{N-i-2} \right) \quad (5.8)$$

and

$$f_2^+(x,y) = f_1^+(y,1-x) \quad (5.9)$$

$$f_2^-(x,y) = f_1^-(y,1-x) \quad (5.10)$$

Moreover, given $\rho_t^{(i)}$, $\rho_{t+1}^{(i)}$ has mean $f_i(\rho_t^{(1)},\rho_t^{(2)})$ and variance $g_i(\rho_t^{(1)},\rho_t^{(2)})/n^2$, for $i = 1, 2$, where

$$f_1(x,y) = x f_1^+(x,y) + (1-x) f_1^-(x,y), \quad (5.11)$$

$$f_2(x,y) = y f_2^+(x,y) + (1-y) f_2^-(x,y), \quad (5.12)$$

and

$$g_1(x,y) = x f_1^+(x,y)(1-f_1^+(x,y)) + (1-x) f_1^-(x,y)(1-f_1^-(x,y)), \quad (5.13)$$

$$g_2(x,y) = y f_2^+(x,y)(1-f_2^+(x,y)) + (1-y) f_2^-(x,y)(1-f_2^-(x,y)). \quad (5.14)$$

Proof. The statement follows from the fact that in the MF approximation it is assumed that a node has degree $N-1$, each node is active with probability $\rho_t^{(j)}$, for

$j = 1, 2$, and has an edge to the other grid with probability β, independently of other nodes; and any pair of nodes is considered as independent. □

Based on the above Lemma, the processes can be well approximated by the means $f_1(x, y)$ and $f_2(x, y)$ since the variances, $g_i(\rho_t^{(1)}, \rho_t^{(2)})/n^2$, for $i = 1, 2$, are negligible for large n. It also follows from Lemma 29 that

$$f_2(x, y) = f_1(y, 1 - x). \tag{5.15}$$

In order to simplify the following consideration we denote $f_1(x, y)$ by $f(x, y \mid \epsilon, \beta, N)$, so that this function is given by

$$\begin{aligned}
&f(x, y \mid \epsilon, \beta, N) = \\
&\quad \beta\left(\epsilon\left(\sum_{i=0}^{\lfloor\frac{N-3}{2}\rfloor}\binom{N-1}{i}x^i(1-x)^{N-i-1} + y\binom{N-1}{\lfloor\frac{N-1}{2}\rfloor}x^{\lfloor\frac{N-1}{2}\rfloor}(1-x)^{\lceil\frac{N-1}{2}\rceil}\right)+\right. \\
&\left.(1-\epsilon)\left(\sum_{i=\lfloor\frac{N+1}{2}\rfloor}^{N-1}\binom{N-1}{i}x^i(1-x)^{N-i-1} + (1-y)\binom{N-1}{\lfloor\frac{N-1}{2}\rfloor}x^{\lfloor\frac{N-1}{2}\rfloor}(1-x)^{\lceil\frac{N-1}{2}\rceil}\right)\right) \\
&\quad + (1-\beta)\left(\epsilon\sum_{i=0}^{\lfloor\frac{N}{2}\rfloor}\binom{N}{i}x^i(1-x)^{N-i} + (1-\epsilon)\sum_{i=\lfloor\frac{N}{2}\rfloor+1}^{N}\binom{N}{i}x^i(1-x)^{N-i}\right)
\end{aligned} \tag{5.16}$$

Thus, the density functions of active nodes from the first and second grids evolve according to

$$\begin{aligned}
x_{n+1} &= f(x_n, y_n|\epsilon, \beta, N) \\
y_{n+1} &= f(y_n, 1 - x_n|\epsilon, \beta, N)
\end{aligned} \tag{5.17}$$

For the sake of simplicity of the stability analysis, let us assume that the closed neighborhood size of a node is $N = 5$, that is, square grids are considered. For $N = 5$, the model takes the following form

$$
\begin{cases}
x_{n+1} = f_1(x_n, y_n|\epsilon,\beta) = f(x_n, y_n|\epsilon,\beta,5) = \\
\beta\left((1-\epsilon)\left(x_n^4 + 4x_n^3(1-x_n) + 6x_n^2(1-x_n)^2(1-y_n)\right)\right. \\
\qquad \left. + \epsilon\left(6x_n^2(1-x_n)^2 y_n + 4x_n(1-x_n)^3 + (1-x_n)^4\right)\right) \\
+ (1-\beta)\left((1-\epsilon)\left(x_n^5 + 5x_n^4(1-x_n) + 10x_n^3(1-x_n)^2\right)\right. \\
\qquad \left. + \epsilon\left(10x_n^2(1-x_n)^3 + 5x_n(1-x_n)^4 + (1-x_n)^5\right)\right), \\
\\
y_{n+1} = f_2(x_n, y_n|\epsilon,\beta) = f(y_n, 1-x_n|\epsilon,\beta,5) = \\
\beta\left((1-\epsilon)\left(y_n^4 + 4y_n^3(1-y_n) + 6y_n^2(1-y_n)^2 x_n\right)\right. \\
\left. + \epsilon\left(6y_n^2(1-y_n)^2(1-x_n) + 4y_n(1-y_n)^3 + (1-y_n)^4\right)\right) \\
+ (1-\beta)\left((1-\epsilon)\left(y_n^5 + 5y_n^4(1-y_n) + 10y_n^3(1-y_n)^2\right)\right. \\
\left. + \epsilon\left(10y_n^2(1-y_n)^3 + 5y_n(1-y_n)^4 + (1-y_n)^5\right)\right).
\end{cases}
\tag{5.18}
$$

Let us denote the right hand side (RHS) of (5.18) by $F_{(\epsilon,\beta)}(x,y)$, that is,

$$
F_{(\epsilon,\beta)}(x,y) = \begin{bmatrix} f_1(x,y|\epsilon,\beta) \\ f_2(x,y|\epsilon,\beta) \end{bmatrix}. \tag{5.19}
$$

In order to study the dynamics of our model, first of all, we have to find the fixed points of the system defined by (5.18). For this purpose, we need to find the solutions of

$$
\begin{cases}
x = f_1(x,y|\epsilon,\beta), \\
y = f_2(x,y|\epsilon,\beta).
\end{cases}
\tag{5.20}
$$

In general, it is hard to find all solutions of system (5.20) analytically. Notice, however, that $(\frac{1}{2},\frac{1}{2})$ is the solution for any $\beta \in [0,1]$ and $\epsilon \in [0,1]$.

It is obvious that for $\beta = 0$ we have two uncoupled grids. In this case, it is enough to study the process only on one torus. Model defined on one torus was considered by Balister, Bollobás, and Kozma [10]. Let us summarize the results

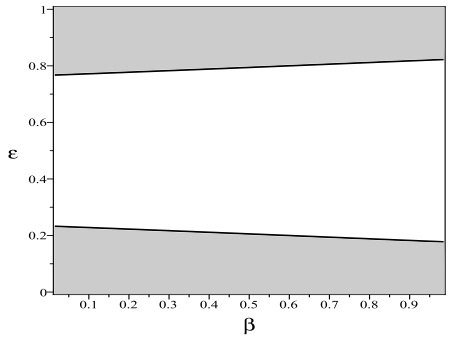

Figure 6: Stability regions of the fixed point $(0.5, 0.5)$ for $\epsilon \in [0, 1]$ and $\beta \in (0, 1]$. The region of instability is marked in gray.

obtained in [10], which also may follow from the general model with $\beta = 0$. There exists a critical value $\epsilon = 7/30$, such that there are two stable and one unstable fixed points for $\epsilon \in [0, 7/30)$, and one unstable fixed point, $1/2$, for $\epsilon \in (7/30, 0.5]$.

In the case of two randomly coupled grids, instability of $(\frac{1}{2}, \frac{1}{2})$ may lead to the appearance of a limit cycle. The Jacobian matrix of $F_{(\epsilon,\beta)}(x, y)$ at the fixed point $(1/2, 1/2)$ is given by

$$DF_{(\epsilon,\beta)}\left(\frac{1}{2}, \frac{1}{2}\right) = \frac{3}{8}(2\epsilon - 1)\begin{bmatrix} \beta - 5 & \beta \\ -\beta & \beta - 5 \end{bmatrix}. \tag{5.21}$$

For any $\beta > 0$ and $\epsilon \in [0, 1]$ the Jacobian $DF_{(\epsilon,\beta)}\left(\frac{1}{2}, \frac{1}{2}\right)$ has a pair of complex conjugate eigenvalues $\lambda, \overline{\lambda}$:

$$\lambda_{1,2}(\epsilon, \beta) = 3/8(2\epsilon - 1)(\beta - 5 \pm i\beta), \tag{5.22}$$

with the corresponding eigenvectors

$$e_{1,2} = \begin{bmatrix} \mp i \\ 1 \end{bmatrix}. \tag{5.23}$$

The fixed point $(1/2, 1/2)$ is stable if $|\lambda| < 1$, that is, when the condition $\frac{3}{8}|2\epsilon - 1|\sqrt{25 - 10\beta + 2\beta^2} < 1$ holds, and unstable if $|\lambda| > 1$; the corresponding regions are shown on Figure 6. Additional analysis is required when $|\lambda| = 1$. Under

this condition an invariant set around the fixed point may appear as a result of Neimark-Sacker bifurcation. More precisely we have the following

Theorem 30. For an arbitrary $\beta \in (0, 1]$ and sufficiently small in absolute value δ, there exist two values of ϵ defined by

$$\epsilon = \frac{1}{2} \pm \frac{8\sqrt{1+\delta}}{6\sqrt{2\beta^2 - 10\beta + 25}}, \tag{5.24}$$

so that the fixed point $(1/2, 1/2)$ is asymptotically stable for $\delta < 0$, and it is an unstable fixed point for $\delta > 0$. Moreover, the the mean-field approximation (5.18) has an asymptotically stable invariant closed curve encircling the fixed point $(1/2, 1/2)$ for $\delta > 0$.

In the next section we prove the above theorem and describe the relation to the process.

Remark 31. The fixed point $(1/2, 1/2)$ is nonlinearly stable at the critical parameter $\delta = 0$.

5.3 Neimark-Sacker bifurcation and phase transition

The Neimark-Sacker bifurcation occurs in a discrete-time dynamical system when a pair of complex conjugate eigenvalues has modulus 1. Thus, for any $\beta \in [0, 1]$ there exists ϵ given by

$$\epsilon^*(\beta) = \frac{\pm 8 + 3\sqrt{2\beta^2 - 10\beta + 25}}{6\sqrt{2\beta^2 - 10\beta + 25}} \tag{5.25}$$

so that the eigenvalues of the system satisfy $|\lambda| = |\overline{\lambda}| = 1$.

To study the Neimark-Sacker bifurcation it is necessary to derive the corresponding normal form. The normal form for Neimark-Sacker bifurcation for a map with a pair of complex conjugate eigenvalues is given by

$$z \mapsto \lambda z + b z^2 \overline{z} + O(|z|^5) \tag{5.26}$$

where $O(|z|^5)$ are higher-order terms starting with at least fifth-order terms, which

can depend smoothly on δ. This bifurcation is also known as Hopf bifurcation for maps.

In order to simplify our analysis we first apply coordinate transformations to get the fixed point at $(0,0)$, and then another transformation to bring the linear part to the simplest form. Hence, we first apply

$$(X_n, Y_n) = \left(x_n - \frac{1}{2}, y_n - \frac{1}{2} \right), \tag{5.27}$$

and the second transformation can be defined using the eigenbasis of (5.21). Let

$$P = \begin{bmatrix} -i & i \\ 1 & 1 \end{bmatrix}, \tag{5.28}$$

then the transformation is given by

$$P^{-1} = \frac{1}{2} \begin{bmatrix} i & 1 \\ -i & 1 \end{bmatrix}. \tag{5.29}$$

Thus, the new complex coordinates $(z_n, \overline{z}_n)$ are obtained by

$$\begin{bmatrix} z_n \\ \overline{z}_n \end{bmatrix} = P^{-1} \begin{bmatrix} X_n \\ Y_n \end{bmatrix}, \tag{5.30}$$

and the inverse of the change of variables is given by

$$\begin{bmatrix} X_n \\ Y_n \end{bmatrix} = P \begin{bmatrix} z_n \\ \overline{z}_n \end{bmatrix}. \tag{5.31}$$

After this transformations system (5.18) can be written as

$$\begin{bmatrix} z_{n+1} \\ \overline{z}_{n+1} \end{bmatrix} = J \begin{bmatrix} z_n \\ \overline{z}_n \end{bmatrix} + \begin{bmatrix} H^1(z_n, \overline{z}_n) \\ H^2(z_n, \overline{z}_n) \end{bmatrix}, \tag{5.32}$$

where $H^j(z_n, \overline{z}_n)$ contains nonlinear terms of degree two and higher, for $j = 1, 2$, and matrix J is defined by

$$J = \begin{bmatrix} \lambda & 0 \\ 0 & \overline{\lambda} \end{bmatrix}, \tag{5.33}$$

where $\lambda, \overline{\lambda}$ is a pair of complex conjugate eigenvalues of the Jacobian $DF_{(\epsilon,\beta)}\left(\frac{1}{2}, \frac{1}{2}\right)$. Clearly, matrix J has the same eigenvalues as the Jacobian.

It is convenient to introduce a new parameter, such that $|\lambda| = 1$ when the new parameter is zero. Let δ be a parameter such that $|\lambda|^2 = 1 + \delta$. Then

$$|\lambda| = \sqrt{1+\delta}$$

and $|\lambda| \,\big|_{\delta=0} = 1$. The original parameters β and ϵ are fixed, and moreover $\epsilon = \epsilon^*(\beta)$, which is given by (5.25). For the following consideration denote $\lambda = \lambda(\delta)$ to emphasize explicit dependence of the eigenvalues on the new parameter.. After this smooth change of parameters the problem reduces to the consideration of bifurcation with respect to δ.

The eigenvalues can be rewritten with respect to the new parameter δ. Clearly, $\lambda + \overline{\lambda} = 2|\lambda| \cos\theta = \mathrm{tr}(J)$, where $\theta = \arg(\lambda)$. Therefore, $\cos\theta = \frac{3(2\epsilon-1)(\beta-5)}{8\sqrt{1+\delta}}$, and for $\epsilon = \epsilon^*(\beta)$ we have

$$\cos\theta \,\big|_{\epsilon=\epsilon^*(\beta)} = \frac{\beta - 5}{\sqrt{1+\delta}\sqrt{2\beta^2 - 10\beta + 25}}. \tag{5.34}$$

Thus, the eigenvalues $\lambda, \overline{\lambda}$, which can be written as $|\lambda|(\cos\theta \pm i \sin\theta)$, are expressed as

$$\sqrt{1+\delta}e^{\pm i\theta} = \frac{\beta - 5}{\sqrt{2\beta^2 - 10\beta + 25}} \pm i\frac{\sqrt{\beta^2 + \delta(2\beta^2 - 10\beta + 25)}}{\sqrt{2\beta^2 - 10\beta + 25}}. \tag{5.35}$$

It is necessary to note that one equation of (5.32) is the complex conjugate of the other. For this reason, it is enough to consider only the first equation in the bifurcation analysis of the system. Let the first equation of (5.32) define a map Q,

that is

$$Q: \qquad z \mapsto \lambda z + H^1(z, \overline{z}), \tag{5.36}$$

we would like to put this map in the normal form for the Neimark-Sacker bifurcation,

$$NS: \qquad z \mapsto \lambda z + B z^2 \overline{z} + O(|z|^4). \tag{5.37}$$

Lemma 32. For a sufficiently small δ, if $\lambda^k(0) \neq 1$, for $k = 1, \ldots, 5$, that is, $\beta \neq 0$ and $\epsilon \neq \{7/30; 23/30\}$, then the map Q defined in (5.36) can be transformed by an invertible parameter-dependent change of complex coordinate

$$z = u + h_2(u, \overline{u}) + c_1 u^3 + c_2 u\, \overline{u}^2 + c_3 \overline{u}^3 + h_4(u, \overline{u}), \tag{5.38}$$

where $h_j(u, \overline{u})$ is a j-th order homogeneous polynomial in u and $\overline{u}$ with coefficients depending on δ, into a map

$$u \mapsto \lambda u + B(\delta)\, u^2\, \overline{u} + O(|u|^5) \tag{5.39}$$

and $B(0) = 30\epsilon - 18\beta\epsilon - 15 + 9\beta + i(3\beta - 6\beta\epsilon)$.

Proof. The desired normal form can be obtained in three steps. If $\lambda^k(0) \neq 1$ for $k = 1, 3$ then by conjugating Q with a suitable diffeomorphism we can annihilate the quadratic terms. After that, conjugating once more with an appropriate diffeomorphism we can remove all cubic terms but $u^2\, \overline{u}$-term, which is called a resonant term, when λ is not a k-th root of unity for $k = 2, 4$. Finally, if $\lambda^5(0) \neq 1$ we can find a diffeomorphism so that the map reduces to the form (5.39). Combining all these steps we obtain (5.38). □

Remark 33. Lemma 32 stated under a stronger condition, i.e., it includes $\lambda^5(0) \neq 1$. This is not necessary for the conclusion, however it holds in this case when the other four conditions are satisfied.

Now we can investigate the type of the Neimark-Sacker bifurcation with respect

to the parameter δ, where β is fixed and ϵ is defined by (5.25).

Lemma 34. The origin is asymptotically stable fixed point for $\delta < 0$. For $\delta > 0$ there exists an asymptotically stable invariant circular set around the origin.

Proof. The normal form with respect to complex coordinates can be written as a system of two equations, where one equation describes the dynamics of the $\arg(u)$, and the other the dynamics of the modulus, $|u|$. Moreover, the equation describing the dynamics of the modulus does not depend on $\arg(u)$, therefore it is possible to describe stability considering only this equation. Hence, we derive the following two conditions

$$\frac{d}{d\delta}|\delta| \ \big|_{\delta=0} = \frac{1}{2}, \tag{5.40}$$

and

$$a = Re\left(\frac{B}{\lambda} \ \big|_{\delta=0}\right) = \frac{-8(4\beta^2 - 20\beta + 25)}{(\beta-5)^2 + \beta^2} < 0, \tag{5.41}$$

for $\beta \in [0, 1]$. These conditions proves the statement. □

Proof of Theorem 30. Combining results from Lemma 34 and Lemma 32 the statement follows. □

Remark 35. The maps $f\left(x_n, y_n|\epsilon, \beta, N\right)$ and $f\left(y_n, 1 - x_n|\epsilon, \beta, N\right)$ are defined as $[0, 1] \to [0, 1]$, that is they are bounded by 1. From this it follows that if ϵ and β are such that $(0.5, 0.5)$ is unstable then the system has either oscillating dynamics or converges to a different fixed point. The region where $(0.5, 0.5)$ is unstable is shown in Figure 6.

CHAPTER 6

HOMOGENEOUS COUPLING OF TWO IDENTICAL SYSTEMS AND INHOMOGENEOUS ATTRACTING SET

The study of oscillatory systems gained a lot of attention during the twentieth century. In particular, questions regarding the dynamics of coupled oscillators and forced systems received great interest. One of the motivations came from applications originating in the consideration of van der Pol oscillators. However, the importance of the problem from a theoretical point of view should never be underestimated since this mechanism can produce chaos.

The coupled limit cycle oscillators are natural examples with flows defined on n-tori. The analysis of coupled systems relies on averaging and perturbation techniques. For example, in the case of two coupled van der Pol oscillators, the orbits lie on $\mathbb{S}^1 \times \mathbb{S}^1 = \mathbb{T}^2 \subset \mathbb{R}^4$. It was shown that two-tori is an attractor and it persists under small perturbation.

Recently, the effects of periodic forcing on flows that perdmit periodic cycles and homoclinic loops/heteroclinic cycles have been extensively studied [53, 55, 77, 76, 50]. It has been shown that this mechanism, which relies on shear, can produce an observable chaos. In particular, the existence of a strange attractor and Sinai-Ruelle-Bowen (SRB) measure with strong statistical properties (e.g., central limit theorem, and exponential decay of correlation) have been proven.

One important detail in the problems mentioned above is the finiteness of interactions. This means that limit cycle oscillators as well as periodic forcing have a periodic influence. This assumption is needed for the application of perturbation theory. One cannot generalize the same idea for coupled heteroclinic cycle oscillators as the time that trajectories spend near saddles goes to infinity. This is nontrivial since orbits spend infinite time near saddles, and thus perturbations can be significant.

In order to describe coupled heteroclinic cycle oscillators we need to understand the geometry of the attracting set. Unfortunately, the existing techniques do not allow for this. In this chapter, we provide some motivation for studying this question by considering numerically bifurcation of coupled heteroclinc cycle oscillators given by Lotka-Volterra equations. The main message is that this mechanism creates a new phenomenon. Also, some description of bifurcation is provided. Then, a simplified problem is considered. A system that has an attracting two-dimensional surface with a boundary that is homeomorphic to a cylinder, and it is formed by the union of equilibria and their unstable manifolds is built.

This chapter is partly based on a joint work with Robert Kozma, and Mikhail Rabinovich, [60].

6.1 Model

In our study, we consider Generalized Lotka-Volterra (GLV) equations. It is known that a system of nonlinear equations can be rewritten as a system of GLV equations after some suitable transformations [38]. The model in the simplest canonical form of Generalized Lotka-Volterra equations is given by

$$\tau_i \frac{dx_i}{dt} = x_i \left(\gamma_i - \sum_{k=1}^{N} a_{ij} x_j \right), \tag{6.1}$$

where $x_i \geq 0$, $\tau_i > 0$, $\gamma_i > 0$, and $a_{i,j} > 0$ for $i, j = 1, \ldots, n$, with $a_{i,i} = 1$ for all i.

System (6.1) has (nontrivial) saddle equilibria that lie on the boundary of the phase space of the form $(0, \ldots, 0, \gamma_i, 0, \ldots, 0)$, where γ_i is the i-th entry, $i = 1, \ldots, n$. Let us denote these equilibria by A_i. If $\lambda_1^{(i)}, ..., \lambda_N^{(i)}$ are eigenvalues of the matrix of the system linearized at A_i, that are ordered as follows
$\mathrm{Re}\lambda_1^{(i)} > ... \geq \mathrm{Re}\lambda_{k_i}^{(i)} > 0 > \mathrm{Re}\lambda_{k_i+1}^{(i)} \geq ... \geq \mathrm{Re}\lambda_N^{(i)}$ then A_i is a saddle with k_i-dimensional unstable manifold.

Denote $1, \ldots, n$ by $[n]$. Consider $S \subset [n]$ given by $S = (i_1, \ldots, i_m)$ where $m \leq n$.

Set S is called a sequence of equilibria of the system (6.1). Let

$I = \{i_k = \pi_k(S) | \pi_k$ is the projection on the k-th coordinate$\}$.

Definition 36. Let S be a sequence of equilibria and assume that all A_i are saddles with a one-dimensional unstable manifold for all $i \in I$ and that there are heteroclinic orbits $\Gamma_{i_{k-1}i_k}$ connecting $A_{i_{k-1}}$ and A_{i_k} such that $\Gamma_{i_{k-1}i_k} \in W^u(A_{i_{k-1}}) \cap W^s(A_{i_k})$, for all $k = 2, \ldots, |I|$. Define

$$\Gamma(S) = \bigcup_{i \in I} A_i \cup \bigcup_{2 \leq k \leq |I|} \Gamma_{i_{k-1}i_k}$$

. Then

1. if $i_1 = i_{|I|}$ then $\Gamma(S)$ is called a heteroclinic cycle and otherwise
2. a heteroclinic sequence

When the unstable manifolds of the saddles are one-dimensional, i.e. $k_i = 1$ for all i, the stability of a heteroclinic cycle depends on the ratios of the compression of the phase volume to the stretching of it in the vicinity of the cycle. These ratios are called saddle values and they can be defined as $\nu_i = -\mathrm{Re}\lambda_2^{(i)}/\mathrm{Re}\lambda_1^{(i)}$. Saddle equilibria A_i is called dissipative if $\nu_i > 1$, and the heteroclinic sequence/cycle is stable if $\nu_i > 1$ for all $i \in I$.

The conditions of the existence and stability of the heteroclinic sequence/cycle with constant uniform stimulation strength $\gamma_i = 1$ for any i are given in [4]. The conditions of existence and stability of the heteroclinic sequence/cycle with arbitrary γ_i were obtained in [5].

6.2 Coupled systems with heteroclinic cycle

We study dynamics of two coupled systems defined by GLV with the heteroclinic cycle. For zero coupling, the parameters of the systems of GLV are chosen in order to obtain heteroclinic cycle dynamics, which exist for a certain parameter range [5].

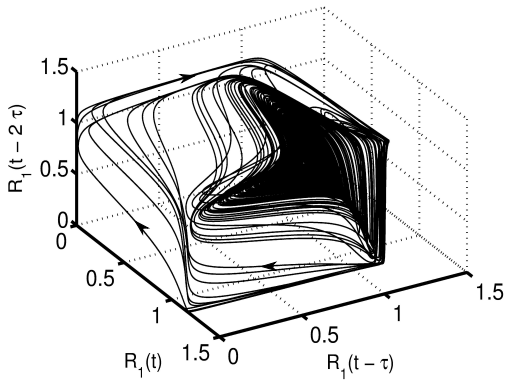

Figure 7: Illustration of the attracting set in the mutually coupled system of Generalized Lotka-Volterra equations.

Let us introduce the notation for sub-systems S_1 and S_2. For simplicity, we consider two systems each of which is defined by three GLV equations (6.1). We reenumerate the variables so that S_1 contains x_1, x_3, and x_5, while S_2 includes x_2, x_4, and x_6. The coupling parameter κ denotes the connection strength from S_1 to S_2.

6.2.1 Numerical study

To analyze in detail the case of reduced/intermediate strength of coupling when quasi-periodic heteroclinic dynamics and chaos co-exist in a mutually coupled system, we performed extensive simulations with various sets of parameters. Let $a_{ij} = \gamma_i/\gamma_j$ the the parameters of the uncoupled systems are $\tau_1 = 1$, $\tau_2 = 1.7$, $\gamma_1 = 1.5, \gamma_2 = 1.2, \gamma_3 = 1.426, \gamma_4 = 1.6, \gamma_5 = 0.956, \gamma_6 = 0.8$.

Takens' theorem [67] can be used to reconstruct high-dimensional attractors from the time series of a variable using time-delayed coordinate embedding. Note that time delay τ can be selected according to the given problem to produce a suitable display of the phase portrait. For example, $x_1(t)$ and its time-lagged copies $x_1(t-\tau)$ and $x_1(t-2\tau)$ are used in Figure 7 to show the three-dimensional phase portrait with time-lagged reconstruction. The case of $\tau = 150$ is used in this display; the direction of the trajectory is illustrated by arrows.

Quantitative evaluation of the Lyapunov exponents shows the coexistence of

heteroclinic cycles and chaos. Namely, we have two positive Lyapunov exponents, where one small negative value is close to zero, another is a small negative exponent, and two others which are large negative exponents. The exact Lyapunov exponent values corresponding to parameters are as follows:
$\lambda_1 = 0.0061 \pm 0.0005, \lambda_2 = 0.0008 \pm 0.0001,$
$\lambda_3 = -0.0019 \pm 0.0015, \lambda_4 = -0.0127 \pm 0.0019, \lambda_5 = -0.6654 \pm 0.0004,$
$\lambda_6 = -1.4409 \pm 0.0002$. We explored a variety of systems close and further away from the heteroclinic cycles. The above conclusions have been confirmed, i.e., we have two positive Lyapunov exponents, one is close to zero, and the rest are negative. Our numerical results show that two different dynamic regimes coexist in a single system with non-oscillatory intrinsic dynamics, similarly to the chimera states described recently in the literature [1].

6.2.2 Analysis

Based on the definition of subsystems S_1 and S_2, clearly two independent stable heteroclinic cycles exist for $\kappa_1 = 0$. Further, it is expected that the two heteroclinic cycles are maintained for very weak coupling $0 < \kappa << \epsilon << 1$.

Theorem 37. There exist values of coupling parameter $0 < k^0 << 1, k^*, k', k$" such that

1. the coupled system exhibits two heteroclinic cycles for $\kappa \in [0, k^0)$;
2. the coupled system converges to a fixed point for $\kappa \in (k^*, k')$;
3. heteroclinic cycle in one system coexists with zero fixed points of the other system for $\kappa \in (k', k")$.

Proof. The equilibrium point attracts trajectories in its neighborhood if it is a dissipative point. However, if the dissipative property of the saddle point changes, i.e. the saddle value is no greater than one due to the increase of κ, then the orbits move in directions away from equilibria. For this reason, when the coupling

parameter is large ($\kappa > k'$), the origin will attract the trajectories of one of the subsystems. Under this scenario, we have one subsystem (i.e. $S1$ or $S2$) embedded in six-dimensions, and this subsystem behaves as in the case of $\kappa = 0$. In other words, considering the phase space $\mathbb{R}^6 = \mathbb{R}^3 \otimes \mathbb{R}^3$, if one subsystem vanishes we deal with the subspace where all coordinates of this subsystem are zero, so that the other subsystem behaves like in the case of $\kappa = 0$.

In the case of $\kappa \in (\kappa^*, k')$, the central eigenspace of each equilibria stays the same. However, the number of stable non-leading eigenvalues is increased to the maximum possible value, thus fixed points appear.

Due to continuity, there exists a $0 < k^0 << 1$, so that the coupled system has two heteroclinic cycles created its subsystems in a corresponding subspace of $\mathbb{R}^6$ for $\kappa < k^0$.

Using dissipativity let us define several quantities, which allow us to separate the whole domain of coupling parameter κ into regions with different types of behavior. The threshold values are expressed as follows:
$\kappa^* = \max_i\{\gamma_{i+1}/\gamma_i\},\ i = 1, \ldots, 6$, where γ_i is the strength of the stimulation of mode i, see (6.1). Further, let us characterize each equilibria. In the following considerations, all indices are written with respect to $(mod\ 6)$ and we make use of the following convention $\{i \in \{0, \ldots, n\} |\ i = n\ (mod\ n)\} = n$. Let us define for each $i = 1, \ldots, 6$ the corresponding set of two numbers $\bar{i} = \{(i \pm 2)\ mod\ 6\}$.

Further notations are: $k^*_{odd} = \max\{k_1, k_3, k_5\}$ and $k^*_{even} = \max\{k_2, k_4, k_6\}$, and indexes defined as $i^*_{odd} = \arg\max\{k^*_{odd}\}$ and $i^*_{even} = \arg\max\{k^*_{even}\}$, where k_i is defined by

$$k_i = \frac{\gamma_{(i+1)}(-\sum_{k\in\bar{i}} \gamma_k a_{ki} + \gamma_i \prod_{k\in\bar{i}} a_{ki})}{\prod_{k\in\bar{i}} (\gamma_k - \gamma_i a_{ki})} \tag{6.2}$$

In the following considerations, we use quantities $k' = \max\{k_{i^*_{odd}-2}, k_{i^*_{odd}+2}\}$ and k" $= \max\{k_{i^*_{even}-2}, k_{i^*_{even}+2}\}$. It is easy to see that k' and k" are larger than the

other thresholds. In the following description, we assume that $k' < k$" unless it is otherwise specified.

The statement follows from the cases considered above with the corresponding values of κ. □

Remark 38. If $k' = k$" then the conclusion still holds with the difference that the behavior corresponding to values between k' and k" does not occur.

6.3 Inhomogeneous graph as an attractor of the GLV system

In [3], a model which is described by n Generalized Lotka-Volterra equations was considered. It was assumed that there is a subset among equilibria (that consists of $1 \leq p \leq n$ equilibria) which are on the axes, such that each equilibrium (saddle) has two unstable directions, see Figure 8. In other words, saddles are sequentially connected by a set of two-dimensional unstable manifold, such that there are heteroclinic orbits connecting O_k to O_{k+1} and O_k to O_{k+2}, for all $k = 1, \ldots, p$.

Here it is assumed that saddles in the sequence are of different types, that is with one and two unstable directions, see Figure 9. For simplicity, let us say that there are heteroclinic orbits connecting O_1 to O_2 and O_1 to O_3, however there is only one heteroclinic orbit connecting O_2 to O_3. In the same way we define the structure of k-th saddle depending whether k is odd or even (up to the change of enumeration of saddles in the sequence).

This case, however, depends on the "strong/weak", "local/non-local" types of heteroclinic orbits for saddles with two-dimensional unstable manifold. Let us consider two cases whereby, the leading unstable eigenvalue of O_{2m+1} corresponds to: the heteroclinic orbit to O_{2m+2}; the heteroclinic orbit to O_{2m+3}. The first case is called "weak", the second is "strong". In both cases, the "attractor" is homeomorphic to a cylinder, however, they are of different dimensions. In the "strong" case the "dimension" is equal to the number of saddles in the sequence, p.

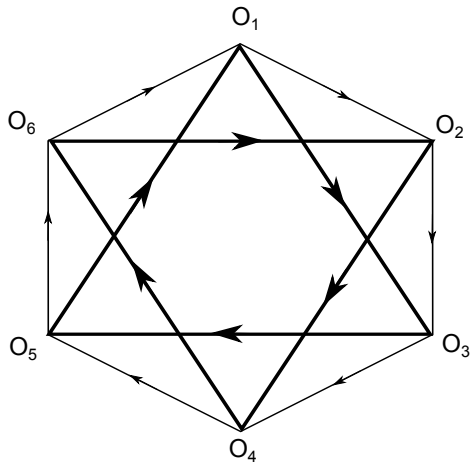

Figure 8: The structure of an attracting set in the phase space considered in [3].

In the "weak" case, the "dimension" is $p/2$. Note, that due to our construction p is divisible by two, i.e. p is even.

In [3], the topological type of the attractor depends on the size of the sequence of saddles. In particular, when p is even, it was shown that the attractor is homeomorphic to a cylinder. Therefore, we can assume that the model with two and one unstable directions is a particular case of the model with two unstable directions only.

In the next argument we consider an arbitrary sequence of three saddles O_k, O_{k+1}, and O_{k+2}, which are joined by heteroclinic orbits as it was described above. Since the consideration is the same for any triple of equilibria, let us take O_1, O_2 and O_3. For simplicity, we assume that $\tau_i = 1$ in (6.1). Then equations (6.1) restricted to three dimensions are given by

$$\begin{aligned}
\frac{dx_1}{dt} &= x_1\left(\gamma_1 - a_{1,2}x_2 - a_{1,3}x_3 - x_1\right)\\
\frac{dx_2}{dt} &= x_2\left(\gamma_2 - a_{2,1}x_1 - a_{2,3}x_3 - x_2\right)\\
\frac{dx_3}{dt} &= x_3\left(\gamma_3 - a_{3,1}x_1 - a_{3,2}x_2 - x_3\right)
\end{aligned} \tag{6.3}$$

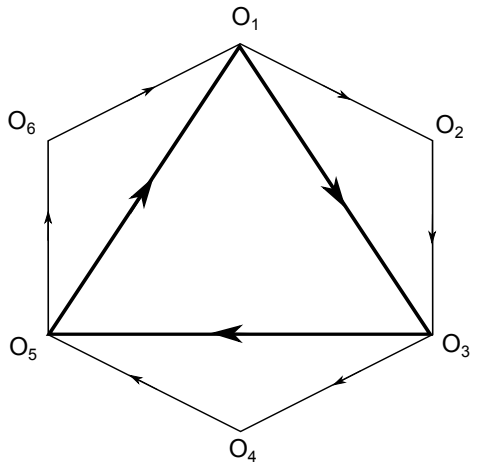

Figure 9: The structure of an attracting set in the phase space of Proposition 40.

For our purposes we define the following planes

$$P_1 := \{\gamma_1 - a_{1,2}x_2 - a_{1,3}x_3 - x_1 = 0\} \tag{6.4}$$

$$P_2 := \{\gamma_2 - a_{2,1}x_1 - a_{2,3}x_3 - x_2 = 0\} \tag{6.5}$$

$$P_3 := \{\gamma_3 - a_{3,1}x_1 - a_{3,2}x_2 - x_3 = 0\} \tag{6.6}$$

and

$$P_{12} := \{x_3 = 0\} \tag{6.7}$$

$$P_{23} := \{x_1 = 0\} \tag{6.8}$$

$$P_{13} := \{x_2 = 0\} \tag{6.9}$$

One may consider two possibilities of local dynamics near equilibrium with two and one unstable directions. It was shown in [3] that planes P_3, P_{23}, P_{13}, and P_{12} enclose a positively invariant region, that is, there are no trajectories which leave the region in positive time. Proofs of the following propositions are similar to the case when each saddle in the sequence has two-dimensional unstable manifold considered in [3].

Proposition 39. If P_3, P_{23}, P_{13}, and P_{12} enclose a positively invariant region then any trajectory in the region which is not in P_{12} goes to O_3.

Proof. In the restricted region system (6.3) has three equilibria O_1, O_2 and O_3 so that O_1 is a saddle with a two-dimensional unstable manifold, O_2 is a saddle with a one-dimensional unstable manifold, and O_3 is a sink.

Any trajectory in a compact positively invariant region has a non-empty ω-limit set. Let us consider an arbitrary trajectory from the region, and let W be a point from the ω-limit set.

Let $O_\epsilon(W)$ be a spherical neighborhood of W with radius ϵ. Also consider another spherical neighborhood of W with radius $\epsilon/2$, $O_{\epsilon/2}(W)$. If a trajectory enters $O_{\epsilon/2}(W)$ then it goes in x_3 direction and spends at least δ in the neighborhood, where δ is the minimum time it takes a representative point from $O_{\epsilon/2}(W)$ to reach a boundary of $O_\epsilon(W)$. Moreover, the growth in the x_3 direction is increased by no less then δS where $dx_3/dt > S > 0$ on $O_{\epsilon/2}(W)$, thus it can never decrease and this happens only a finite number of times, which contradicts that W is in ω-limit set.

Similarly, we can study the other saddles in the restricted region. This construction shows that mapping contracts in the positively invariant region. If we study the saddle with one-dimensional unstable manifold of the original system then we are also able to build a locally contracting map similar to the construction of the Poincaré map. □

Proposition 40. If each unstable manifold $W^u(O_k)$ of saddles in the sequence is contained in the compact forward invariant region defined by P_3, P_{23}, P_{13}, and P_{12}, then $\Gamma = \cup_{k=1}^{n}(W^u(O_k) \cup O_k)$ is asymptotically stable.

Proof. In the previous Proposition we showed that there exists a contracting map in a compact positively invariant regionregion. If we assume that each unstable manifold $W^u(O_k)$ is in the region then we can find a small enough neighborhood of the saddles so that it is in the interior of the region. Using the classical variables in normal form techniques we can find two transversal sections S_0 and S_1 so that

forward solutions starting at S_0 will intersect S_1 before leaving an arbitrary δ-neighborhood of Γ. This together with the previous Proposition shows an existence of a global contraction in δ-neighborhood of Γ, which insures that Γ is asymptotically stable. $\square$

CHAPTER 7

CONCLUDING REMARKS AND FURTHER DIRECTIONS

In this dissertation, I deeply engaged, in collaboration with others, in the study of the dynamics of spatially distributed systems with continuous and discrete time. Discrete time systems considered in this dissertation are defined on random graphs. In particular, I introduced a random graph model $G_{\mathbb{Z}_N^2,p_d}$, where the probability of an edge between a pair of vertices depends on the graph distance between the pair. Several properties of the introduced graph were analyzed. It was shown that the degree distribution of the random graph is approximately Poisson and the diameter is of logarithmic order on the size of the graph.

Many questions about $G_{\mathbb{Z}_N^2,p_d}$ are still open for a deeper exploration. A natural question is what is the graph diameter when $\alpha > 1$? We can generalize this model. One can consider instead of a two-dimensional torus, a higher dimensional one, say, $n-$dimensional. In this case, it is possible to include another parameter β so that the probability of an edge is defined by $p_d = c/(N^\beta d^\alpha)$. It would be interesting to know the properties of the generalized model, in particular the graph diameter in different regimes with respect to α, β, n. It is interesting to determine whether a set of parameters exists where the the diameter is of a smaller order than $\log N$.

Schulman considered an extension of the percolation model where non-local connections are possible [63]. He introduced a long-range percolation graph (LRPG). The diameter of LRPG defined on a finite discrete n-circle was studied by Benjamini and Berger [17], and Coppersmith et al. [29]. However, it is still unknown what is the diameter in several regimes. Since LRPG closely relates to $G_{\mathbb{Z}_N^2,p_d}$ it is possible to apply the technique used for $G_{\mathbb{Z}_N^2,p_d}$ in the study of LRPG.

Probabilistic cellular automaton defined on two randomly coupled square grids was considered. Using mean-field approximation, the existence of limit cycle behavior in the case where vertices of two square grids are of different types was

shown. Also, a similar process was studied yet on a more complicated graph, the introduced random graph $G_{\mathbb{Z}_N^2,p_d}$. First, sharp thresholds on the critical probability of initialization in the case of one type of vertices were derived. Then some bounds for critical probability in the case of two types of vertices were provided.

Janson et al. [42] developed a theory of bootstrap percolation on the Erdős-Rényi random graph $G_{n,p}$. What about the non-monotone version of bootstrap percolation on this graph, i.e., where an active vertex can become inactive? This question is currently open. Another interesting question is related to bootstrap percolation with two types of vertices defined on a square grid, $G_{n,p}$, and $G_{\mathbb{Z}_N^2,p_d}$. What are the critical probabilities in these cases? How far are they from the mean-field approximation?

Systems with continuous time considered in this dissertation are described by generalized Lotka-Volterra (GLV) differential equations. I studied network dynamics of coupled systems each of which has been described by three GLV equations that show my collaborators and I the different potentialities and complexities of these types of systems. Bifurcation with respect to coupling parameters was investigated and a new phenomenon was shown - heteroclinic chimera, i.e., the coexistence of heteroclinic and chaotic dynamics.

Coupled oscillators and forced systems are important subjects. In particular, it is necessary to know the effect of heteroclinic cycle forcing and this will generalize the theory of periodic forcing on flows that admit periodic cycles and homoclinic loops/heteroclininc cycles developed in [53, 55, 77, 76, 50]. However, due to some peculiar properties of the heteroclinic cycle, the techniques used in the study of periodic forcing on flows that permit periodic cycles and homoclinic loops/heteroclinic cycles do not work for this case. A new approach has to be developed. As a first step, one can address this question for a particular case where the system is defined by GLV equations.

In this dissertation, the stability of a discrete dynamical system of estimation error in approximate dynamic programming was also studied based on a universal function approximator. It was shown that the system is uniformly ultimately bounded. This provides a qualitative description of the algorithm.

In the theory of ADP control an important question is still open: what is the rate of convergence? Since many sequential decision problems can be formulated as Markov Decision Processes it is possible to use ADP when traditional techniques may no longer be effective. However, additional deeper analysis of ADP algorithms might improve the performance. This issue together with the stochastic version of ADP are the most important questions in the field both theoretically and for practical applications.

Finally, I would like to note that some of the considered questions may have potential applications in neurobiology, social dynamics, and decision making. Recent developments in neuroimaging, including functional magnetic resonance imaging (fMRI) and electroencephalography (EEG), have provided the possibility to study brain dynamics in high spatio-temporal resolution. Also, significant efforts have been made in analyzing connectivity in the brain. It is supposed that problems and models, which have been considered here, can be used in theoretical studies based on experimental data.

The graph model introduced in this dissertation is also motivated by the structure and operation of the neuropil, the densely connected neural tissue of the cortex [34]. The human brain contains about 10^{11} neurons. Typically, a neuron has several thousands of connections to other neurons through synapses, thus the human brain has $\sim 10^{15}$ synaptic connections. Most of the connections are short and limited to the neuron's direct neighborhood (in some metric), forming the so-called dendritic arbor. In addition, the neurons have a few long connections (axons), which extend further away from their cell body. In general, there are

several thousands of short connections in the dendritic arbor for one distant connection represented by a long axon. We use $G_{\mathbb{Z}_N^2,p_d}$ to model the combined effect of mostly short connections and a few long connections. Brains are more likely to contain more shorter connections than longer ones, a fact captured in the definition of p_d, as p_d is decreasing in the graph distance d.

There are two types of neurons in the brain, namely excitatory and inhibitory ones. The type of neuron describes its function in the brain, e.g., excitatory (inhibitory) neurons excite (inhibit) the neurons to which they are connected. It is known that there are many more excitatory neurons than inhibitory neurons in the cortex; the ratio of inhibitory to excitatory neurons is typically 1/4 [33]. Based on neurobiological studies, it is expected that pure excitatory populations can maintain a non-zero background activation level, while interacting excitatory and inhibitory populations are able to produce limit cycle oscillations [34]. In this dissertation, the focused was on conditions required to sustain a non-zero activity level in pure excitatory networks.

Some of our rigorous mathematical results may provide useful insights in the neural processes described above. It is expected that future studies can provide an evidence on the benefits of the theoretical results to neurobiology.

REFERENCES

[1] D.M. Abrams, and S.H. Strogatz, *Chimera states for coupled oscillators*, Physical review letters, **93**, 174102, 2004.

[2] M. Abu-Khalaf, and F.L. Lewis, *Nearly optimal control laws for nonlinear systems with saturating actuators using a neural network HJB approach*, Automatica, **41**:779-791, 2005.

[3] V.S. Afraimovich, G. Moses, and T. Young, : *Two dimensional heteroclinic attractor in the generalized Lotka-Volterra system*, Nonlinearity, 2016, to appear. arXiv:1509.04570.

[4] V.S. Afraimovich, M.I. Rabinovich, and P. Varona, *Heteroclinic contours in neural ensembles and the winnerless competition principle*, Int. J. Bifurcation and Chaos,**14** (4):1195-1208, 2004.

[5] V.S. Afraimovich, V. Zhigulin, and M.I. Rabinovich, *On the origin of reproducible sequential activity in neural circuts*, Chaos, **14** (4):1123-1129, 2004.

[6] M. Aizenman and J. Lebowitz, *Metastability effects in bootstrap percolation*, J. of Physics A, **21**:3801-3813, 1988.

[7] M. Aizenman, H. Kesten, and C.M. Newman, *Uniqueness of the infinite cluster and continuity of connectivity functions for short and long range percolation*, Commun. Math. Phys., **111**:505-531, 1987.

[8] A. Al-Tamimi, F.L. Lewis, and M. Abu-Khalaf, *Model-free Q-learning designs for linear discrete-time zero-sum games with application to H-infinity control*, Automatica, **43**:473-481, 2007.

[9] P. Balister, B. Bollobás, J. R. Johnson, and M. Walters, *Random Majority Percolation*, Random Structures Algorithms, **36** (3):315-340, 2010.

[10] P. Balister, B. Bollobás, and R. Kozma, *Large deviations for mean field models of probabilistic cellular automata*, Random Structures & Algorithms, **29** (3):399-415, 2006.

[11] J. Balogh, B. Bollobás, H. Duminil-Copin, and R. Morris, *The sharp thresholdfor bootstrap percolation in all dimensions*, Trans. Amer. Math. Soc. **364** (5):2667-2701, 2012.

[12] A. Barron, *Universal approximation bounds for superpositions of a sigmoidal function*, IEEE Transactions on Information Theory, **39**:930-944, 1993.

[13] A. Barron, *Approximation and estimation bounds for artificial neural networks*, Machine Learning, **14**:113-143, 1994.

[14] A.D. Barbour, L. Holst, and S. Janson, *Poisson Approximation*, Clarendon Press, Oxford, 1992.

[15] A.G. Barto, R.S. Sutton, and C.W. Anderson, *Neuronlike elements that can solve difficult learning control problems*, IEEE Transactions on Systems Man and Cybernetics, **13**:835-846, 1983.

[16] R. Bellman, *The theory of dynamic programming*, The RAND Corporation, Paper P-550, 1954.

[17] I. Benjamini, and N. Berger, *The diameter of long-range percolation clusters on finite cycles*, Random Structures & Algorithms, **19** (2):102-111, 2001.

[18] D.P. Bertsekas, and J.N. Tsitsiklis, *Neuro-dynamic programming*, MA, Athena Scientific, 1996.

[19] M. Biskup, L. Chayes, and N. Crawford, *Mean-Field Driven First-Order Phase Transitions in Systems with Long-Range Interactions*, J. of Statistical Physics, **122** (6):1139-1193, 2006.

[20] B. Bollobas, *Random graphs*, Academic Press, Orlando, 1985.

[21] B. Bollobas, and O. Riordan, *Percolation*, Cambridge University Press, Cambridge, UK, 2006.

[22] B. Bollobás, H. Duminil-Copin, R. Morris, and P.J. Smith, *Universality of two-dimensional critical cellular automata*, preprint, 2014. arXiv:1406.6680v2.

[23] B. Bollobás, P.J. Smith, and A.J. Uzzell, *Monotone cellular automata in a random environment*, Combin. Probab. Comput., **24** 4:687-722, 2015.

[24] B. Bollobás, and F. R. K. Chung, *The Diameter of a Cycle Plus a Random Matching*, SIAM J. Disc. Math., **1** (3):328-333, 1988.

[25] B. Bollobás, S. Janson, and O. Riordan, *The phase transition in inhomogeneous random graphs*, Random Structures & Algorithms, **31** (1):3-122, 2007.

[26] A.E. Bryson, and Y.C. Ho, *Applied optimal control*, Washington, DC: Hemisphere, 1975.

[27] J. Chalupa, P.L. Leath, and G.R. Reich. *Bootstrap percolation on a Bethe lattice*, Journal of Physics C, **12** (1):L31, 1979.

[28] F.R.K. Chung, and L. Lu, *The Diameter of Sparse Random Graphs*, Advances in Applied Mathematics, **26** (4):256-279, 2001.

[29] D. Coppersmith, D. Gamarnik, and M. Sviridenko, *The diameter of a long-range percolation graph*, Random Structures & Algorithms, **21** (1):1-13, 2002.

[30] H. Einarsson, J. Lengler, F. Mousset, K. Panagiotouy, and A. Steger, *Bootstrap Percolation with Inhibition*, preprint, 2015. arXiv:1410.3291v2.

[31] P. Erdős, and A. Rényi, *On random graphs I.* Publicationes Mathematicae Debrecen, **5**:290-297, 1959.

[32] P. Erdős, and A. Rényi, *On the evolution of random graphs*, Magyar Tudoamányos Akadémia, Mat. Kut. Int. Közl., **5**:17-61, 1960.

[33] W. J. Freeman, *Mass action in the Nervous system*, Academic Press, New York, 1975.

[34] W.J. Freeman, *Mechanism and significance of global coherence in scalp EEG*, Current Opinion in Neurobiology, **31**:199-205, 2015.

[35] E. N. Gilbert, *Random graphs*, Annals of Mathematical Statistics **30**:1141-1144, 1959.

[36] E. N. Gilbert, *Random plane networks*, J. Soc. Indust. Appl. Math. **9**:533-543, 1961.

[37] H. He, *Self-Adaptive Systems for Machine Intelligence*, Wiley, 2011.

[38] B. Hernandez-Bermejo, V. Fairen, and B. Leon, *Algebraic recasting of nonlinear systems of ODEs into universal formats*, J. Phys. A: Math. Gen., **31**:2415, 1998.

[39] M.W. Hirsch, S. Smale, and R.L. Devaney, *Differential equations, dynamical systems, and an introduction to chaos*, 2nd ed., Elsevier Academic Press, 2004.

[40] A. E. Holroyd, *Sharp metastability threshold for two-dimensional bootstrap percolation*, Probability Theory and Related Fields, **125**:195-224, 2003.

[41] R. Ilin, R. Kozma, *Stability of coupled excitatory-inhibitory neural populations and application to control of multi-stable systems*, Phys. Lett. A, **360** (1):66-83, 2006.

[42] S. Janson, T. Łuczak, T. Turova, and T. Vallier, *Bootstrap percolation on the random graph $G_{N,p}$*, The Annals of Applied Probability, **22** (5):1989-2047, 2012.

[43] S. Janson, R. Kozma, M. Ruszinkó, and Y. Sokolov, *Bootstrap percolation on a random graph coupled with a lattice*, submitted, 2015. arXiv:1507.07997v2.

[44] A. Klenke, and L. Mattner, *Stochastic ordring of classical discrete distributions*, Adv. Appl. Prob., **42**:392-410, 2010.

[45] R. Kozma, M. Puljic, P. Balister, B. Bollobas, and W. J. Freeman, *Phase transitions in the neuropercolation model of neural populations with mixed local and non-local interactions*, Biological Cybernetics, **92** (6):367-379, 2005.

[46] R. Kozma, and Y. Sokolov, *Improved Stability Criteria of ADP Control for Efficient Context-Aware Decision Support Systems*. Int. Conf. on Awareness Science and Technology (iCAST2013), pp. 41-46, Aizu-Wakamatsu, Japan, November 2-4, 2013, IEEE Press, 2013. doi:10.1109/ICAwST.2013.6765406

[47] L. Le Cam, *An approximation theorem for the Poisson binomial distribution*, Pacific Journal of Mathematics, **10**:1181-1197, 1960.

[48] G.G. Lendaris, *Adaptive dynamic programming approach to experience-based systems identification and control*, Neural Networks, **22** (5):822, 2009.

[49] F. Lewis, and D. Liu, (Eds), *Reinforcement Learning and Approximate Dynamic Programming for Feedback Control*, Wiley-IEEE Press, 2012.

[50] K. K. Lin and L.-S. Young, *Shear-induced chaos*, Nonlinearity, **21**:899-922, 2008.

[51] F. Liu, J. Sun, J. Si, W. Guo, and S. Mei, *A boundness result for the direct heuristic dynamic programming*, Neural Networks, **32**:229-235, 2012.

[52] A. Michel, L. Hou, and D. Liu, *Stability of dynamical system*, Birkhauser, 2008.

[53] A. Mohapatra and W. Ott, *Homoclinic loop, heteroclinic cycle and rank-one chaos*, SIAM J. Applied Dynamical Systems, **14**:107-131, 2015.

[54] M. E. J. Newman, and D.J. Watts, *Scaling and percolation in the small-world network model*, Phys. Rev. E, **60**:7332 - 7342, 1999.

[55] W. Ott, *Strange attractors in periodically-kicked degenerate Hopf bifurcations*, Comm. Math. Phys., **281**:775-791, 2008.

[56] W.B. Powell, *Approximate dynamic programming*, Wiley, 2011.

[57] D. Prokhorov, and D.C. Wunsch, *Adaptive critic Designs*, IEEE Trans. on Neural Netw., **8** (5):997-1007, 1997.

[58] M. Puljic, R. Kozma, *Noise mediate Intermittent Synchronization of behaviors in the Random Cellular Automaton Model of Neural Populations*, Proc. ALIFEX, MIT Press, 2006.

[59] M.I. Rabinovich, P. Varona, A.I. Selverston, H.D.I. Abarbanel. *Dynamical Principles in Neuroscience*. Reviews of Modern Physics, **78** (4):1213, 2006.

[60] M.I. Rabinovich, Y. Sokolov and R. Kozma *Robust sequential working memory recall in heterogeneous cognitive networks*, Front. Syst. Neurosci. **8**:220, 2014. doi:10.3389/fnsys.2014.00220.

[61] J. Sarangapani, *Neural network control of nonlinear discrete-time systems*, Taylor and Francis, 2006.

[62] R.H. Schonmann, *On the behaviour of some cellular automata related to bootstrap percolation*, Annals of Probability, **20**:174-193, 1992.

[63] L. S. Schulman, *Long-range percolation in one dimension*, J.Phys. A, **16**:L639-L641, 1983.

[64] J., Si, A.G. Barto, W.B. Powell, and D.C. Wunsch, *Handbook of learning and approximate dynamic programming.* Piscataway, NJ: IEEE Press, 2004.

[65] Y. Sokolov, R. Kozma, *Stability of dynamic brain models in neuropercolation approximation*, Proc. of 2014 IEEE Int. Conf. on Systems, Man, and Cybernetics, October 2014, San Diego, CA, USA, 2230-2233, IEEE Press, 2014. doi:10.1109/SMC.2014.6974256

[66] Y. Sokolov, R. Kozma, L.D. Werbos, and P.J. Werbos, *Complete stability analysis of a heuristic approximate dynamic programming control design*, Automatica, **59**:9-18, 2015. doi:10.1016/j.automatica.2015.06.001.

[67] F. Takens, *Detecting strange attractors in turbulence*, in Lecture Notes in Mathematics, vol. 898, D. A. Rand and L. S. Young, eds. Springer-Verlag, 366381, 1981.

[68] Talagrand, M., *Mean Field Models for Spin Glasses*, Vol. 1 & 2, Springer-Verlag Berlin Heidelberg, 2011.

[69] T. Turova, and T. Vallier, *Bootstrap percolation on a graph with random and local connections*, J. of Statistical Physics, **160** (5):1249-1276, 2015.

[70] A.C.D. van Enter, *Proof of Straley's argument for bootstrap percolation*, J. Statist. Phys., **48**:943-945, 1987.

[71] G.K. Venayagamoorthy, R.G. Harley, and D.C. Wunsch, *Dual heuristic programming excitation neurocontrol for generatos in a multimachine power system*, IEEE Trans. on Industry Applications, **39** (2):382-394, 2003.

[72] D. Vrabie, and F.L. Lewis, *Generalized policy iteration for continuous-time systems*, In Proceeding of Int. joint Conf. on Neural Networks, New York:IEEE, 3224-3231, 2009.

[73] J. von Neumann, *Theory of self-reproducing automata*, University of Illinois Press, 1966.

[74] J. von Neumannm, O. Morgenstern, *Theory of games and economic behavior*, Princeton Univ. Press, 1944.

[75] D. J. Watts, and S. H. Strogatz, *Collective dynamics of 'small-world' networks*, Nature, **393**:440-442, 1998.

[76] Q. Wang and L.-S. Young, *From invariant curves to strange attractors*, Comm. Math. Phys., **225**:275-304, 2002.

[77] Q. Wang and L.-S. Young, *Strange attractors in periodically-kicked limit cycles and Hopf bifurcations*, Comm. Math. Phys., **240**:509-529, 2003.

[78] D. Wang, D. Liu, Q. Wei, D. Zhao, and N. Jin, *Optimal control of unknown nonaffine nonlinear discrete-time systems based on adaptive dynamic programming*, Automatica, **48**:1825-1832, 2012.

[79] P.J. Werbos, *Beyond regression: New Tools for Prediction and Analysis in the Behavioral Science*, Ph.D. thesis, Committee on Applied Mathematics, Harvard Univ., Cambridge, MA, 1974.

[80] P.J. Werbos, *Consistency of HDP applied to a simple reinforcement learning problem*, Neural Networks, **3**:179-189, 1990.

[81] P.J. Werbos, *Stable Adaptive Control Using New critic Designs*, preprint, 2012. arXiv:adap-org/9810001.

[82] D.A. White, and D.A. Sofge, (Eds.) *Handbook of Intelligent Control: Neural, Fuzzy, and Adaptive Approaches*, Chapters 3, 10 and 13, 1992.

[83] H. Zhang, Q. Wei, and D. Liu, *An iterative adaptive dynamic programming method for solving a class of nonlinear zero-sum differential games*, Automatica, **47** (1):207-214, 2011.

[84] J. Zhang, H. Zhang, Y. Luo, and H. Liang, *Nearly optimal control scheme using adaptive dynamic programming based on generalized fuzzy hyperbolic model*, ACTA Automatica Sinica, **39** (2):142-148, 2013.

[85] H. Zhang, D. Liu, Y. Luo, and D. Wang, *Adaptive Dynamic Programming for Control: Algorithms and Stability.* London:Springer-Verlag, 2013.